UNIVERSITÄT SIEGEN

Ralf Siebert

Mechanical integrators for the optimal control in multibody dynamics

Herausgeber: Peter Betsch

Schriftenreihe des Lehrstuhls für Numerische Mechanik

Band V

Mechanical integrators for the optimal control in multibody dynamics

Dissertation
zur Erlangung des akademischen Grades
Doktor-Ingenieur

vorgelegt von
Dipl.-Math. Ralf Siebert
aus Heinsberg

eingereicht dem
Department Maschinenbau
der Universität Siegen

Referent:	Prof. Dr.-Ing. habil. Peter Betsch
Korreferent:	Prof. Dr. Moritz Diehl
Vorsitzender:	Prof. Dr.-Ing. Oliver Nelles

Tag der mündlichen Prüfung:
31. 08. 2012

Impressum
Prof. Dr.-Ing. habil. Peter Betsch
Lehrstuhl für Numerische Mechanik
Universität Siegen
57068 Siegen
ISSN 1866-1203
URN urn:nbn:de:hbz:467-6520
Zugl.: Siegen, Univ., Diss., 2012

Abstract

The present thesis deals with inverse multibody dynamics problems. In particular, optimal control problems will be treated, which are governed by differential-algebraic equations. The main goal therein is the minimization of the control effort, which is necessary for moving a multibody system from one configuration to another. A basic task therefore is the formulation of the underlying equations of motion. Main focus will be on the formulation of the equations of motion with natural coordinates, which facilitates the design of structure-preserving time-stepping schemes. It is well known that schemes preserving basic properties of the mechanical system algorithmically exhibit superior stability properties in comparison to standard integrators. The application of these schemes within optimal control problems requires a consistent incorporation of the control torques. A convincing way for the incorporation of the control torques will be proposed in this contribution. In addition to the schemes based on the rotationless formulation, also an energy-momentum conserving time-stepping scheme based on quaternions will be presented. Although the quaternion-based scheme turns out to be competitive in the forward dynamics of rigid bodies, the extension to multibody problems is not as straightforward and easy to handle as with the rotationless formulation in terms of natural coordinates. Therefore quaternions will not be applied within optimal control problems in this thesis. Regarding optimal control of multibody systems, new energy-momentum consistent direct transcription methods in terms of natural coordinates will be presented. In a first step, the equations of motion obtained by a reduction process via the discrete null space method will be applied. The arising results will be compared with those achieved by a formulation of the equations of motion with the widely used minimal coordinates. In a second step, the original equations of motion in form of differential-algebraic equations will serve as basis for the formulation of the optimal control problem. In addition to the direct transcription methods mentioned before, a novel optimal control method based on indirect transcription will be presented. The newly proposed method conserves the Hamiltonian corresponding to the optimal control problem. It is worth mentioning that this method is directly related to previously developed energy consistent schemes in forward dynamics.

Keywords: Multibody Systems, Differential-Algebraic Equations, Rotationless Formulation, Quaternions, Energy-Momentum Consistency, Optimal Control, Actuation, Direct Transcription, Indirect Transcription, Conservation of the Hamiltonian

Zusammenfassung

Die vorliegende Arbeit behandelt Problemstellungen der inversen Mehrkörperdynamik. Insbesondere werden Optimalsteuerungsprobleme untersucht, die mittels differential-algebraischer Gleichungen beschrieben werden. Das Hauptziel besteht in der Minimierung des Steuerungsaufwands, der benötigt wird, um ein Mehrkörpersystem von einer Konfiguration in eine andere zu bewegen. Eine wichtige Aufgabe dafür ist die Formulierung der zu Grunde liegenden Bewegungsgleichungen. Hauptaugenmerk wird dabei auf die Formulierung der Bewegungsgleichungen mit natürlichen Koordinaten gelegt, die die Konstruktion von Struktur erhaltenden Zeitintegratoren ermöglichen. Es ist bekannt, dass sich Verfahren, die grundlegende mechanische Eigenschaften algorithmisch erhalten, durch überlegene numerische Stabilitätseigenschaften im Vergleich zu Standardintegratoren auszeichnen. Die Anwendung von diesen Verfahren innerhalb von Optimalsteuerungsproblemen erfordert einen konsistenten Einbau von Steuerungsmomenten. Ein überzeugender Weg für den Einbau von Steuerungsmomenten wird in dieser Arbeit vorgeschlagen. Zusätzlich zu den Integratoren aufbauend auf der rotationsfreien Formulierung wird ergänzend ein Energie-Impulserhaltendes Zeitschrittverfahren basierend auf Quaternionen vorgestellt. Zwar stellt sich das Quaternionen gestützte Verfahren als konkurrenzfähig in der Vorwärtsdynamik von Starrkörpern heraus, die Erweiterung auf Mehrkörperprobleme ist allerdings nicht so direkt und einfach zu handhaben wie bei der rotationsfreien Formulierung basierend auf natürlichen Koordinaten. Daher werden die Quaternionen innerhalb von den Optimalsteuerungsproblemen in dieser Arbeit nicht verwendet. In Bezug auf die optimale Steuerung von Mehrkörpersystemen werden neuartige Energie-Impuls-konsistente direkte Transkriptionsverfahren beruhend auf natürlichen Koordinaten vorgestellt. In einem ersten Schritt werden Bewegungsgleichungen verwendet, die über eine Reduktion mittels der diskreten Nullraum-Methode gewonnen werden. Die Resultate werden verglichen mit denen, die man durch eine Formulierung der Bewegungsgleichungen mit den weit verbreiteten minimalen Koordinaten erhält. In einem zweiten Schritt dienen die ursprünglichen Bewegungsgleichungen in Form von differential-algebraischen Gleichungen als Basis für die Formulierung von den Optimalsteuerungsproblemen. Zusätzlich zu den bereits erwähnten direkten Transkriptionsmethoden wird auch eine neuartige Optimalsteuerungsmethode basierend auf indirekter Transkription eingeführt. Die besagte Methode erhält die zu dem Optimalsteuerungsproblem zugehörige Hamiltonfunktion. Es ist erwähnenswert, das diese Methode direkten Bezug hat zu früher entwickelten Energie-konsistenten Verfahren in der Vorwärtsdynamik.

Schlagwörter: Mehrkörpersysteme, Differential-Algebraische Gleichungen, Rotationsfreie Formulierung, Quaternionen, Energie-Impuls-Konsistenz, Optimalsteurung, Aktuierung, Direkte Transkription, Indirekte Transkription, Erhaltung der Hamilton-Funktion

Vorwort

Die vorliegende Arbeit entstand in der Zeit von 2007 bis 2012 im Rahmen meiner Tätigkeit als wissenschaftlicher Mitarbeiter am Lehrstuhl für Numerische Mechanik der Universität Siegen.

Besonders bedanken möchte ich mich bei Herrn Prof. Dr.-Ing. Peter Betsch für die fachliche Unterstützung und Motivation bei der Erarbeitung dieser Dissertation sowie die Übernahme des Hauptreferates.

Ebenfalls danken möchte ich Herrn Prof. Dr. Moritz Diehl für die Übernahme des Korreferates, das damit gezeigte Interesse an dieser Arbeit und zahlreiche wertvolle Anmerkungen.

Außerdem möchte ich allen Mitarbeitern des Lehrstuhls für Numerische Mechanik für die angenehme Arbeitsatmosphäre und Zusammenarbeit danken.

Siegen, September 2012

Ralf Siebert

Contents

1. Introduction

In the present thesis, numerical methods for treating optimal control of mechanical multibody systems will be developed. To preserve resources, energy-optimal movements become more and more important. Hence, the main focus will be on the minimization of the control effort which is necessary for moving a multibody system from a specific initial to a specific end position. Areas of application of such problems are the simulation of optimal movements in robotics, biomechanics, or space flights. In the literature, also minimum-time optimal control problems have been investigated intensely. However, those kind of problems will not be treated in this work.

Equations of motion describing a multibody system depend strongly on the choice of coordinates. In most of the classical works, generalized or minimal coordinates such as Euler angles for describing the orientation of a rigid body in space have been used. This approach leads to equations of motion in form of ordinary differential equations (ODEs), which typically exhibit a high degree of nonlinearity. Additionally, the well-known singularities of the 3-parameter descriptions of finite rotations have to be taken into account. An essentially different form of the equations of motion arises if redundant coordinates are employed. In that case, the equations of motion take the form of differential-algebraic equations (DAEs) of index 3. The application of DAEs facilitates both the treatment of mechanical systems with closed loops and a straightforward extension to flexible multibody dynamics. Moreover, the simply structured form of those equations permits the usage of consistent numerical integrators such as energy-momentum schemes.

In this work, recent developments of consistent numerical integrators for multibody dynamics will be extended to optimal control problems. Consistent integrators reproduce basic mechanical properties of the underlying system like momentum, angular momentum, and energy correctly. These consistency properties lead to increased robustness and stability of the mechanical integrator. Furthermore, consistent integrators facilitate the application of large time step sizes, which may lead to reduced computational costs. Finally, it will be shown in this thesis that conservation properties similar to those present in a mechanical system also exist for optimal control problems. Similar to the forward dynamics case, a special discretization of the optimality conditions can be found which yields the corresponding algorithmic conservation property of the optimal control problem.

1.1. Literature review

A short survey of literature published during the last 50 years concerning the content of this thesis will be given below.

A large number of textbooks treating optimal control theory exist, among these are the works of Athans & Falb [5], Bryson & Ho [33], Sontag [98], and Pinch [88]. Since continuous solutions of optimal control problems can only be calculated for special cases, practical optimal control techniques make use of computational methods. Several differing numerical approaches are available for the solution of the boundary value problems which arise when treating optimal control problems. Surveys of the different numerical optimal control methods are given in the works of Betts [21, 22] and Binder et al. [25]. A basic distinction can be made concerning the way the discretization will be done. The necessary conditions of optimality may be derived before the discretization of the equations of motion. This yields an indirect method. A main issue within an indirect method is the explicit formulation of the involved systems of costate differential equations, which makes the calculation of first- and second-order derivatives of the equations of motion necessary. Alternatively, direct methods can be employed, where the discretization of the equations of motion will be done before formulating the optimal control problem. Several direct methods have been applied in the past for the solution of optimal control problems. Among these are direct multiple shooting methods due to Bock & Plitt [27] (see also Diehl et al. [42]) and direct collocation methods (see, for example, von Stryk [103] and Hargraves & Paris [60]). A hybrid approach combining direct collocation and indirect multiple shooting can be found in von Stryk & Bulirsch [104]. Also direct transcription methods are often referred to in the literature, but direct transcription methods and direct collocation methods can be regarded the same (see, for example, Hull [64]). Works regarding direct transcription are those of Enright & Conway [45], Betts and co-workers [24, 23], and Engelsone et al. [44]. Besides the numerical optimal control approaches falling into the classes of collocation or multiple shooting, also single shooting methods have been applied in the past (see, for example, Hicks & Ray [63], Hannemann & Marquardt [59] and Hartwich et al. [61]). However, for highly unstable system the application of single shooting methods seems not to be recommended (see, for example, Ascher et al. [4]). The mentioned direct approaches have in common that the constrained optimal control problem will be transformed into a finite dimensional nonlinear program which can be solved by standard 'Sequential Quadratic Programming' (SQP) methods (see, for example, Barclay et al. [6] and Boggs & Tolle [28]). The underlying 'Quadratic Programming' (QP) problems therein can be solved, for example, by 'interior-point' (IP) methods. In some cases, relations between direct methods for optimal control and discretized costate equations arising in indirect methods can be elaborated. In the work of Hager [58] (see also Bonnans & Laurent-Varin [29]), it has been shown that the discretization of the necessary conditions of optimality within an indirect method by use of symplectic partitioned Runge-Kutta methods is equivalent to direct collocation.

Starting with the pioneering works by Simo and co-workers [97, 96, 95], a lot of effort has gone into the development of energy-momentum consistent time-stepping schemes. This is due to the well-known superior numerical stability and robustness properties of the structure-preserving integrators in comparison to standard integrators (see, for example, Goicolea & Garcia Orden [51] and Gonzalez and co-workers [52, 54]). Energy-momentum consistent integrators have been shown to be especially beneficial in the context of flexible multibody dynamics (see, for example, Bauchau & Bottasso [7], Puso [89], Betsch & Steinmann [15] and Betsch et al. [10]). It is well-known that the midpoint rule is sufficient for the consistency of energy for maximum quadratic Hamilton functions (see, for example, Wood [107]). However, to achieve an energy consistent scheme for general nonlinear Hamilton functions, the discrete derivative introduced by Gonzalez [53] is required. Various approaches applying the discrete derivative have been introduced, see Gonzalez [53] for a specific second-order method and Groß et al. [57] for higher-order schemes. As a special case, applicable for one-dimensional systems with general nonlinear potential functions, the Greenspan formula introduced in Greenspan [55] can be mentioned. Besides the energy-momentum consistent schemes, also variational integrators leading to angular momentum consistency are widely-used (see, for example, Marsden & West [80] and Lew et al. [75]).

In many works use has been made of generalized or minimal coordinates. While the corresponding system of equations describing the motion is of minimal size, the equations of motion exhibit a high degree of nonlinearity. As an additional drawback, the well-known singularities of the Euler angles or other 3-parameter representations of finite rotations have to be considered. The mentioned drawbacks can be circumvented by application of the so-called rotationless formulation based on the natural coordinates introduced in Garcia de Jalon et al. [47] (see also Garcia de Jalon [46], von Schwerin [102], Kraus et al. [66], and Cossalter & Lot [40]). A fundamental characteristic of natural coordinates is the constant mass matrix leading to simply structured equations of motion. The rotationless formulation has a wide area of application, such as in rigid body dynamics (see, for example, Betsch & Steinmann [16]), for the description of multibody systems (see, for example, Betsch & Leyendecker [11] and Betsch & Uhlar [19]), and even for multibody systems containing flexible components (see, for example, Betsch & Steinmann [18], Betsch et al. [10], and Sänger [92]). A major benefit of the rotationless formulation is the facility of discretizing the corresponding equations of motion with consistent time-stepping schemes. To reduce the large number of equations and unknowns present in the rotationless formulation, the discrete null space method with nodal reparametrization can been applied (see, for example, Betsch [9], Betsch & Leyendecker [11], Leyendecker et al. [76], and Uhlar [99]). It is worth mentioning that the reduction process does not effect the consistency properties of the employed integration scheme. In addition to the already mentioned choices of coordinates, also quaternions have been used in the past in rigid body dynamics (see, for example, Haug [62] and Nikravesh [85]). In comparison to the rotationless formulation, the quaternion formulation is characterized by

less redundant coordinates. However, it exhibits a higher degree of nonlinearity (see Betsch & Siebert [12]) due to the configuration dependent mass matrix.

Several works deal with numerical approaches for the optimal control of multibody systems. In Agrawal et al. [1] a multiple shooting method in combination with a generalized coordinates formulation of the equations of motion has been employed for the optimal control of a robot manipulator. A different indirect multiple shooting method has been presented in the recent work of Callies & Rentrop [37]. In the works of Büskens and co-workers [35, 34] the optimal control of industrial robots described by a minimal set of coordinates has been treated. A deeper insight into the discrete costate variables of the employed direct multiple shooting method is given in Büskens & Maurer [36]. Also preserving integrators have been applied in previous works concerning optimal control of multibody systems. An energy consistent direct transcription method has been introduced in Bottasso & Croce [31] (see also Bottasso et al. [32]). Therein, the underlying discrete equations of motion take the form of differential-algebraic equations. A variational integrator yielding consistency of angular momentum served as basis for the formulation of a direct transcription optimal control method in the works of Leyendecker et al. [77] and Ober–Blöbaum et al. [86]. The arising optimal control methods therein are referred to as 'Discrete mechanics and optimal control' (DMOC) for unconstrained systems and 'Discrete mechanics and optimal control for constrained systems' (DMOCC) otherwise. A direct transcription method based on an energy-momentum scheme has been developed in the recent work of Betsch et al. [13]. The formulation with differential-algebraic equations arising when using redundant coordinates has been avoided in [77, 86, 13] through the use of the discrete null space method. Only few works are concerned with optimal control described with equations of motion in form of differential-algebraic equations. Notable exceptions are the works of Bottasso and co-workers [32, 31], von Schwerin [102], and Kraus et al. [65] focussed on real multibody systems as well as the more theoretical works of Kunkel & Mehrmann [69], Gerdts [48, 49], Gerdts & Kunkel [50], and Müller [83, 84].

1.2. Outline

In the following, a short summary of each chapter of this thesis will be given. Thereby the main issues of each chapter will be pointed out for the reader.

Chapter 2 provides basics for the formulation of the optimal control problems which will be treated in this work. The continuous augmented cost function has to be formulated. Calculating partial derivatives yields the continuous necessary conditions of optimality. Deriving the continuous necessary conditions of optimality and discretizing them results in an indirect method. Another possibility is discretizing the equations of motion of the underlying mechanical system first and formulating the discrete augmented cost function afterwards. The latter proceeding yields a direct method. While direct methods will be employed in

Chapters 6 and 7, an indirect method will be used in Chapter 8. Additionally, it will be emphasized that transcription or collocation methods will be used in this work. Shooting or multiple shooting methods will only be touched in this thesis. Finally, it will be shown that fulfilment of the necessary conditions of optimality involves conservation of the Hamiltonian. The latter can also be reached in the discrete case within the newly derived Hamiltonian conserving indirect optimal control method elaborated later in Chapter 8.

Chapter 3 introduces the equations of motion describing the dynamical behaviour of the mechanical multibody systems. In a first step, the equations of motion in the so-called rotationless formulation take the form of differential-algebraic equations (DAEs) with index 3. A special discretization of the equations will be applied to achieve a mechanical integrator which is algorithmically consistent concerning basic properties of the underlying mechanical system. For this aim, a special discretization for both the input of the controls and the incorporation of linear viscous friction will be introduced. The arising basic energy-momentum scheme will serve as basis for the formulation of the optimal control problems in Chapter 7. Furthermore, a reduction process will be performed by application of the discrete null space method with nodal reparametrization. Additionally, a generalized coordinates formulation of the equations of motion with midpoint evaluation will be achieved by a reduction process. Both reduced equations of motion will be applied in Chapter 6 within optimal control problems.

Chapter 4 presents the rotationless formulation of spatial rigid body dynamics. Therein, direction cosines will be employed for describing the orientation of the rigid bodies. A key property of the rotationless formulation is the constant and diagonal mass matrix. The application of the rotationless formulation necessitates the incorporation of internal constraints due to the rigidity. Furthermore, the extension to constrained multibody systems is directly suitable. For that purpose, two of the basic kinematic joints will be treated in detail, namely the revolute and the prismatic joint. Consequently, external constraints due to the kinematic joints have to be added. A basic task for achieving an energy and angular momentum consistent integrator is the adequate discretization of the involved vectors and matrices in the equations of motion. In Chapter 4, the main focus will be on the consistent incorporation of control torques and linear viscous friction. At the end, the consistency properties will be demonstrated within an appropriate numerical example.

Chapter 5 proposes the main ideas of Betsch & Siebert [12], where quaternions have been used for the formulation of the equations of motion for a rigid body in space. It is well known that unit quaternions are well-suited for the singularity-free description of finite rotations. The quaternion formulation of the equations of motion contains a configuration dependent mass matrix. An invertible mass matrix is mandatory for the transition to the Hamilton equations of motion. The latter can be achieved by a size reduction of the mass matrix in the director formulation. The quaternion-based Hamilton equations of motion serve as starting point for the design of an energy-momentum conserving time-stepping scheme.

For this aim, the kinetic energy has to be formulated with quadratic invariants and the discrete derivative introduced by Gonzalez in [53] has to be applied. The conservation properties of the newly derived scheme will be demonstrated within a numerical example. At the end, problems regarding the extension to flexible multibody dynamics within an energy-momentum scheme will be mentioned. Due to these problems, the quaternions will not be applied in the optimal control problems later on.

Chapter 6 combines the contents of Chapter 2 with those of the Chapters 3 and 4. Equations of motion with eliminated algebraic constraints in the discrete setting as well as equations of motion in purely differential form from the outset will be used as basis for the formulation of the mechanical optimal control problem. In particular, both the reduced energy-momentum scheme and a generalized coordinates formulation with midpoint evaluation will be employed. Two multibody systems will be investigated in the present chapter. In a first step, a 3-link robot manipulator will be used as an example of a planar multibody system. Furthermore, a space robot, whose change in orientation is induced by three rotors will be examined within optimal control. This example is qualified for testing all algorithmic consistency properties of the mechanical integrator. The effects of limited controls and linear viscous friction will be demonstrated within these examples. A direct transcription method will be used for the calculation of the optimal movement. The arising nonlinear programming problem will be solved by the SQP solver fmincon in MATLAB.

In Chapter 7 the basic energy-momentum scheme will serve as basis for the description of the mechanical optimal control problem. Consequently, the equations of motion contain constraints, which leads to differential-algebraic equations. The present approach will be employed within two examples. Firstly, the optimal control of an underactuated overhead crane as an example of a point mass system will be investigated. Secondly, the 3-link robot manipulator introduced earlier in Chapter 6 will be explored. Therein, the orientation of the involved three rigid bodies will be specified using directors. As in Chapter 6, the calculation of the optimal movement will be done by use of a direct transcription method. Furthermore, the arising nonlinear programming problem will be solved by the SQP solver fmincon in MATLAB. The results will be compared with those achieved by the approaches of Chapter 6.

Chapter 8 supplies a newly derived Hamiltonian conserving indirect optimal control method. Based on observations in the forward dynamics case, namely the consistency of the discrete energy, similarities will be studied in the optimal control case, leading to the conservation of the underlying discrete Hamiltonian. It is well known that the Hamiltonian is conserved along an optimal solution in the continuous case. For reaching the same in the discrete case, a special midpoint evaluation of the costate equations, respectively a consistent variant thereof, turns out to be necessary. Notice that the midpoint evaluation of the state equations leads to a trapezoidal evaluation of the costate equations within a direct transcription method. Finally, it will be shown that for systems with

one degree of freedom a formula can be applied for the costate equations, which is inspired by the Greenspan formula introduced in Greenspan [55] for the state equations. Systems with several degrees of freedom necessitate a formula which has similarities to the discrete derivative introduced in Gonzalez [53] for the state equations.

2. Basics of optimal control

In the last 50 years a large number of methods have been developed for solving nonlinear optimal control problems. Since analytical solutions for optimal control problems only exist for special cases, the application of numerical methods is of decisive importance. A major distinguishing feature for numerical optimal control methods is the way in which the necessary conditions of optimality are derived. One possibility is deriving the continuous necessary conditions of optimality first and discretizing them afterwards. This approach yields an indirect optimal control method. The basics for an indirect method will be given in this chapter. A special indirect method, which inherits essential features from the continuous optimal control problem, will be introduced in Chapter 8. However, most of the recent works are based on direct optimal control methods. To derive a direct optimal control method, the equations of motion will be discretized first before formulating the optimal control problem. Based on fundamentals given in this chapter, examples of direct methods will be introduced in Chapters 6 and 7.

Three different direct numerical optimal control methods are commonly utilized in recent works. Collocation or transcription methods can be found for example in the works of Betts and co-workers [24, 23] or Stryk & Bulirsch [104]. An alternative approach is given by the multiple shooting method introduced in Bock & Plitt [27]. Additionally, the single shooting method can be mentioned which can be found in Hicks & Ray [63]. Transcription will be the method of choice in this thesis in the later Chapters 6, 7, and 8.

While, of course, several ways for describing the dynamics of a mechanical system exist, in this chapter no differences will be made between the possible formulations. The mechanical system may be described by differential-algebraic equations (DAEs). Optimal control of multibody systems described with equations of motion in DAE-form have been rarely investigated in the past. Notable exceptions are the works of Bottasso et al. [32], Bottasso & Croce [31], von Schwerin [102], and Kraus et al. [65]. In this thesis, the DAE-based optimal control of multibody systems will be the topic of Chapter 7. In most of the works, pure differential equations have been used for describing the mechanical systems. Those ordinary differential equations may result from the well known generalized coordinates formulation. Alternatively, a reduction process from a redundant formulation based on DAEs can be applied to eliminate the algebraic constraints in the discrete setting. In the context of multibody systems, the mentioned reduction process has been introduced in the work of Betsch & Leyendecker [11] and will be illustrated in Chapter 3 in more detail. Within

optimal control problems, this method has been applied in Leyendecker et al. [77] and Betsch et al. [13]. In this thesis, the latter will be the topic of Chapter 6.

2.1. Continuous optimal control

First of all, a dynamical system will be considered, which, for generality, can be described by a set of differential-algebraic equations

$$\mathbf{0} = \boldsymbol{f}(\boldsymbol{x}, \dot{\boldsymbol{x}}, \boldsymbol{u}) \tag{2.1}$$

where $\boldsymbol{x}$ is the state vector, which may contain the configuration vector, the velocity vector, and the vector of Lagrange-multipliers, $\boldsymbol{u}$ is the control vector and a superposed dot denotes differentiation with respect to time. The size of the state vector $\boldsymbol{x}$ is equal to the number of equations of motion in Eq. (2.1) and will be specified later for the different time-stepping schemes in Chapter 3. Additionally, suppose that the system is subjected to inequality constraints of the form

$$\mathbf{0} \geq \boldsymbol{c}(\boldsymbol{x}, \boldsymbol{u}) \tag{2.2}$$

Here, the differential-algebraic equations as well as the inequality constraints will be valid for a given time interval $I = [t_0, t_f]$ with fixed final time t_f. In this work, the problem of optimal control is to determine the states $\boldsymbol{x}$ and the controls $\boldsymbol{u}$ that minimize a cost function of the form

$$\mathfrak{J} = \int_{t_0}^{t_f} \mathcal{L}(\boldsymbol{u}) \, dt \tag{2.3}$$

where the integral costs only depend on the controls $\boldsymbol{u}$ and will be specified later in Section 6.1. To achieve proper conditions for optimality, one has to define an augmented cost function by adjoining the equations of motion in Eq. (2.1) as well as the inequality constraints given by Eq. (2.2) to the cost function in Eq. (2.3) through the use of Lagrange-multipliers $\boldsymbol{\lambda}^f$ respectively $\boldsymbol{\lambda}^c$ and the final conditions for the dynamical system

$$\boldsymbol{\psi}(\boldsymbol{x}(t_f)) = \mathbf{0} \tag{2.4}$$

by use of the Lagrange-multipliers $\boldsymbol{\mu}$. The continuous augmented cost function then takes the form

$$\tilde{\mathfrak{J}} = \boldsymbol{\mu} \cdot \boldsymbol{\psi}(\boldsymbol{x}(t_f)) + \int_{t_0}^{t_f} \mathcal{L}(\boldsymbol{u}) + \begin{bmatrix} \boldsymbol{\lambda}^f \\ \boldsymbol{\lambda}^c \end{bmatrix} \cdot \begin{bmatrix} \boldsymbol{f}(\boldsymbol{x}, \dot{\boldsymbol{x}}, \boldsymbol{u}) \\ \boldsymbol{c}(\boldsymbol{x}, \boldsymbol{u}) \end{bmatrix} \, dt \tag{2.5}$$

Calculating the derivatives of $\tilde{\mathfrak{J}}$ with respect to all independent variables and setting them to zero yields the necessary conditions of optimality (NCO), which consist of the equations of motion in Eq. (2.1) together with the inequality constraints in Eq. (2.2) as state equations, the costate equations, the control equations and the final conditions. The NCO may serve as basis for an indirect optimal control method.

Conservation of the Hamiltonian The general continuous equations of motion, which have been introduced in Eq. (2.1), can alternatively be presented in the form

$$\boldsymbol{C}\,\dot{\boldsymbol{x}} = \bar{\boldsymbol{f}}(\boldsymbol{x}, \boldsymbol{u}) \tag{2.6}$$

where the constant diagonal-matrix $\boldsymbol{C}$ consists of ones and zeros on its diagonal, depending on the number of differential respectively algebraic equations. Here, the inequality constraints are, for the sake of simplicity, neglected. Thus, the upper index in the Lagrange-multipliers is unnecessary at this point and will be left out. The continuous Hamiltonian is defined by

$$\mathcal{H}(\boldsymbol{x}, \boldsymbol{u}, \boldsymbol{\lambda}) = -\mathcal{L}(\boldsymbol{u}) + \boldsymbol{\lambda} \cdot \bar{\boldsymbol{f}}(\boldsymbol{x}, \boldsymbol{u}) \tag{2.7}$$

and can be used for deriving the continuous necessary conditions of optimality (NCO), which take the form

$$\begin{aligned} \boldsymbol{0} &= \boldsymbol{C}\,\dot{\boldsymbol{x}} - \bar{\boldsymbol{f}}(\boldsymbol{x}, \boldsymbol{u}) \\ \boldsymbol{0} &= \boldsymbol{C}\,\dot{\boldsymbol{\lambda}} + \nabla_{\boldsymbol{x}}\mathcal{H}(\boldsymbol{x}, \boldsymbol{u}, \boldsymbol{\lambda}) \\ \boldsymbol{0} &= \nabla_{\boldsymbol{u}}\mathcal{H}(\boldsymbol{x}, \boldsymbol{u}, \boldsymbol{\lambda}) \end{aligned} \tag{2.8}$$

They consist of the equations of motion as state equations in Eq. $(2.8)_1$, the costate equations in Eq. $(2.8)_2$ and the control equations in Eq. $(2.8)_3$. Fulfilment of the NCO involves conservation of the Hamiltonian, which can be proven in the following way:

$$\begin{aligned} \dot{\mathcal{H}}(\boldsymbol{x}, \boldsymbol{u}, \boldsymbol{\lambda}) &= \nabla_{\boldsymbol{x}}\mathcal{H}(\boldsymbol{x}, \boldsymbol{u}, \boldsymbol{\lambda}) \cdot \dot{\boldsymbol{x}} + \nabla_{\boldsymbol{u}}\mathcal{H}(\boldsymbol{x}, \boldsymbol{u}, \boldsymbol{\lambda}) \cdot \dot{\boldsymbol{u}} + \nabla_{\boldsymbol{\lambda}}\mathcal{H}(\boldsymbol{x}, \boldsymbol{u}, \boldsymbol{\lambda}) \cdot \dot{\boldsymbol{\lambda}} \\ &= -\boldsymbol{C}\,\dot{\boldsymbol{\lambda}} \cdot \dot{\boldsymbol{x}} + \boldsymbol{0} \cdot \dot{\boldsymbol{u}} + \bar{\boldsymbol{f}}(\boldsymbol{x}, \boldsymbol{u}) \cdot \dot{\boldsymbol{\lambda}} \\ &= -\boldsymbol{C}\,\dot{\boldsymbol{\lambda}} \cdot \dot{\boldsymbol{x}} + \boldsymbol{C}\,\dot{\boldsymbol{x}} \cdot \dot{\boldsymbol{\lambda}} \\ &= 0 \end{aligned} \tag{2.9}$$

Here, the NCO in Eq. (2.8) and the definition of the Hamiltonian in Eq. (2.7) have been employed.

2.2. Discrete optimal control

First of all, some fundamental words have to be said about the discretization applied in this work. The whole time interval $I = [t_0, t_f]$ will be divided into N time intervals $[t_k, t_{k+1}]$, which, to simplify matters, all have the time step size $h = t_{k+1} - t_k$. The discretization yields $N+1$ discretization points or time nodes for the evaluation of the state vector $\boldsymbol{x}_k$ $(k = 0, ..., N)$. The size of the discrete state vectors is equal to the size of the corresponding continuous quantities. This convention of notation will be used even if parts of the state vectors are not evaluated at the time nodes in a specific time-stepping scheme, which is valid in the case of Lagrange-multipliers arising in the equations of motion. Thus, the discrete state vectors sometimes contain components which do not appear in

the equations of motion and consequently do not affect the optimization process. Furthermore, the starting states $\boldsymbol{x}_0$ will be incorporated directly in the equations of motion, the final states $\boldsymbol{x}_f$ will be enforced through final conditions

$$\boldsymbol{\psi}(\boldsymbol{x}_N) = \boldsymbol{0} \tag{2.10}$$

The time derivative of the state vector $\dot{\boldsymbol{x}}$ will be approximated with the difference quotient, thus

$$\dot{\boldsymbol{x}}_{k,k+1} \approx \frac{1}{h}(\boldsymbol{x}_{k+1} - \boldsymbol{x}_k) \tag{2.11}$$

Lagrange-multipliers $\boldsymbol{\lambda}^f_{k,k+1}$ respectively $\boldsymbol{\lambda}^c_{k,k+1}$ $(k = 0, ..., N-1)$ have to be introduced for enforcing the discretized differential parts of the state equations as well as those inequality constraints which are appropriate for the components of the states $\boldsymbol{x}_{k,k+1}$ and the control forces $\boldsymbol{u}_{k,k+1}$. Additionally, Lagrange-multipliers $\boldsymbol{\lambda}^f_{k+1}$ respectively $\boldsymbol{\lambda}^c_{k+1}$ $(k = 0, ..., N-1)$ will be introduced for those algebraic equality and inequality constraints which are appropriate for the components of the configuration vector at the $N+1$ time discretization points. Again, the size of the discrete Lagrange-multipliers is equal to the size of the corresponding continuous quantities. Obviously, only a selection of the discrete Lagrange-multipliers are really applied later in the optimization process. If the continuous state equations contain algebraic constraints, the states $\boldsymbol{x}_{k,k+1}$ have to be introduced for the Lagrange-multipliers. As before, the size of the discrete state vectors is equal to the size of the corresponding continuous quantities. Again, only some parts of these discrete state vectors are really needed in the equations of motion and thus in the optimization process. If the corresponding continuous state equations do not contain algebraic constraints, those states can be neglected. Furthermore, the states $\boldsymbol{x}_{k,k+1}$, the control forces $\boldsymbol{u}_{k,k+1}$, and the Lagrange-multipliers $\boldsymbol{\lambda}^f_{k,k+1}$ respectively $\boldsymbol{\lambda}^c_{k,k+1}$ $(k = 0, ..., N-1)$ are assumed to be constant on each of the N time intervals.

At this point, the discrete analogy of the procedure given in Section 2.1 will be introduced. The general form of the discrete equations of motion and the discrete inequality constraints is given by

$$\boldsymbol{0} = \boldsymbol{f}(\boldsymbol{x}_k, \boldsymbol{x}_{k+1}, \boldsymbol{x}_{k,k+1}, \boldsymbol{u}_{k,k+1}) \tag{2.12}$$

respectively

$$\boldsymbol{0} \geq \boldsymbol{c}(\boldsymbol{x}_{k+1}, \boldsymbol{x}_{k,k+1}, \boldsymbol{u}_{k,k+1}) \tag{2.13}$$

thus depend only on the state vectors $\boldsymbol{x}_k$ and $\boldsymbol{x}_{k+1}$ at the limits of each time interval, and the state vector $\boldsymbol{x}_{k,k+1}$ as well as the control vector $\boldsymbol{u}_{k,k+1}$, which are assumed to be constant on each time interval. The number of discrete states $\boldsymbol{x}_{k+1}$ and $\boldsymbol{x}_{k,k+1}$ which are really involved as unknowns in the equations of motion is equal to the number of discrete equations of motion in Eq. (2.12). In a discrete optimal control problem, the states and controls have to be determined such that the discrete cost function

$$\mathfrak{J}^d = \sum_{k=0}^{N-1} \mathcal{L}(\boldsymbol{u}_{k,k+1}) \cdot h \tag{2.14}$$

will be minimized. This is the discrete analogon of the continuous version in Eq. (2.3). To achieve proper discrete necessary conditions for optimality, one has to define a discrete augmented cost function by adjoining the discrete equations of motion given in Eq. (2.12) as well as the discrete inequality constraints given in Eq. (2.13) to the discrete cost function in Eq. (2.14). This will be done by introduction of the abbreviations $\bar{\boldsymbol{\lambda}}^f$ and $\bar{\boldsymbol{\lambda}}^c$ which contain all of the arising necessary components of the Lagrange-multipliers. Obviously, the number of components of those vectors has to be equal to the number of equations in Eq. (2.12), respectively inequalities in Eq. (2.13). Additionally, Lagrange-multipliers $\boldsymbol{\mu}$ are required for the final conditions of the dynamical system in Eq. (2.10). Finally, the discrete augmented cost function takes the form

$$\tilde{\mathfrak{J}}^d = \boldsymbol{\mu} \cdot \boldsymbol{\psi}(\boldsymbol{x}_N) + \sum_{k=0}^{N-1} \mathcal{L}(\boldsymbol{u}_{k,k+1}) \cdot h + \begin{bmatrix} \bar{\boldsymbol{\lambda}}^f \\ \bar{\boldsymbol{\lambda}}^c \end{bmatrix} \cdot \begin{bmatrix} \boldsymbol{f}(\boldsymbol{x}_k, \boldsymbol{x}_{k+1}, \boldsymbol{x}_{k,k+1}, \boldsymbol{u}_{k,k+1}) \\ \boldsymbol{c}(\boldsymbol{x}_{k+1}, \boldsymbol{x}_{k,k+1}, \boldsymbol{u}_{k,k+1}) \end{bmatrix} \tag{2.15}$$

Calculating partial derivatives of $\tilde{\mathfrak{J}}^d$ and setting them to zero yield the discrete necessary conditions of optimality (DNCO). The optimality conditions which are calculated with this proceeding, serve as basis for direct optimal control approaches.

Conservation of the discrete Hamiltonian The general discrete equations of motion, which have been introduced in Eq. (2.12), can alternatively be presented in the form

$$\boldsymbol{C} \cdot \frac{1}{h}(\boldsymbol{x}_{k+1} - \boldsymbol{x}_k) = \bar{\boldsymbol{f}}(\boldsymbol{x}_k, \boldsymbol{x}_{k+1}, \boldsymbol{x}_{k,k+1}, \boldsymbol{u}_{k,k+1}) \tag{2.16}$$

As in the continuous case, the inequality constraints are, for the sake of simplicity, neglected. Again, the upper index in the Lagrange-multiplier is unnecessary from now on. Furthermore, the discrete Hamiltonian is defined by

$$\mathcal{H}^d_{k,k+1} = -\mathcal{L}(\boldsymbol{u}_{k,k+1}) + \bar{\boldsymbol{\lambda}} \cdot \bar{\boldsymbol{f}}(\boldsymbol{x}_k, \boldsymbol{x}_{k+1}, \boldsymbol{x}_{k,k+1}, \boldsymbol{u}_{k,k+1}) \tag{2.17}$$

and can be used for deriving the discrete necessary conditions of optimality (DNCO), which take the form

$$\begin{aligned} \boldsymbol{0} &= \boldsymbol{C} \cdot \frac{1}{h}(\boldsymbol{x}_{k+1} - \boldsymbol{x}_k) - \bar{\boldsymbol{f}}(\boldsymbol{x}_k, \boldsymbol{x}_{k+1}, \boldsymbol{x}_{k,k+1}, \boldsymbol{u}_{k,k+1}) \\ \boldsymbol{0} &= \boldsymbol{C} \cdot \frac{1}{h}(\boldsymbol{\lambda}_{k,k+1} - \boldsymbol{\lambda}_{k-1,k}) + (\nabla_{\boldsymbol{x}} \mathcal{H}^d)_{k-1,k,k+1} \\ \boldsymbol{0} &= \nabla_{\boldsymbol{u}} \mathcal{H}(\boldsymbol{x}_k, \boldsymbol{x}_{k+1}, \boldsymbol{u}_{k,k+1}, \boldsymbol{\lambda}_{k,k+1}) \end{aligned} \tag{2.18}$$

where the first term in Eq. $(2.18)_2$ can be interpreted as an approximation of the first term in Eq. $(2.8)_2$ by a difference quotient. Notice that the assumed constant time step size is mandatory for the application of the difference quotient for this term. The second term in Eq. $(2.18)_2$ can be obtained by differentiating the discrete Hamiltonian of a specific time step with respect to $\boldsymbol{x}_{k+1}$ and $\boldsymbol{x}_{k,k+1}$ and the discrete Hamiltonian of the following time step with respect to $\boldsymbol{x}_k$ and $\boldsymbol{x}_{k-1,k}$. Consequently, the second term in Eq. $(2.18)_2$ may depend on all of the

discrete quantities arising within two consecutive time steps. Finally, the DNCO consist of the discrete equations of motion as state equations in Eq. $(2.18)_1$, the discrete costate equations in Eq. $(2.18)_2$ and the discrete control equations in Eq. $(2.18)_3$.

In the continuous case, fulfilment of the NCO involves conservation of the Hamiltonian. In the discrete case, fulfilment of the DNCO generally yields conservation of the discrete Hamiltonian only in the limit case of vanishing time step sizes. However, in some cases, a special discretization of the NCO can be found which yields conservation of the discrete Hamiltonian even for large time step sizes, that is

$$\mathcal{H}^d_{k,k+1} = \mathcal{H}^d_{k-1,k} \tag{2.19}$$

This desirable feature can be seen as analogy to the energy consistency in forward dynamics problems, which leads to unconditional numerical stability of the corresponding integrators. Similar benefits can be expected from the mentioned Hamiltonian conserving discretizations of the NCO. Investigations concerning this topic will be done later in Chapter 8.

2.3. Review of numerical optimal control methods

In the current section, pros and cons of practical optimal control problems taken mainly from the surveys of Betts [21], Binder et al. [25], and Diehl [41] will be outlined. Concerning this matter, main focus will be on indirect optimal control methods based on the calculus of variations as well as the most practical direct optimal control methods, direct collocation and direct multiple shooting. Further methods have been investigated in the past. Dynamic programming seems to have only little practical applicability due to the so-called 'curse of dimensionality' (see, for example, Diehl et al. [42]). Furthermore, the essential drawback of single shooting methods is the sensitivity of the method regarding to the chosen initial guess. Small changes early in the trajectory can produce large errors at the end of the trajectory. Consequently, the review will be restricted on three types of practical optimal control methods.

Indirect optimal control methods Mainly three differing types of indirect optimal control methods based on the Pontryagin maximum principle have been further investigated in the past. Among them are gradient methods, indirect multiple shooting, and indirect collocation. Several practical drawbacks of indirect methods in comparison to direct methods can be mentioned. Analytical expressions of all arising gradients have to be provided for an indirect method. This makes it necessary that the user of an indirect method has knowledge and experience in the solution of optimal control problems. Additionally, indirect methods require suitable initial guesses for the states and the costates to start the iterative process (see Binder et al. [25]). However, indirect optimal control

methods provide a large freedom for the way the costate equations will be discretized. In this regard, a discretization of the costate equations can be found which yields a numerical method with the beneficial property that the discrete optimal control solution inherits basic properties from the corresponding continuous solution. An example of such an indirect method will be introduced in Chapter 8 of this thesis. It is worth mentioning that within direct optimal control methods such a special discretization of the costate equations is not feasible. In particular, the midpoint-type evaluation of the state equations automatically yields a trapezoidal-type evaluation of the costate equations. An additional midpoint-type evaluation of the costate equations, which in some cases leads to special conservation properties, is, apart from some very simple special cases, only feasible in indirect methods.

Direct collocation or direct transcription As a basic property of direct collocation or direct transcription methods, the simultaneous treatment of simulation and optimization can be stated. Following the process described in Section 2.2, the corresponding methods are based on formulating the discrete augmented cost function with discrete equations of motion as nonlinear constraints. While those constraints can be violated during the optimization procedure, they have to be satisfied at the solution. This is a severe difference to the shooting methods treating simulation and optimization sequentially. As an important disadvantage of direct collocation methods, the very large number of equations and variables have to be mentioned. However, the needed gradients exhibit a very sparse structure which can be exploited for practical collocation methods. Initial guesses of the states for the whole time interval are needed which can be seen as advantage, if knowledge of the states is available. As a crucial advantage in comparison to single shooting methods, the possibility of treating highly unstable systems as well as inequality constraints and active set changes can be stated. Furthermore, the discrete costates present in direct collocation are reliable estimates for the costates of the corresponding continuous optimal control problem. Secondary, informations about the switching structure can be obtained. Hence, those informations received from the discrete optimal control problem can be exploited for highly accurate indirect optimal control methods. In this regard, the hybrid approach introduced in Stryk & Bulirsch [104] combines direct collocation with indirect multiple shooting. Direct collocation will be the direct method of choice in the Chapters 6 and 7 of this thesis.

Direct multiple shooting While a detailed description of direct multiple shooting methods can be found in the literature (see, for example, Bock & Plitt [27] and Leineweber et al. [72, 73]), the following text restricts itself on basic properties as well as the pros and cons of direct multiple shooting in contrast to direct collocation. Correspondingly, direct multiple shooting methods treat simulation and optimization sequentially in each of the shooting segments and simultaneously on the whole time interval. Hence, direct multiple shooting can be seen as a hybrid method combining properties of direct single shooting and direct

collocation. In comparison to direct collocation, the arising system of equations in direct multiple shooting is of lower dimension, but has a less sparse structure, which may yield increased computational costs. In each of the shooting segments, direct multiple shooting methods behave like direct single shooting methods with all of the pros and cons. As written in the works of Diehl and co-workers [43, 42] the major advantage of direct multiple shooting compared to direct collocation is the possibility of using adaptive, error controlled solvers for the state equations in each of the shooting intervals. The use of adaptivity in state-of-the-art ODE or DAE solvers typically yields an increased accuracy. Additionally, the method is well suited for parallel computing, since the solution of the simulation problem is decoupled from the calculation of the derivatives on different multiple shooting segments. However, direct multiple shooting will not be the method of choice in this work.

3. Equations of motion

In a first step, the equations of motion in the so-called rotationless formulation take the form of differential-algebraic equations (DAEs) with index 3. Equations of motion specified with DAEs were rarely used in the past for the formulation of optimal control problems in multibody dynamics. Notable exceptions are the works of Bottasso et al. [32], Bottasso & Croce [31], von Schwerin [102], and Kraus et al. [65]. In the present work, the DAEs will serve as basis for the formulation of the optimal control problems in Chapter 7. The discretization of the equations of motion will be done by application of an energy and angular momentum consistent integrator.

In a first step, however, equations of motion obtained by a reduction process will be applied. This leads to a formulation of the equations of motion with eliminated algebraic constraints in the discrete setting. In particular, the discrete null space method with nodal reparametrization (see Betsch & Leyendecker [11] and Betsch & Uhlar [19]) will be employed. The reduced equations of motion will be applied in Chapter 6 within optimal control problems. This has been done previously in the work of Leyendecker et al. [77]. In contrast to the aforementioned work, where a variational integrator leading to angular momentum consistency has been used, in this work, an energy and angular momentum consistent time-stepping scheme will be applied.

Finally, those optimal control formulations based on the discrete null space method with nodal reparametrization will be compared with optimal control problems based on the widely-used generalized coordinates. The corresponding formulation of the equations of motion can also be achieved by a reduction process from the rotationless formulation. In contrast to the discretizations mentioned before, the discretization of the generalized coordinates formulation will neither be energy nor angular momentum consistent.

3.1. Dynamics of constrained mechanical systems with size reduction

In the present work, discrete mechanical systems subject to constraints which are holonomic and scleronomic will be considered. Due to the specific rotationless formulation employed in this work, the equations of motion for multibody

systems can be written in the form of Eq. (2.1). In particular,

$$\boldsymbol{f}(\boldsymbol{x}, \dot{\boldsymbol{x}}, \boldsymbol{u}) = \begin{bmatrix} \dot{\boldsymbol{q}} - \boldsymbol{v} \\ \boldsymbol{M}\dot{\boldsymbol{v}} + \boldsymbol{F}_{\text{int}} + \boldsymbol{F}_{\text{ext}} \\ \boldsymbol{\Phi}(\boldsymbol{q}) \end{bmatrix} \tag{3.1}$$

with the vector of internal forces

$$\boldsymbol{F}_{\text{int}} = \boldsymbol{G}(\boldsymbol{q})^T \boldsymbol{\gamma} + \boldsymbol{B}(\boldsymbol{q})^T \boldsymbol{a}(\boldsymbol{q}, \boldsymbol{v}) \tag{3.2}$$

and the vector of external forces

$$\boldsymbol{F}_{\text{ext}} = \nabla_{\boldsymbol{q}} \boldsymbol{V} + \boldsymbol{B}(\boldsymbol{q})^T \boldsymbol{u} \tag{3.3}$$

where $\boldsymbol{q} \in \mathbb{R}^n$ is the configuration vector and $\boldsymbol{v} \in \mathbb{R}^n$ the velocity vector.

As mentioned before, an essential property of the rotationless formulation, which, beside the generalized coordinates formulation, will be applied in this work, is the constant and symmetric mass matrix $\boldsymbol{M} \in \mathbb{R}^{n \times n}$. Using this mass matrix, the kinetic energy can be written as

$$T(\dot{\boldsymbol{q}}) = \frac{1}{2} \dot{\boldsymbol{q}} \cdot \boldsymbol{M} \dot{\boldsymbol{q}} \tag{3.4}$$

Here, the gradient of the potential energy $\nabla_{\boldsymbol{q}} \boldsymbol{V} \in \mathbb{R}^n$ is assumed to be constant, which is the case if it is a pure gravitational force.

Moreover, $\boldsymbol{\Phi}(\boldsymbol{q}) \in \mathbb{R}^m$ is a vector of geometric constraint functions, $\boldsymbol{G}(\boldsymbol{q}) = \nabla_{\boldsymbol{q}} \boldsymbol{\Phi}(\boldsymbol{q}) \in \mathbb{R}^{m \times n}$ the corresponding constraint Jacobian, and $\boldsymbol{\gamma} \in \mathbb{R}^m$ the vector of Lagrange-multipliers. The configuration space of the system is given by

$$Q = \{ \boldsymbol{q} \in \mathbb{R}^n \mid \boldsymbol{\Phi}(\boldsymbol{q}) = \boldsymbol{0} \} . \tag{3.5}$$

The geometric constraints give rise to kinematic constraints, which follow from the consistency condition $\dot{\boldsymbol{\Phi}} = \boldsymbol{0}$ on velocity level. Accordingly, the kinematic constraints assume the formulation

$$\boldsymbol{G}(\boldsymbol{q}) \boldsymbol{v} = \boldsymbol{0} \tag{3.6}$$

Suppose the matrix $\boldsymbol{P}(\boldsymbol{q}) \in \mathbb{R}^{n \times (n-m)}$ is the null space matrix corresponding to the Jacobian $\boldsymbol{G}$, that is the equation

$$\boldsymbol{G}(\boldsymbol{q}) \boldsymbol{P}(\boldsymbol{q}) = \boldsymbol{0} \tag{3.7}$$

is valid. Admissible velocities $\boldsymbol{v} \in T_{\boldsymbol{q}} Q$ may be written in the form

$$\boldsymbol{v} = \boldsymbol{P}(\boldsymbol{q}) \boldsymbol{\nu} \tag{3.8}$$

with independent, generalized velocities $\boldsymbol{\nu} \in \mathbb{R}^{n-m}$. While the null space matrix $\boldsymbol{P}$ can be employed for calculating the redundant velocities $\boldsymbol{v}$ from the generalized

velocities $\boldsymbol{\nu}$, there is also need for a matrix $\boldsymbol{B}(\boldsymbol{q}) \in \mathbb{R}^{(n-m)\times n}$, which can be applied for the reverse way, that is

$$\boldsymbol{\nu} = \boldsymbol{B}(\boldsymbol{q})\boldsymbol{v} \tag{3.9}$$

Apparently, the equation

$$\boldsymbol{B}(\boldsymbol{q})\boldsymbol{P}(\boldsymbol{q}) = \boldsymbol{I} \tag{3.10}$$

has to be valid for such a transformation matrix $\boldsymbol{B}$. Some examples of those matrices will be introduced later in Chapter 4. In particular, the transformation matrices for a single rigid body, for revolute pairs and for prismatic pairs will be elaborated. Some further kinematic pairs have been treated in Leyendecker et al. [77].

Next, the incorporation of friction forces as well as external control forces and torques into the rotationless formulation of the equations of motion will be treated. Starting point for the present consideration is the Rayleigh dissipation function given by

$$\mathcal{D}(\boldsymbol{\nu}) = \frac{1}{2}\boldsymbol{\nu} \cdot \boldsymbol{K}\boldsymbol{\nu} \tag{3.11}$$

In this term, $\boldsymbol{K} \in \mathbb{R}^{(n-m)\times(n-m)}$ is a matrix consisting of damping constants k_i on its diagonal. Calculating the partial derivative with respect to the generalized velocities yields the generalized friction forces

$$\boldsymbol{a}(\boldsymbol{\nu}) = \frac{\partial \mathcal{D}}{\partial \boldsymbol{\nu}} = \boldsymbol{K}\boldsymbol{\nu} \tag{3.12}$$

While Eq. (3.12) contains generalized velocities, the equations of motion given in Eq. (3.1) only contain redundant velocities. Hence, Eq. (3.9) has to be applied for the reformulation of the generalized friction forces by use of the redundant velocities. The generalized friction forces then take the form

$$\boldsymbol{a}(\boldsymbol{q}, \boldsymbol{v}) = \boldsymbol{K}\boldsymbol{B}(\boldsymbol{q})\boldsymbol{v} \tag{3.13}$$

Furthermore, by inserting Eq. (3.9) into the Rayleigh dissipation function in Eq. (3.11) and taking the partial derivative with respect to the redundant velocities, a representation of the redundant friction forces can be found. To specify, the redundant friction forces necessary for Eq. (3.1) can be computed by premultiplication of Eq. (3.13) by the transpose of the transformation matrix. In the same way, the redundant external control forces and torques appearing in the equations of motion given in Eq. (3.1) will be calculated from the corresponding generalized ones $\boldsymbol{u} \in \mathbb{R}^{n-m}$.

At this point, all matrices and vectors appearing in the equations of motion in Eq. (3.1) have been described. Summing up, these equations of motion specify a general mechanical multibody system containing forces and torques acting on the involved bodies and friction forces acting in the kinematic joints. Additionally, holonomic constraints for describing the system can be added. Finally, the

equations of motion given in Eq. (3.1) form a set of index-3 DAEs. Those equations of motion can be directly derived from the classical Lagrange equations of motion of the first kind.

To demonstrate the last statement, the augmented Lagrange function has to be formulated by

$$L(\boldsymbol{q}, \dot{\boldsymbol{q}}, \boldsymbol{\lambda}) = T(\dot{\boldsymbol{q}}) - V(\boldsymbol{q}) - \boldsymbol{\gamma} \cdot \boldsymbol{\Phi}(\boldsymbol{q}) \tag{3.14}$$

where the kinetic energy is given by Eq. (3.4), $V(\boldsymbol{q})$ is the potential energy, and the constraint function $\boldsymbol{\Phi}(\boldsymbol{q})$ will be incorporated through the use of the Lagrange-multipliers $\boldsymbol{\gamma}$. The Lagrange equations of motion of the first kind for a friction-afflicted multibody system with additional external forces generally take the form

$$\begin{aligned} \mathbf{0} &= \frac{d}{dt}\left(\frac{\partial L}{\partial \dot{\boldsymbol{q}}}\right) - \frac{\partial L}{\partial \boldsymbol{q}} + \frac{\partial \mathcal{D}}{\partial \dot{\boldsymbol{q}}} + \boldsymbol{B}(\boldsymbol{q})^T \boldsymbol{u} \\ \mathbf{0} &= \boldsymbol{\Phi}(\boldsymbol{q}) \end{aligned} \tag{3.15}$$

where the Rayleigh dissipation function is given in Eq. (3.11) and the last term is due to the external redundant control forces and torques. Calculating the derivatives yields

$$\begin{aligned} \mathbf{0} &= \boldsymbol{M}\ddot{\boldsymbol{q}} + \nabla_{\boldsymbol{q}} \boldsymbol{V} + \boldsymbol{G}(\boldsymbol{q})^T \boldsymbol{\gamma} + \boldsymbol{B}(\boldsymbol{q})^T \boldsymbol{a}(\boldsymbol{q}, \boldsymbol{v}) + \boldsymbol{B}(\boldsymbol{q})^T \boldsymbol{u} \\ \mathbf{0} &= \boldsymbol{\Phi}(\boldsymbol{q}) \end{aligned} \tag{3.16}$$

By inserting the additional relation $\boldsymbol{v} = \dot{\boldsymbol{q}}$, the final form of the Lagrange equations of motion of the first kind is given by

$$\begin{aligned} \mathbf{0} &= \dot{\boldsymbol{q}} - \boldsymbol{v} \\ \mathbf{0} &= \boldsymbol{M}\dot{\boldsymbol{v}} + \nabla_{\boldsymbol{q}} \boldsymbol{V} + \boldsymbol{G}(\boldsymbol{q})^T \boldsymbol{\gamma} + \boldsymbol{B}(\boldsymbol{q})^T \boldsymbol{a}(\boldsymbol{q}, \boldsymbol{v}) + \boldsymbol{B}(\boldsymbol{q})^T \boldsymbol{u} \\ \mathbf{0} &= \boldsymbol{\Phi}(\boldsymbol{q}) \end{aligned} \tag{3.17}$$

Obviously, the equations of motion in Eq. (3.17) coincide with those given in Eq. (3.1).

If the function $\boldsymbol{f}$ in Eq. (3.1) will be taken for the formulation of the optimal control problem, the state vector $\boldsymbol{x}$ consists of the configuration vector $\boldsymbol{q}$, the velocity vector $\boldsymbol{v}$ and the vector of Lagrange-multipliers $\boldsymbol{\gamma}$. Then, the function $\boldsymbol{f}$ has to be inserted into Eq. (2.1).

Size reduction To achieve a formulation of the equations of motion in purely differential form without any algebraic constraints, a size reduction consisting of two steps will be done in the following. Straightforward, by applying Eq. (3.8), a reduced form of the kinetic energy with a reduced mass matrix can be calculated.

Specifically, premultiplication by the transpose of the null space matrix $\boldsymbol{P}$ yields an alternative reduced formulation of the equations of motion consisting of the

$2n$ equations

$$\begin{aligned} \mathbf{0} &= \dot{\boldsymbol{q}} - \boldsymbol{v} \\ \mathbf{0} &= \boldsymbol{P}(\boldsymbol{q})^T \left\{ \boldsymbol{M}\dot{\boldsymbol{v}} + \boldsymbol{F}_{\text{int}} + \boldsymbol{F}_{\text{ext}} \right\} \\ \mathbf{0} &= \boldsymbol{\Phi}(\boldsymbol{q}) \end{aligned} \tag{3.18}$$

with the remaining parts of the vector of internal forces

$$\boldsymbol{F}_{\text{int}} = \boldsymbol{B}(\boldsymbol{q})^T \boldsymbol{a}(\boldsymbol{q}, \boldsymbol{v}) \tag{3.19}$$

and the vector of external forces given in Eq. (3.3).

A further size reduction can be done by expressing the redundant coordinates $\boldsymbol{q} \in \mathbb{R}^n$ in terms of local coordinates of minimal size $\boldsymbol{\theta} \in \mathbb{R}^{n-m}$, that is $\boldsymbol{q} = \boldsymbol{q}(\boldsymbol{\theta})$. Then, one of the possible null space matrices is equal to the Jacobian of the coordinate transformation, that is $\boldsymbol{P}(\boldsymbol{q}) = \nabla_{\boldsymbol{\theta}} \boldsymbol{q}(\boldsymbol{\theta})$. Since the constraints are fulfilled automatically due to the reparametrization, the system is reduced to $2n - m$ first-order differential equations. The function $\boldsymbol{f}$, which then has to be inserted into Eq. (2.1), takes the form

$$\boldsymbol{f}(\boldsymbol{x}, \dot{\boldsymbol{x}}, \boldsymbol{u}) = \begin{bmatrix} \dot{\boldsymbol{q}} - \boldsymbol{v} \\ \boldsymbol{P}(\boldsymbol{q})^T \left\{ \boldsymbol{M}\dot{\boldsymbol{v}} + \boldsymbol{F}_{\text{int}} + \boldsymbol{F}_{\text{ext}} \right\} \end{bmatrix} \tag{3.20}$$

where the internal and the external forces are given by Eq. (3.19) respectively Eq. (3.3). Here, the state vector $\boldsymbol{x}$ consists of the local coordinates $\boldsymbol{\theta}$ and the velocities $\boldsymbol{v}$. $\boldsymbol{\theta}$ can be used for the calculation of the configuration vector $\boldsymbol{q} = \boldsymbol{q}(\boldsymbol{\theta})$.

3.2. Basic and reduced energy-momentum scheme

Concerning the direct discretization of the equations of motion, the methodology developed by Gonzalez [53] will be employed. Consider the state space coordinates $\boldsymbol{q}_k \in Q$ and $\boldsymbol{v}_k \in \mathbb{R}^n$ at t_k, the discrete equations of motion for a representative time interval are given by Eq. (2.12). Specifically,

$$\boldsymbol{f}(\boldsymbol{x}_k, \boldsymbol{x}_{k+1}, \boldsymbol{x}_{k,k+1}, \boldsymbol{u}_{k,k+1}) = \begin{bmatrix} \boldsymbol{q}_{k+1} - \boldsymbol{q}_k - h\, \boldsymbol{v}_{k+\frac{1}{2}} \\ \boldsymbol{M}(\boldsymbol{v}_{k+1} - \boldsymbol{v}_k) + h(\boldsymbol{F}^d_{\text{int}} + \boldsymbol{F}^d_{\text{ext}}) \\ \boldsymbol{\Phi}(\boldsymbol{q}_{k+1}) \end{bmatrix} \tag{3.21}$$

with the vector of discrete internal forces

$$\boldsymbol{F}^d_{\text{int}} = \boldsymbol{G}(\boldsymbol{q}_{k+\frac{1}{2}})^T \boldsymbol{\gamma}_{k,k+1} + \boldsymbol{B}(\boldsymbol{q}^{k+\frac{1}{2}})^T \boldsymbol{a}(\boldsymbol{q}^{k+\frac{1}{2}}, \boldsymbol{v}_{k+\frac{1}{2}}) \tag{3.22}$$

and the vector of discrete external forces

$$\boldsymbol{F}^d_{\text{ext}} = \nabla_{\boldsymbol{q}} \boldsymbol{V} + \boldsymbol{B}(\boldsymbol{q}^{k+\frac{1}{2}})^T \boldsymbol{u}_{k,k+1} \tag{3.23}$$

where the Lagrange-multipliers $\boldsymbol{\gamma}_{k,k+1}$ are assumed to be constant in every time interval and $\boldsymbol{q}_{k+\frac{1}{2}} = (\boldsymbol{q}_{k+1}+\boldsymbol{q}_k)/2$ as well as $\boldsymbol{v}_{k+\frac{1}{2}} = (\boldsymbol{v}_{k+1}+\boldsymbol{v}_k)/2$. In the sequel, the above scheme will be called the basic energy-momentum scheme (BEM).

The advantageous algorithmic consistency properties, which are contained in the basic energy-momentum scheme, are linked to the special evaluation of the matrices in Eq. (3.21). As said before, the gradient of the potential energy is assumed to be constant, which makes a special evaluation unnecessary. The same is valid for the mass matrix in the rotationless formulation of multibody systems employed in this work. The constraint function $\boldsymbol{\Phi}$ here is at most quadratic. In that case, simple midpoint evaluation of the corresponding Jacobian $\boldsymbol{G}$ leads to the consistency of energy and angular momentum. If the formulation would involve a higher degree of nonlinearity, a formulation of the constraints $\boldsymbol{\Phi}$, the potential energy V and the kinetic energy T with quadratic invariants and application of the discrete gradient as introduced in Gonzalez [53] would be necessary.

The mass matrix necessary for formulating the kinetic energy is constant within the rotationless formulation based on natural coordinates, which contains direction cosines for describing the orientation of the rigid bodies. The corresponding rigid body formulation will be presented in Chapter 4. In contrast to this, the kinetic energy in the quaternion-based rigid body formulation contains a configuration dependent mass matrix. To obtain the advantageous algorithmic consistency properties in the quaternion-based rigid body formulation, a formulation of the kinetic energy with quadratic invariants and application of the discrete gradient introduced by Gonzalez in [53] will become necessary. Further details on that topic can be found in Chapter 5.

Concerning the rotationless formulation, additionally, a discrete null space matrix has to be found, which satisfies the following two properties:

- In the limit of vanishing time steps, the discrete version has to coincide with the continuous one. That is,

$$\boldsymbol{P}(\boldsymbol{q}_{k+\frac{1}{2}}) \rightarrow \boldsymbol{P}(\boldsymbol{q}_k) \text{ as } \boldsymbol{q}_{k+1} \rightarrow \boldsymbol{q}_k \tag{3.24}$$

- The discrete null space matrix $\boldsymbol{P}(\boldsymbol{q}_{k+\frac{1}{2}})$ has full rank and satisfies the equations

$$\boldsymbol{G}(\boldsymbol{q}_{k+\frac{1}{2}})\,\boldsymbol{P}(\boldsymbol{q}_{k+\frac{1}{2}}) = \boldsymbol{0} \tag{3.25}$$

  for $\boldsymbol{q}_{k+\frac{1}{2}} = (\boldsymbol{q}_k + \boldsymbol{q}_{k+1})/2$ with $\boldsymbol{q}_k, \boldsymbol{q}_{k+1} \in Q$.

Analogously to the continuous case, discrete redundant velocities can be obtained by applying the formula

$$\boldsymbol{v}_{k+\frac{1}{2}} = \boldsymbol{P}(\boldsymbol{q}_{k+\frac{1}{2}})\boldsymbol{\nu}_{k,k+1} \tag{3.26}$$

where the quantity $\boldsymbol{\nu}_{k,k+1}$, which does not appear explicitly in the time-stepping scheme, can be interpreted as discrete generalized velocities. Conversely, the discrete generalized velocities needed for calculating the generalized friction forces

can be obtained by application of

$$\boldsymbol{\nu}_{k,k+1} = \boldsymbol{B}(\boldsymbol{q}^{k+\frac{1}{2}})\boldsymbol{v}_{k+\frac{1}{2}} \tag{3.27}$$

Obviously, the equation

$$\boldsymbol{B}(\boldsymbol{q}^{k+\frac{1}{2}})\boldsymbol{P}(\boldsymbol{q}_{k+\frac{1}{2}}) = \boldsymbol{I} \tag{3.28}$$

has to be valid in the discrete case for the transformation matrix $\boldsymbol{B}$. At this point, generalized friction forces can be obtained by applying the formula

$$\boldsymbol{a}(\boldsymbol{q}^{k+\frac{1}{2}}, \boldsymbol{v}_{k+\frac{1}{2}}) = \boldsymbol{K}\boldsymbol{B}(\boldsymbol{q}^{k+\frac{1}{2}})\boldsymbol{v}_{k+\frac{1}{2}} \tag{3.29}$$

It has to be pointed out that a special evaluation of the transformation matrix is necessary for achieving the intended algorithmic consistency properties. The mentioned special evaluation will be designated by the upper index in the configuration vector, that is $\boldsymbol{q}^{k+\frac{1}{2}}$. It is worth mentioning that the upper index in $\boldsymbol{q}^{k+\frac{1}{2}}$ does not denote a midpoint evaluation itself, but results from a nonlinear function $\bar{\boldsymbol{g}}$ of the midpoint evaluation $\boldsymbol{q}_{k+\frac{1}{2}}$, that is

$$\boldsymbol{q}^{k+\frac{1}{2}} = \bar{\boldsymbol{g}}(\boldsymbol{q}_{k+\frac{1}{2}}) \tag{3.30}$$

Further details on that topic will be given in Chapter 4 for a single rigid body as well as for kinematic pairs.

Finally, if the function $\boldsymbol{f}$ in Eq. (3.21) will be taken for the formulation of the optimal control problem the discrete state vector $\boldsymbol{x}_k$ contains the configuration vector $\boldsymbol{q}_k$ and the velocity vector $\boldsymbol{v}_k$ at the time discretization points. The additional part due to the Lagrange-multipliers $\boldsymbol{\gamma}_k$, which do not appear in the BEM, can be neglected for the optimization. Furthermore, the state vector $\boldsymbol{x}_{k,k+1}$ contains the vector of Lagrange-multipliers $\boldsymbol{\gamma}_{k,k+1}$ assumed to be constant in every time interval. The additional parts due the configuration vector $\boldsymbol{q}_{k,k+1}$ and the velocity vector $\boldsymbol{v}_{k,k+1}$ do not appear in the BEM, and thus can be neglected. Then, the function $\boldsymbol{f}$ has to be inserted into Eq. (2.12).

Reduced energy-momentum scheme (REM) Similar to the continuous reduction process given at the end of Section 3.1, now the discrete analogy will be devised. Premultiplication by the transpose of $\boldsymbol{P}(\boldsymbol{q}_{k+\frac{1}{2}})$ yields an alternative reduced formulation of the BEM consisting of the $2n$ equations

$$\begin{aligned}
\boldsymbol{0} &= \boldsymbol{q}_{k+1} - \boldsymbol{q}_k - h\, \boldsymbol{v}_{k+\frac{1}{2}} \\
\boldsymbol{0} &= \boldsymbol{P}(\boldsymbol{q}_{k+\frac{1}{2}})^T \left\{ \boldsymbol{M}(\boldsymbol{v}_{k+1} - \boldsymbol{v}_k) + h(\boldsymbol{F}^d_{\text{int}} + \boldsymbol{F}^d_{\text{ext}}) \right\} \\
\boldsymbol{0} &= \boldsymbol{\Phi}(\boldsymbol{q}_{k+1})
\end{aligned} \tag{3.31}$$

with the remaining parts of the vector of discrete internal forces

$$\boldsymbol{F}^d_{\text{int}} = \boldsymbol{B}(\boldsymbol{q}^{k+\frac{1}{2}})^T \boldsymbol{a}(\boldsymbol{q}^{k+\frac{1}{2}}, \boldsymbol{v}_{k+\frac{1}{2}}) \tag{3.32}$$

and the vector of discrete external forces in Eq. (3.23).

To achieve the favored formulation of the equations of motion without any constraints, a further reduction step has to be accomplished by a reparametrization of the remaining unknowns. For open-loop multibody systems, it is generally feasible to find a vector of local coordinates $\boldsymbol{\theta} \in \mathbb{R}^{n-m}$ which can be used for the parametrization of the configuration vectors $\boldsymbol{q}_k = \boldsymbol{q}(\boldsymbol{\theta}_k)$. Additionally, the discrete velocities can be calculated in every time step by applying the formula

$$\boldsymbol{v}_k(\boldsymbol{q}_0, ..., \boldsymbol{q}_k, \boldsymbol{v}_0) = (-1)^k \left\{ \frac{2}{h} \left[(-1)^k \boldsymbol{q}_k + 2 \sum_{i=1}^{k-1} (-1)^i \boldsymbol{q}_i + \boldsymbol{q}_0 \right] + \boldsymbol{v}_0 \right\} \tag{3.33}$$

which results from Eq. $(3.31)_1$. Notice that the discrete velocities depend on all configurations from t_0 to t_k. This has to be taken into account for the calculation of the derivatives (see Eq. (A.12) provided in Appendix A). Finally, only $n - m$ equations remain for the description of the mechanical system. The function $\boldsymbol{f}$ which then has to be inserted into Eq. (2.12) takes the form

$$\boldsymbol{f}(\boldsymbol{x}_k, \boldsymbol{x}_{k+1}, \boldsymbol{u}_{k,k+1}) = \boldsymbol{P}(\boldsymbol{q}_{k+\frac{1}{2}})^T \left\{ \boldsymbol{M}(\boldsymbol{v}_{k+1} - \boldsymbol{v}_k) + h(\boldsymbol{F}^d_{\text{int}} + \boldsymbol{F}^d_{\text{ext}}) \right\} \tag{3.34}$$

where the discrete internal and external forces are given by Eq. (3.32) respectively Eq. (3.23). Here, the discrete state vector $\boldsymbol{x}_k$ only consists of the local coordinates $\boldsymbol{\theta}_k$. $\boldsymbol{\theta}_k$ can be used for the calculation of both the configuration $\boldsymbol{q}_k = \boldsymbol{q}(\boldsymbol{\theta}_k)$ and the velocity $\boldsymbol{v}_k(\boldsymbol{q}_0, ..., \boldsymbol{q}_k, \boldsymbol{v}_0)$.

3.3. Connection with generalized coordinates

One of the main goals of this work is the comparison between the above described EM-schemes and the well-known generalized coordinates formulation. To establish the relation, the vector of generalized coordinates $\tilde{\boldsymbol{q}}$, together with its relation to the redundant coordinates

$$\boldsymbol{q} = \boldsymbol{q}(\tilde{\boldsymbol{q}}) \tag{3.35}$$

has to be found. Together with the null space matrix $\boldsymbol{P}$ introduced in Section 3.1, this relation can be used for the calculation of a null space matrix $\boldsymbol{P}(\tilde{\boldsymbol{q}})$. The same is valid for the transformation matrix $\boldsymbol{B}(\tilde{\boldsymbol{q}})$. The configuration dependent mass matrix $\tilde{\boldsymbol{M}}(\tilde{\boldsymbol{q}})$, which is necessary in the generalized coordinates formulation, can be obtained by applying the formula

$$\tilde{\boldsymbol{M}}(\tilde{\boldsymbol{q}}) = \boldsymbol{P}(\tilde{\boldsymbol{q}})^T \boldsymbol{M} \boldsymbol{P}(\tilde{\boldsymbol{q}}) \tag{3.36}$$

Additionally, a matrix $\dot{\boldsymbol{P}}(\tilde{\boldsymbol{q}}, \tilde{\boldsymbol{v}})$ containing the time derivatives of the components of $\boldsymbol{P}(\tilde{\boldsymbol{q}})$ has to be found. Both the gradient of the potential energy and the transformation matrix can be derived from the redundant formulation by premultiplication of the transpose of $\boldsymbol{P}(\tilde{\boldsymbol{q}})$.

Finally, the function $\boldsymbol{f}$ to be inserted into the continuous augmented cost function given in Eq. (2.5) takes the form

$$\boldsymbol{f}(\boldsymbol{x}, \dot{\boldsymbol{x}}, \boldsymbol{u}) = \begin{bmatrix} \dot{\tilde{\boldsymbol{q}}} - \tilde{\boldsymbol{v}} \\ \tilde{\boldsymbol{M}}(\tilde{\boldsymbol{q}}) \dot{\tilde{\boldsymbol{v}}} + \boldsymbol{P}(\tilde{\boldsymbol{q}})^T (\tilde{\boldsymbol{F}}_{\text{int}} + \tilde{\boldsymbol{F}}_{\text{ext}}) \end{bmatrix} \tag{3.37}$$

with the vector of internal forces

$$\tilde{\boldsymbol{F}}_{\text{int}} = \boldsymbol{B}(\tilde{\boldsymbol{q}})^T \boldsymbol{K} \tilde{\boldsymbol{v}} \tag{3.38}$$

and the vector of external forces

$$\tilde{\boldsymbol{F}}_{\text{ext}} = \boldsymbol{M}\dot{\boldsymbol{P}}(\tilde{\boldsymbol{q}}, \tilde{\boldsymbol{v}})\tilde{\boldsymbol{v}} + \nabla_{\boldsymbol{q}} \boldsymbol{V} + \boldsymbol{B}(\tilde{\boldsymbol{q}})^T \boldsymbol{u} \tag{3.39}$$

Eventually, the transition to the discrete setting will be done by applying the midpoint rule for the configuration vector $\tilde{\boldsymbol{q}}$ and the velocity $\tilde{\boldsymbol{v}}$.

The function $\boldsymbol{f}$, which then has to be inserted into Eq. (2.12), takes the form

$$\boldsymbol{f}(\boldsymbol{x}_k, \boldsymbol{x}_{k+1}, \boldsymbol{u}_{k,k+1}) = \begin{bmatrix} \tilde{\boldsymbol{q}}_{k+1} - \tilde{\boldsymbol{q}}_k - h\, \tilde{\boldsymbol{v}}_{k+\frac{1}{2}} \\ \tilde{\boldsymbol{M}}(\tilde{\boldsymbol{q}}_{k+\frac{1}{2}})(\tilde{\boldsymbol{v}}_{k+1} - \tilde{\boldsymbol{v}}_k) + h\, \boldsymbol{P}(\tilde{\boldsymbol{q}}_{k+\frac{1}{2}})^T (\tilde{\boldsymbol{F}}^d_{\text{int}} + \tilde{\boldsymbol{F}}^d_{\text{ext}}) \end{bmatrix} \tag{3.40}$$

with the vector of discrete internal forces

$$\tilde{\boldsymbol{F}}^d_{\text{int}} = \boldsymbol{B}(\tilde{\boldsymbol{q}}_{k+\frac{1}{2}})^T \boldsymbol{K} \tilde{\boldsymbol{v}}_{k+\frac{1}{2}} \tag{3.41}$$

and the vector of discrete external forces

$$\tilde{\boldsymbol{F}}^d_{\text{ext}} = \boldsymbol{M}\dot{\boldsymbol{P}}(\tilde{\boldsymbol{q}}_{k+\frac{1}{2}}, \tilde{\boldsymbol{v}}_{k+\frac{1}{2}})\tilde{\boldsymbol{v}}_{k+\frac{1}{2}} + \nabla_{\boldsymbol{q}} \boldsymbol{V} + \boldsymbol{B}(\tilde{\boldsymbol{q}}_{k+\frac{1}{2}})^T \boldsymbol{u}_{k,k+1} \tag{3.42}$$

In principle, the elimination of the velocities could be achieved similarly to the procedure illustrated in Section 3.2. However, the use of generalized coordinates complicates this size reduction significantly. Furthermore, the higher degree of nonlinearity in the generalized coordinates formulation complicates the calculation of the derivatives.

4. Rigid body dynamics

In the following, a short account of the rotationless formulation of spatial rigid body dynamics will be given. This approach is directly suitable for the extension to constrained multibody systems specified by the DAEs in Eq. (3.1). The rotationless formulation of rigid bodies is based on direction cosines. A key property is the constant and diagonal mass matrix, which is an important advantage of the rotationless formulation in comparison to the widely used classical Euler's equations for rigid bodies, where generalized coordinates are employed. Also quaternions where used often in the past (Haug [62], Nikravesh [85]). Although the quaternion formulation relies on less redundant coordinates, it exhibits a higher degree of nonlinearity (Betsch & Siebert [12]). Properties of the mentioned quaternion formulation of rigid body dynamics as well as the problematic extension to multibody systems will be described in Chapter 5 in detail. Further details on the rotationless formulation for multibody systems consisting of rigid components, which are investigated in this work, can be found in Betsch & Steinmann [16], Betsch & Leyendecker [11], Betsch & Uhlar [19] and Leyendecker et al. [77].

The present constrained formulation of rigid bodies as well as multibody systems relies on redundant coordinates. Both the internal constraints due to the rigidity of the bodies and the external constraints due to kinematic pairs turn out to be at most quadratic. This property has advantages for the advocated energy and momentum consistent integration (see Section 3.2).

Basically, the rotationless formulation does not contain rotational or translational degrees of freedom along with associated joint torques or forces. While in previous work an augmentation technique has been applied for the incorporation of such degrees of freedom (see, for example, Betsch & Uhlar [19] and Uhlar & Betsch [100]), this will not be preferred here. One of the disadvantages is the necessary additional components for the constraint function and the resultant more complicated gradients, which are known to be a crucial part of optimal control problems. Additionally, it has been shown that the augmentation technique used in Betsch & Uhlar [19] suffers from singularities (see Sänger et al. [93]). An alternative augmentation technique illustrated in Bottasso & Croce [31] seems not to be afflicted by singularities. However, the energy and angular momentum consistent discretization for this augmentation technique is a challenging task. In this work, a transformation matrix is used for the incorporation of the controls as previously done in Leyendecker et al. [77]. Additionally, this matrix is employed for the inclusion of linear viscous friction. To achieve the con-

sistency properties, a special evaluation of this matrix turns out to be required (see Betsch et al. [13]).

4.1. Spatial rigid body

In the present work, use will be made of twelve redundant coordinates for the description of the position and the orientation of the spatial rigid body depicted in Fig. 4.1. For one single rigid body, the vector of redundant coordinates is given by

$$\boldsymbol{q} = \begin{bmatrix} \boldsymbol{\varphi} \\ \boldsymbol{d}_1 \\ \boldsymbol{d}_2 \\ \boldsymbol{d}_3 \end{bmatrix} \tag{4.1}$$

where $\boldsymbol{\varphi} \in \mathbb{R}^3$ is the position vector of the center of mass and $\boldsymbol{d}_1, \boldsymbol{d}_2, \boldsymbol{d}_3$ are the directors, which constitute the columns of the rotation tensor $\boldsymbol{R} \in SO(3)$ and thus specify the orientation of the rigid body.

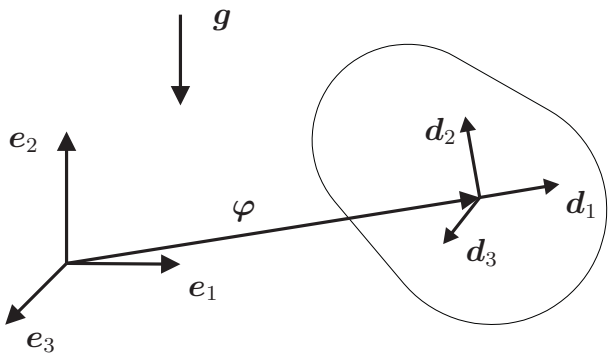

Figure 4.1.: Spatial rigid body

In the sequel, all of the coordinates are referred to a right-handed orthogonal basis $\{\boldsymbol{e}_1, \boldsymbol{e}_2, \boldsymbol{e}_3\}$, which plays the role of an inertial frame. The directors are assumed to constitute a right-handed body frame which coincides with the principal axes of the rigid body. Since the directors are fixed in the body and moving with it, they have to stay orthonormal for all times. This gives rise to six independent geometric (or holonomic) constraints $\Phi^i_{\text{int}}(\boldsymbol{q}) = 0$. The functions $\Phi^i_{\text{int}} : \mathbb{R}^{12} \to \mathbb{R}$ may be arranged in the vector of internal constraint functions

$$\boldsymbol{\Phi}_{\text{int}}(\boldsymbol{q}) = \begin{bmatrix} \frac{1}{2}(\boldsymbol{d}_1 \cdot \boldsymbol{d}_1 - 1) \\ \frac{1}{2}(\boldsymbol{d}_2 \cdot \boldsymbol{d}_2 - 1) \\ \frac{1}{2}(\boldsymbol{d}_3 \cdot \boldsymbol{d}_3 - 1) \\ \boldsymbol{d}_1 \cdot \boldsymbol{d}_2 \\ \boldsymbol{d}_1 \cdot \boldsymbol{d}_3 \\ \boldsymbol{d}_2 \cdot \boldsymbol{d}_3 \end{bmatrix} \tag{4.2}$$

With regard to the internal constraints, the configuration space of the free rigid body may now be written in the form

$$Q_{\text{free}} = \left\{ \boldsymbol{q} \in \mathbb{R}^{12} \mid \boldsymbol{\Phi}_{\text{int}}(\boldsymbol{q}) = \boldsymbol{0}, (\boldsymbol{d}_1 \times \boldsymbol{d}_2) \cdot \boldsymbol{d}_3 = +1 \right\} \tag{4.3}$$

The motion of the free rigid body can now be specified by means of the DAEs. In the following, it is for simplicity assumed that the axes of the body frame are aligned with the principal axes of the body. Accordingly, the mass matrix $\boldsymbol{M} \in \mathbb{R}^{12\times 12}$ is given by

$$\boldsymbol{M} = \begin{bmatrix} m\boldsymbol{I}_3 & \boldsymbol{0}_3 & \boldsymbol{0}_3 & \boldsymbol{0}_3 \\ \boldsymbol{0}_3 & \mathcal{E}_1\boldsymbol{I}_3 & \boldsymbol{0}_3 & \boldsymbol{0}_3 \\ \boldsymbol{0}_3 & \boldsymbol{0}_3 & \mathcal{E}_2\boldsymbol{I}_3 & \boldsymbol{0}_3 \\ \boldsymbol{0}_3 & \boldsymbol{0}_3 & \boldsymbol{0}_3 & \mathcal{E}_3\boldsymbol{I}_3 \end{bmatrix} \tag{4.4}$$

where m is the total mass of the rigid body and $\mathcal{E}_1, \mathcal{E}_2, \mathcal{E}_3$ are the principal values of the Euler tensor relative to the center of mass, which can be related to the classical polar momentum of inertia about the center of mass, $\boldsymbol{\mathcal{J}}$, via the relationship

$$\boldsymbol{\mathcal{J}} = (\text{tr}\boldsymbol{\mathcal{E}})\boldsymbol{I}_3 - \boldsymbol{\mathcal{E}} \tag{4.5}$$

If gravity is acting on the body, the potential energy reads

$$V(\boldsymbol{q}) = mg\, \boldsymbol{\varphi} \cdot \boldsymbol{e}_2 \tag{4.6}$$

where g is the gravitational acceleration. Furthermore, the constraint Jacobian corresponding to the free rigid body $\boldsymbol{G}_{\text{int}} = \nabla_q \boldsymbol{\Phi}_{\text{int}}(\boldsymbol{q})$ is given by

$$\boldsymbol{G}_{\text{int}}(\boldsymbol{q}) = \begin{bmatrix} \boldsymbol{0}^T & \boldsymbol{d}_1^T & \boldsymbol{0}^T & \boldsymbol{0}^T \\ \boldsymbol{0}^T & \boldsymbol{0}^T & \boldsymbol{d}_2^T & \boldsymbol{0}^T \\ \boldsymbol{0}^T & \boldsymbol{0}^T & \boldsymbol{0}^T & \boldsymbol{d}_3^T \\ \boldsymbol{0}^T & \boldsymbol{d}_2^T & \boldsymbol{d}_1^T & \boldsymbol{0}^T \\ \boldsymbol{0}^T & \boldsymbol{d}_3^T & \boldsymbol{0}^T & \boldsymbol{d}_1^T \\ \boldsymbol{0}^T & \boldsymbol{0}^T & \boldsymbol{d}_3^T & \boldsymbol{d}_2^T \end{bmatrix} \tag{4.7}$$

Additionally, the angular momentum of the rigid body with respect to the origin of the inertial frame is given by

$$\boldsymbol{J} = m\, \boldsymbol{\varphi} \times \dot{\boldsymbol{\varphi}} + \sum_{i=1}^{3} \mathcal{E}_i\, \boldsymbol{d}_i \times \dot{\boldsymbol{d}}_i \tag{4.8}$$

Similar to the procedure described in Section 3.1, a matrix with full column rank fulfilling Eq. (3.7) has to be found for the size reduction by the null space method. The matrix

$$\boldsymbol{P}_{\text{int}}(\boldsymbol{q}) = \begin{bmatrix} \boldsymbol{I}_3 & \boldsymbol{0}_3 \\ \boldsymbol{0}_3 & -\hat{\boldsymbol{d}}_1 \\ \boldsymbol{0}_3 & -\hat{\boldsymbol{d}}_2 \\ \boldsymbol{0}_3 & -\hat{\boldsymbol{d}}_3 \end{bmatrix} \tag{4.9}$$

perfectly qualifies as null space matrix. Here, the hat-vector matrix in the spatial case, which is needed for describing the null space matrix, is given by

$$\begin{bmatrix} \hat{a} \\ b \\ c \end{bmatrix} = \begin{bmatrix} 0 & -c & b \\ c & 0 & -a \\ -b & a & 0 \end{bmatrix} \tag{4.10}$$

and serves as alternative notation for the cross-product, that is $\hat{\boldsymbol{a}}\,\boldsymbol{b} = \boldsymbol{a} \times \boldsymbol{b}$.

Following the proceeding described at the end of Section 3.2, the first reduction step can be accomplished by premultiplication of the transpose of the null space matrix introduced in Eq. (4.9), which will be evaluated in the midpoint. A further reduction step has to be done by the reparametrization of the unknowns. For this aim, the rotation matrix has to be parametrized by the rotation vector $\boldsymbol{\theta} \in \mathbb{R}^3$. This can be done by application of the Rodrigues formula given by

$$\boldsymbol{R}(\boldsymbol{\theta}) = \exp(\hat{\boldsymbol{\theta}}) = \boldsymbol{I}_3 + \frac{\sin ||\boldsymbol{\theta}||}{||\boldsymbol{\theta}||}\,\hat{\boldsymbol{\theta}} + \frac{1}{2}\left(\frac{\sin\left(\frac{||\boldsymbol{\theta}||}{2}\right)}{\frac{||\boldsymbol{\theta}||}{2}}\right)^2 \hat{\boldsymbol{\theta}}^2 \tag{4.11}$$

The latter can be interpreted as closed form expression of the exponential map (see Marsden & Ratiu [79]). Consequently, the discrete directors can be calculated by

$$(\boldsymbol{d}_i)_k = \boldsymbol{R}(\boldsymbol{\theta})(\boldsymbol{d}_i)_0 \tag{4.12}$$

Notice that the application of Eq. (4.12) leads to absolute rotations. This is in contrast to previous work regarding the discrete null space method (Betsch & Leyendecker [11], Betsch & Uhlar [19]), where incremental rotations have been employed. This will be done for two reasons. Firstly, the use of absolute rotations has benefits concerning the boundary conditions on configuration level. In particular, the angles can be used directly without use of a representation by a sum, which would be necessary, if incremental rotations are used. Secondly, the application of incremental rotations would require the calculation of more complicated gradients, because, in that case, every configuration vector depends on every preceding incremental angle. The arising gradients then have a lower-diagonal structure instead of a diagonal structure, thus are much less sparse. However, it has to be stated that the formulation with absolute rotations may suffer from singularities, which is not the case for the formulation with incremental rotations.

At this point, the rotationless formulation for the dynamics of a spatial rigid body is completely given for the case of a conservative system. The content proposed so far is in agreement with the one given earlier for example in Betsch & Steinmann [16], Betsch [9], and Betsch & Leyendecker [11]. Obviously, mechanical systems which will be investigated within optimal control are nonconservative systems, that is, the systems are actuated by control forces and torques. Additionally, the systems may be afflicted by friction. For approaching those nonconservative systems, use will be made of a transformation matrix as previously done in Leyendecker et al. [77].

Incorporation of control torques and forces In the following, a few results concerning the control input will be assembled. Consider the single rigid body depicted in Fig. 4.2, which is actuated by control forces $\boldsymbol{u}_{\boldsymbol{\varphi}} \in \mathbb{R}^3$ directed towards the center of mass and control torques $\boldsymbol{u}_{\boldsymbol{\theta}} \in \mathbb{R}^3$. Notice that external control forces are not excluded, because the resulting forces can be split into those control forces $\boldsymbol{u}_{\boldsymbol{\varphi}} \in \mathbb{R}^3$ acting on the center of mass and control torques $\boldsymbol{u}_{\boldsymbol{\theta}} \in \mathbb{R}^3$. Assuming $\boldsymbol{u} = (\boldsymbol{u}_{\boldsymbol{\varphi}}, \boldsymbol{u}_{\boldsymbol{\theta}})$ as control vector and $\boldsymbol{B} = \boldsymbol{B}_{\text{int}}$ as transformation matrix suitable for the control input, the work of the control forces for this fully actuated rigid body is given by

$$W = \int_{t_0}^{t} \boldsymbol{u} \cdot \boldsymbol{\nu} \, dt = \int_{t_0}^{t} \boldsymbol{u} \cdot \boldsymbol{B}(\boldsymbol{q}) \, \boldsymbol{v} \, dt = \int_{t_0}^{t} (\boldsymbol{B}(\boldsymbol{q})^T \boldsymbol{u}) \cdot \boldsymbol{v} \, dt \tag{4.13}$$

where Eq. (3.9) has been applied. Notice that the generalized control forces and torques $\boldsymbol{u} \in \mathbb{R}^6$ and the generalized velocities $\boldsymbol{\nu} \in \mathbb{R}^6$ are work-conjugated. The same is valid for the corresponding redundant quantities, that is the redundant control forces and torques $\boldsymbol{B}(\boldsymbol{q})^T \boldsymbol{u} \in \mathbb{R}^{12}$ and the redundant velocities $\boldsymbol{v} \in \mathbb{R}^{12}$.

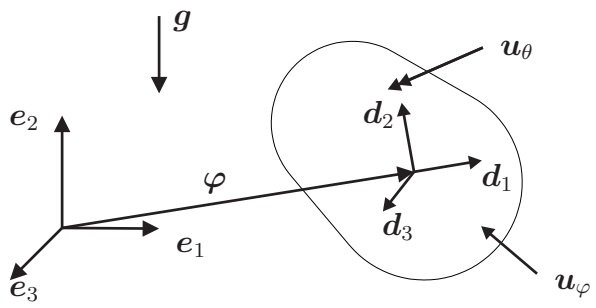

Figure 4.2.: Spatial rigid body: Control input

In the next step, a suitable transformation matrix necessary for the incorporation of control forces and torques will be calculated. Remember that such a transformation matrix has to fulfil the defining condition between the null space matrix and the transformation matrix given in Eq. (3.10). For the present actuation of the single rigid body, the mentioned transformation matrix takes the form

$$\boldsymbol{B}_{\text{int}}(\boldsymbol{q})^T = \boldsymbol{P}_{\text{int}}(\boldsymbol{q}) \begin{bmatrix} \boldsymbol{I}_3 & \boldsymbol{0}_3 \\ \boldsymbol{0}_3 & \frac{1}{2}\boldsymbol{I}_3 \end{bmatrix} \tag{4.14}$$

with the null space matrix introduced in Eq. (4.9). To proove the defining condition given in Eq. (3.10), the product of the transformation and the null space matrix has to be calculated, that is

$$\boldsymbol{B}_{\text{int}}(\boldsymbol{q}) \, \boldsymbol{P}_{\text{int}}(\boldsymbol{q}) = \begin{bmatrix} \boldsymbol{I}_3 & \boldsymbol{0}_3 \\ \boldsymbol{0}_3 & \boldsymbol{X}(\boldsymbol{q}) \end{bmatrix} \tag{4.15}$$

with the orthogonality property for the directors given by

$$\begin{aligned} \boldsymbol{X}(\boldsymbol{q}) &= -\frac{1}{2}\sum_{i=1}^{3} \hat{\boldsymbol{d}}_i\, \hat{\boldsymbol{d}}_i \\ &= -\frac{1}{2}\sum_{i=1}^{3} (\boldsymbol{d}_i \otimes \boldsymbol{d}_i - \{\boldsymbol{d}_i \cdot \boldsymbol{d}_i\}\, \boldsymbol{I}_3) \\ &= -\frac{1}{2}(\boldsymbol{I}_3 - 3\, \boldsymbol{I}_3) \\ &= \boldsymbol{I}_3 \end{aligned} \tag{4.16}$$

Hence, the defining condition is fulfilled. In particular, the transpose of the transformation matrix introduced in Eq. (4.14) maps the generalized control forces and torques $\boldsymbol{u} \in \mathbb{R}^6$ to the corresponding redundant ones $\boldsymbol{B}(\boldsymbol{q})^T \boldsymbol{u} \in \mathbb{R}^{12}$, which then can be incorporated directly in the underlying equations of motion given by Eq. (3.1).

Incorporation of linear viscous friction Below, results concerning the incorporation of linear viscous friction will be illustrated. Again, a single rigid body will be considered. Assuming

$$\boldsymbol{K} = \operatorname{diag}(\boldsymbol{k}_{\boldsymbol{\varphi}}, \boldsymbol{k}_{\boldsymbol{\theta}}) \tag{4.17}$$

as matrix consisting of the damping constants which belong to the translational friction forces $\boldsymbol{a}_{\boldsymbol{\varphi}}$ and the rotational friction forces $\boldsymbol{a}_{\boldsymbol{\theta}}$, on its diagonal. Additionally, $\boldsymbol{B} = \boldsymbol{B}_{\text{int}}$ plays the role of a transformation matrix. Then, the dissipation for the rigid body is given by

$$D = \int_{t_0}^{t} (\boldsymbol{K}\boldsymbol{\nu}) \cdot \boldsymbol{\nu}\, dt = \int_{t_0}^{t} (\boldsymbol{K}\boldsymbol{B}(\boldsymbol{q})\, \boldsymbol{v}) \cdot \boldsymbol{B}(\boldsymbol{q})\, \boldsymbol{v}\, dt \tag{4.18}$$

where Eq. (3.9) as well as the Rayleigh dissipation function in Eq. (3.11) have been employed.

As shown in the last paragraph, the relation between the null space matrix and the transformation matrix given in Eq. (3.10) is fulfilled. As mentioned in Section 3.1, the transformation matrix maps the redundant velocity vectors to the corresponding generalized ones, which then can be used for the formulation of the generalized friction forces $\boldsymbol{a}(\boldsymbol{q}, \boldsymbol{v})$. Inversely, the transpose of the transformation matrix maps the generalized friction forces to the corresponding redundant ones. Finally, the arising vectors can be incorporated directly in the underlying equations of motion given by Eq. (3.1).

Balance of linear momentum, angular momentum and energy Next, the fundamental mechanical balance laws for the rigid body will be elaborated. In a first step, generalized forces $\tilde{\boldsymbol{u}} = (\tilde{\boldsymbol{u}}_{\boldsymbol{\varphi}}, \tilde{\boldsymbol{u}}_{\boldsymbol{\theta}})$ consisting of the generalized control forces $\boldsymbol{u}$ and the generalized friction forces $\boldsymbol{a}(\boldsymbol{q}, \boldsymbol{v})$ will be introduced by

$$\tilde{\boldsymbol{u}} = \boldsymbol{u} + \boldsymbol{a}(\boldsymbol{q}, \boldsymbol{v}) = \boldsymbol{u} + \boldsymbol{K}\boldsymbol{B}(\boldsymbol{q})\, \boldsymbol{v} \tag{4.19}$$

where use has been made of Eq. (3.13).

As a first mechanical balance law, the balance of linear momentum can be mentioned, which states that the time derivative of the linear momentum is equal to the sum of the resulting forces given by $\tilde{\boldsymbol{u}}_{\boldsymbol{\varphi}}$ and the gravitational forces $mg\,\boldsymbol{e}_2$. Additionally, the balance law of angular momentum for a spatial rigid body will be treated. The balance law for angular momentum states that the time derivative of the angular momentum is equal to the sum of the torques, which result from both the resulting forces $\tilde{\boldsymbol{u}}_{\boldsymbol{\varphi}}$ as well as the gravitational forces $mg\,\boldsymbol{e}_2$ and the resulting torques $\tilde{\boldsymbol{u}}_{\boldsymbol{\theta}}$, thus

$$\frac{d}{dt}\boldsymbol{J} = \boldsymbol{\varphi} \times (\tilde{\boldsymbol{u}}_{\boldsymbol{\varphi}} + mg\,\boldsymbol{e}_2) + \boldsymbol{X}(\boldsymbol{q})^T\,\tilde{\boldsymbol{u}}_{\boldsymbol{\theta}} \tag{4.20}$$

The total angular momentum of the rigid body therein has been introduced in Eq. (4.8), the matrix $\boldsymbol{X}(\boldsymbol{q})$ in Eq. (4.15). Obviously, the matrix $\boldsymbol{X}(\boldsymbol{q})$ should not change the resulting generalized torques $\tilde{\boldsymbol{u}}_{\boldsymbol{\theta}}$, which are incorporated into the equations of motion. In the continuous case, the latter is fulfilled due to the orthogonality property of the directors accounted for in Eq. (4.16). Additionally, the mentioned orthogonality property is mandatory for achieving the balance of angular momentum. Furthermore, the balance of energy can be written as

$$\frac{d}{dt}\,(T + V + W + D) = 0 \tag{4.21}$$

By application of $\dot{\boldsymbol{q}} = \boldsymbol{v} = (\boldsymbol{v}_{\boldsymbol{\varphi}}, \boldsymbol{v}_1, \boldsymbol{v}_2, \boldsymbol{v}_3)$, the time derivative of the kinetic energy for the rigid body is given by

$$\frac{d}{dt}\,T = m\,\boldsymbol{v}_{\boldsymbol{\varphi}} \cdot \dot{\boldsymbol{v}}_{\boldsymbol{\varphi}} + \sum_{i=1}^{3} \mathcal{E}_i\,\boldsymbol{v}_i \cdot \dot{\boldsymbol{v}}_i \tag{4.22}$$

where use has been made of Eq. (3.4), Eq. (4.1) and Eq. (4.4). Taking into account Eq. (4.6), the time derivative of the potential energy reads

$$\frac{d}{dt}\,V = mg\;\dot{\boldsymbol{\varphi}} \cdot \boldsymbol{e}_2 \tag{4.23}$$

Finally, the time derivative of the work of the control forces and the dissipation can be written as

$$\frac{d}{dt}(W + D) = \tilde{\boldsymbol{u}} \cdot \boldsymbol{\nu} = \tilde{\boldsymbol{u}} \cdot \boldsymbol{B}(\boldsymbol{q})\,\boldsymbol{v} \tag{4.24}$$

where use has been made of Eq. (4.13), Eq. (4.18) and Eq. (4.19).

Consistent incorporation of control torques and forces While $\boldsymbol{B}_{\text{int}}$ has to be applied in the BEM, the control input in the REM only makes necessary the use of the constant identity matrix $\boldsymbol{I}_6$. However, the calculation of the discrete work of the control forces requires such a transformation matrix. By application of Eq. (3.27), the discrete analogon of Eq. (4.13) is given by

$$W_k = h \cdot \sum_{i=0}^{k-1} \boldsymbol{u}_{i,i+1} \cdot \boldsymbol{\nu}_{i,i+1} = h \cdot \sum_{i=0}^{k-1} \boldsymbol{u}_{i,i+1} \cdot \boldsymbol{B}(\boldsymbol{q}^{i+\frac{1}{2}})\,\boldsymbol{v}_{i+\frac{1}{2}} \tag{4.25}$$

The evaluation of the transformation matrix has basic implications on the consistency properties of the energy-momentum scheme, which is used in this work. The error, which arises through the control input, is equal to zero when directly using the identity matrix $\boldsymbol{I}_6$. Also the consistency properties are not affected by the discretization. If the BEM is used, the midpoint evaluation makes necessary a special evaluation of the control input matrix $\boldsymbol{B}$ to fulfil the discrete analogon of Eq. (3.10). Details of this special evaluation, which has been introduced in Betsch et al. [13], will be specified in the following.

Remember that the directors are the columns of the rotation matrix. A suitable rotation matrix has to fulfil the orthogonality condition given by

$$\boldsymbol{R}\,\boldsymbol{R}^T = \boldsymbol{I} \tag{4.26}$$

Due to the midpoint evaluation of the directors, the orthogonality condition for the corresponding rotation matrix is generally not fulfilled in the midpoint of each time interval, that is

$$\boldsymbol{R}_{k+\frac{1}{2}}\,\boldsymbol{R}_{k+\frac{1}{2}}^T \neq \boldsymbol{I} \tag{4.27}$$

To avoid this error in the discrete setting, the discrete counterpart $\boldsymbol{R}^{k+\frac{1}{2}}$ of the discrete rotation matrix $\boldsymbol{R}_{k+\frac{1}{2}}$, consisting of contravariant directors, has to be calculated. As mentioned earlier in Section 3.2, the upper index in $\boldsymbol{R}^{k+\frac{1}{2}}$ does not denote a midpoint evaluation itself, but results from a nonlinear function of the midpoint evaluation $\boldsymbol{R}_{k+\frac{1}{2}}$. The necessary proceeding is as follows: In a first step, a discrete rotation matrix will be calculated from the covariant directors by application of the relation

$$\boldsymbol{R}_{k+\frac{1}{2}} = \begin{bmatrix} (\boldsymbol{d}_1)_{k+\frac{1}{2}} & (\boldsymbol{d}_2)_{k+\frac{1}{2}} & (\boldsymbol{d}_3)_{k+\frac{1}{2}} \end{bmatrix} \tag{4.28}$$

Afterwards, a discrete rotation matrix consisting of contravariant directors can be obtained by application of the formula

$$\boldsymbol{R}^{k+\frac{1}{2}} = \boldsymbol{R}_{k+\frac{1}{2}}^{-T} \tag{4.29}$$

Notice that the above discrete rotation matrix fulfils the defining orthogonality condition, that is

$$\boldsymbol{R}^{k+\frac{1}{2}}\,\boldsymbol{R}_{k+\frac{1}{2}}^T = \boldsymbol{I} \tag{4.30}$$

Finally, the contravariant directors are the columns of the discrete rotation matrix, that is

$$\begin{bmatrix} (\boldsymbol{d}^1)^{k+\frac{1}{2}} & (\boldsymbol{d}^2)^{k+\frac{1}{2}} & (\boldsymbol{d}^3)^{k+\frac{1}{2}} \end{bmatrix} = \boldsymbol{R}^{k+\frac{1}{2}} \tag{4.31}$$

In the following, the orientation of the spatial rigid body will be reformulated with directors.

Using the recently introduced contravariant configuration vectors $\boldsymbol{q}^{k+\frac{1}{2}}$, consisting of the original position vector $\boldsymbol{\varphi}_{k+\frac{1}{2}}$ and the contravariant directors $(\boldsymbol{d}^i)^{k+\frac{1}{2}}$ for $i = 1, 2, 3$, the discrete transformation matrix takes the form

$$\boldsymbol{B}_{\text{int}}(\boldsymbol{q}^{k+\frac{1}{2}})^T = \boldsymbol{P}_{\text{int}}(\boldsymbol{q}^{k+\frac{1}{2}}) \begin{bmatrix} \boldsymbol{I}_3 & \boldsymbol{0}_3 \\ \boldsymbol{0}_3 & \frac{1}{2}\boldsymbol{I}_3 \end{bmatrix} \tag{4.32}$$

Now calculate

$$\boldsymbol{B}_{\mathrm{int}}(\boldsymbol{q}^{k+\frac{1}{2}})\,\boldsymbol{P}_{\mathrm{int}}(\boldsymbol{q}_{k+\frac{1}{2}}) = \begin{bmatrix} \boldsymbol{I}_3 & \boldsymbol{0}_3 \\ \boldsymbol{0}_3 & \boldsymbol{X}(\boldsymbol{q}_{k+\frac{1}{2}}, \boldsymbol{q}^{k+\frac{1}{2}}) \end{bmatrix} \tag{4.33}$$

where

$$\begin{aligned} \boldsymbol{X}(\boldsymbol{q}_{k+\frac{1}{2}}, \boldsymbol{q}^{k+\frac{1}{2}}) &= -\frac{1}{2}\sum_{i=1}^{3}(\hat{\boldsymbol{d}}^i)^{k+\frac{1}{2}}\,(\hat{\boldsymbol{d}}_i)_{k+\frac{1}{2}} \\ &= -\frac{1}{2}\sum_{i=1}^{3}((\boldsymbol{d}_i)_{k+\frac{1}{2}} \otimes (\boldsymbol{d}^i)^{k+\frac{1}{2}} - \{(\boldsymbol{d}^i)^{k+\frac{1}{2}} \cdot (\boldsymbol{d}_i)_{k+\frac{1}{2}}\}\,\boldsymbol{I}_3) \\ &= -\frac{1}{2}\,(\boldsymbol{I}_3 - 3\,\boldsymbol{I}_3) \\ &= \boldsymbol{I}_3 \end{aligned} \tag{4.34}$$

Consequently, the defining condition for the transformation matrix given in Eq. (3.28) is fulfilled in the discrete case.

Consistent incorporation of linear viscous friction By use of Eq. (3.27), the discrete analogon of Eq. (4.18) is given by

$$D_k = h \cdot \sum_{i=0}^{k-1}(\boldsymbol{K}\boldsymbol{\nu}_{i,i+1}) \cdot \boldsymbol{\nu}_{i,i+1} = h \cdot \sum_{i=0}^{k-1}(\boldsymbol{K}\boldsymbol{B}(\boldsymbol{q}^{i+\frac{1}{2}})\,\boldsymbol{v}_{i+\frac{1}{2}}) \cdot \boldsymbol{B}(\boldsymbol{q}^{i+\frac{1}{2}})\,\boldsymbol{v}_{i+\frac{1}{2}} \tag{4.35}$$

where the transformation matrix $\boldsymbol{B}$, evaluated in the midpoint, has been applied. Here again, the midpoint evaluation makes necessary a special evaluation of the control input matrix $\boldsymbol{B}$ to fulfil the discrete analogon of Eq. (3.10). As for the case of the control input, the use of the recently introduced contravariant configuration vectors leads to the fulfilment of the defining condition for the transformation matrix given in Eq. (3.28).

Discrete balance of linear momentum, angular momentum and energy Next, the discrete analogies of the continuous fundamental mechanical balance laws for the rigid body will be treated. For this aim, discrete generalized forces $\tilde{\boldsymbol{u}}_{k,k+1} = (\tilde{\boldsymbol{u}}_{\boldsymbol{\varphi}_{k,k+1}}, \tilde{\boldsymbol{u}}_{\boldsymbol{\theta}_{k,k+1}})$ will be introduced by

$$\tilde{\boldsymbol{u}}_{k,k+1} = \boldsymbol{u}_{k,k+1} + \boldsymbol{a}(\boldsymbol{q}^{k+\frac{1}{2}}, \boldsymbol{v}_{k+\frac{1}{2}}) = \boldsymbol{u}_{k,k+1} + \boldsymbol{K}\boldsymbol{B}(\boldsymbol{q}^{k+\frac{1}{2}})\boldsymbol{v}_{k+\frac{1}{2}} \tag{4.36}$$

where use has been made of Eq. (3.29).

The discrete balance of linear momentum states that the time derivative of the linear momentum approximated by the difference quotient is equal to the sum of the resulting discrete forces $\tilde{\boldsymbol{u}}_{\boldsymbol{\varphi}_{k,k+1}}$ and the constant gravitational forces $mg\,\boldsymbol{e}_2$. Additionally, the discrete balance law of angular momentum for a spatial rigid body given by

$$\frac{1}{h}(\boldsymbol{J}_{k+1} - \boldsymbol{J}_k) = \boldsymbol{\varphi}_{k+\frac{1}{2}} \times (\tilde{\boldsymbol{u}}_{\boldsymbol{\varphi}_{k,k+1}} + mg\,\boldsymbol{e}_2) + \boldsymbol{X}(\boldsymbol{q}_{k+\frac{1}{2}}, \boldsymbol{q}^{k+\frac{1}{2}})^T\,\tilde{\boldsymbol{u}}_{\boldsymbol{\theta}_{k,k+1}} \tag{4.37}$$

will be treated. To obtain the discrete balance law of angular momentum, the time derivative of the angular momentum in the corresponding continuous balance law in Eq. (4.20) has been approximated by application of the difference quotient. By use of $\boldsymbol{v}_k = (\boldsymbol{v}_{\varphi_k}, \boldsymbol{v}_{1_k}, \boldsymbol{v}_{2_k}, \boldsymbol{v}_{3_k})$, the discrete total angular momentum of the rigid body therein is defined by

$$\boldsymbol{J}_k = m\,\boldsymbol{\varphi}_k \times \boldsymbol{v}_{\varphi_k} + \sum_{i=1}^{3} \mathcal{E}_i\,\boldsymbol{d}_{i_k} \times \boldsymbol{v}_{i_k} \tag{4.38}$$

Furthermore, the matrix $\boldsymbol{X}(\boldsymbol{q}_{k+\frac{1}{2}}, \boldsymbol{q}^{k+\frac{1}{2}})$ introduced in Eq. (4.33) should not change the discrete resulting generalized torques $\tilde{\boldsymbol{u}}_{\boldsymbol{\theta}_{k,k+1}}$, which are incorporated into the discrete equations of motion. Notice that the recently described evaluation of this matrix given in Eq. (4.34) is mandatory for that property. In particular, the latter is necessary for achieving the discrete balance of angular momentum. Furthermore, to obtain the discrete balance of energy, the time derivatives of the kinetic energy, the potential energy, the work of the control forces, and the dissipation in Eq. (4.21) will be approximated by application of the difference quotient. Hence, the discrete balance of energy reads

$$\frac{1}{h}\{(T_{k+1} + V_{k+1} + W_{k+1} + D_{k+1}) - (T_k + V_k + W_k + D_k)\} = 0 \tag{4.39}$$

The time derivative of the velocity in Eq. (4.22) will also be approximated by the difference quotient, thus

$$\begin{aligned} T_{k+1} - T_k &= m\,\boldsymbol{v}_{\varphi_{k+\frac{1}{2}}} \cdot (\boldsymbol{v}_{\varphi_{k+1}} - \boldsymbol{v}_{\varphi_k}) + \sum_{i=1}^{3} \mathcal{E}_i\,\boldsymbol{v}_{i_{k+\frac{1}{2}}} \cdot (\boldsymbol{v}_{i_{k+1}} - \boldsymbol{v}_{i_k}) \\ &= m\,(||\boldsymbol{v}_{\varphi_{k+1}}||^2 - ||\boldsymbol{v}_{\varphi_k}||^2) + \sum_{i=1}^{3} \mathcal{E}_i\,(||\boldsymbol{v}_{i_{k+1}}||^2 - ||\boldsymbol{v}_{i_k}||^2) \end{aligned} \tag{4.40}$$

Additionally, the change of the potential energy from time t_k to t_{k+1} is given by

$$V_{k+1} - V_k = mg\,(\boldsymbol{\varphi}_{k+1} - \boldsymbol{\varphi}_k) \cdot \boldsymbol{e}_2 \tag{4.41}$$

Finally, the change of the work of the control forces and the dissipation from time t_k to t_{k+1} can be written as

$$(W_{k+1}+D_{k+1})-(W_k+D_k) = h\cdot\tilde{\boldsymbol{u}}_{k,k+1}\cdot\boldsymbol{\nu}_{k,k+1} = h\cdot\tilde{\boldsymbol{u}}_{k,k+1}\cdot\boldsymbol{B}(\boldsymbol{q}^{k+\frac{1}{2}})\,\boldsymbol{v}_{k+\frac{1}{2}} \tag{4.42}$$

where use has been made of Eq. (4.25), Eq. (4.35) and Eq. (4.36). Notice that the discrete generalized velocity $\boldsymbol{\nu}_{k,k+1}$ consists of the translational velocity $\boldsymbol{v}_{\varphi_{k+\frac{1}{2}}}$, which is evaluated in the midpoint, and $\boldsymbol{\omega}_{k,k+1}$, which can be interpreted as the discrete angular velocity of the rigid body.

Application to optimal control In the case of a fully actuated rigid body, the function $\boldsymbol{f}$, which then has to be inserted into Eq. (2.1), takes the form of Eq. (3.20). Function $\boldsymbol{f}$ can be used as basis for the optimal control of a single rigid body.

4.2. Kinematic pairs

This section illustrates the present approach by considering two rigid bodies interconnected by a kinematic joint, which has been investigated earlier for example in Betsch & Leyendecker [11] for the case of conservative mechanical systems. In this thesis the extension to nonconservative system will be approached. For this aim, use will be made of a transformation matrix as previously done in Leyendecker et al. [77].

A multibody system will be described as an assembly of individual rigid bodies. For two spatial rigid bodies, interconnected by one kinematic joint, the procedure consists of the following two steps.

In a first step, the contributions of each individual body are collected in appropriate system vectors and matrices. Hence, the configuration vector $\boldsymbol{q} \in \mathbb{R}^{24}$ for two linked spatial rigid bodies is given by

$$\boldsymbol{q} = \begin{bmatrix} \boldsymbol{q}^1 \\ \boldsymbol{q}^2 \end{bmatrix} \tag{4.43}$$

along with the constant and diagonal 24×24 mass matrix

$$\boldsymbol{M} = \begin{bmatrix} \boldsymbol{M}^1 & \boldsymbol{0}_{12} \\ \boldsymbol{0}_{12} & \boldsymbol{M}^2 \end{bmatrix} \tag{4.44}$$

Moreover the constraints of rigidity are outlined in the vector

$$\boldsymbol{\Phi}_{\text{int}}(\boldsymbol{q}) = \begin{bmatrix} \boldsymbol{\Phi}^1_{\text{int}}(\boldsymbol{q}^1) \\ \boldsymbol{\Phi}^2_{\text{int}}(\boldsymbol{q}^2) \end{bmatrix} \tag{4.45}$$

with the corresponding constraint Jacobian

$$\boldsymbol{G}_{\text{int}}(\boldsymbol{q}) = \begin{bmatrix} \boldsymbol{G}^1_{\text{int}}(\boldsymbol{q}^1) & \boldsymbol{0} \\ \boldsymbol{0} & \boldsymbol{G}^2_{\text{int}}(\boldsymbol{q}^2) \end{bmatrix} \tag{4.46}$$

In a second step, the interconnection between the rigid bodies in a multibody system is specified by a number of external constraints summed up in the vector $\boldsymbol{\Phi}_{\text{ext}}(\boldsymbol{q})$. Accordingly, the kinematic pair is characterized by the constraints summarized in

$$\boldsymbol{\Phi}(\boldsymbol{q}) = \begin{bmatrix} \boldsymbol{\Phi}_{\text{int}}(\boldsymbol{q}) \\ \boldsymbol{\Phi}_{\text{ext}}(\boldsymbol{q}) \end{bmatrix} \tag{4.47}$$

with the corresponding constraint Jacobian

$$\boldsymbol{G}(\boldsymbol{q}) = \begin{bmatrix} \boldsymbol{G}_{\text{int}}(\boldsymbol{q}) \\ \boldsymbol{G}_{\text{ext}}(\boldsymbol{q}) \end{bmatrix} \tag{4.48}$$

Similar to the case of a single rigid body described in Section 4.1, a matrix $\boldsymbol{P}$ with full column rank fulfilling Eq. (3.7) has to be found to accomplish the size

reduction by the null space method. One of the possible null space matrices can be calculated by

$$\boldsymbol{P}(\boldsymbol{q}) = \boldsymbol{P}_{\text{int}}(\boldsymbol{q})\ \boldsymbol{P}_{\text{ext}}(\boldsymbol{q}) \tag{4.49}$$

where the 24×12 matrix $\boldsymbol{P}_{\text{int}}$ assumes the form

$$\boldsymbol{P}_{\text{int}}(\boldsymbol{q}) = \begin{bmatrix} \boldsymbol{P}^1_{\text{int}}(\boldsymbol{q}^1) & \boldsymbol{0} \\ \boldsymbol{0} & \boldsymbol{P}^2_{\text{int}}(\boldsymbol{q}^2) \end{bmatrix} \tag{4.50}$$

Moreover, the external null space matrix $\boldsymbol{P}_{\text{ext}}$ has to be found for all of the different kinematic pairs. In the following sections, the procedure will be specified for two primitive kinematic pairs, namely revolute and prismatic pairs.

Application to optimal control In the case of a fully actuated kinematic pair, the function $\boldsymbol{f}$, which then has to be inserted into Eq. (2.1), takes the form of Eq. (3.20). Function $\boldsymbol{f}$ can be used as basis for the optimal control of a kinematic pair.

Revolute pair

Most of the multibody systems employed in this work contain revolute joints. Hence, the necessary background for the revolute pair depicted in Fig. 4.3 will be given below.

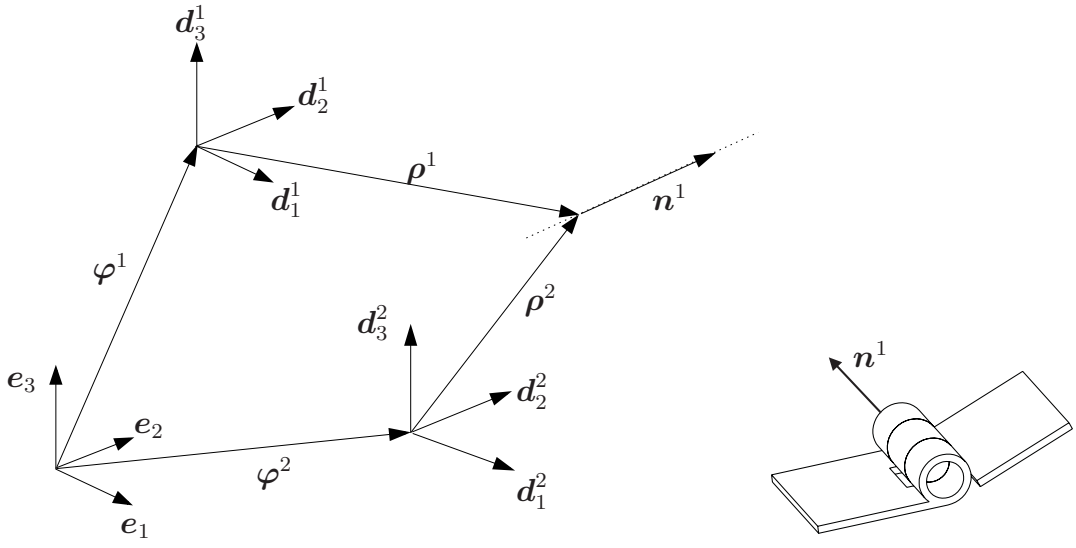

Figure 4.3.: Revolute pair

For the introduction of revolute joints, 5 additional constraint functions of the form

$$\boldsymbol{\Phi}_{\text{ext}}(\boldsymbol{q}) = \begin{bmatrix} \boldsymbol{\varphi}^2 - \boldsymbol{\varphi}^1 + \boldsymbol{\rho}^2 - \boldsymbol{\rho}^1 \\ \boldsymbol{n}^1 \cdot \boldsymbol{d}_1^2 - \mu_1 \\ \boldsymbol{n}^1 \cdot \boldsymbol{d}_2^2 - \mu_2 \end{bmatrix} \tag{4.51}$$

are required, where the unit vector

$$\boldsymbol{n}^1 = \sum_{i=1}^{3} n_i^1 \, \boldsymbol{d}_i^1 \tag{4.52}$$

is fixed at the first body and specifies the rotation axis. The location of the joint on each body is characterized by

$$\boldsymbol{\rho}^\alpha = \sum_{i=1}^{3} \rho_i^\alpha \, \boldsymbol{d}_i^\alpha \;,\; \alpha = 1, 2 \tag{4.53}$$

Additionally, the constants μ_1 and μ_2 need to be consistent. The corresponding 5×24 constraint Jacobian

$$\boldsymbol{G}_{\text{ext}}(\boldsymbol{q}) = \begin{bmatrix} -\boldsymbol{I}_3 & -\rho_1^1 \boldsymbol{I}_3 & -\rho_2^1 \boldsymbol{I}_3 & -\rho_3^1 \boldsymbol{I}_3 & \boldsymbol{I}_3 & \rho_1^2 \boldsymbol{I}_3 & \rho_2^2 \boldsymbol{I}_3 & \rho_3^2 \boldsymbol{I}_3 \\ \boldsymbol{0}^T & n_1^1 (\boldsymbol{d}_1^2)^T & n_2^1 (\boldsymbol{d}_1^2)^T & n_3^1 (\boldsymbol{d}_1^2)^T & \boldsymbol{0}^T & (\boldsymbol{n}^1)^T & \boldsymbol{0}^T & \boldsymbol{0}^T \\ \boldsymbol{0}^T & n_1^1 (\boldsymbol{d}_2^2)^T & n_2^1 (\boldsymbol{d}_2^2)^T & n_3^1 (\boldsymbol{d}_2^2)^T & \boldsymbol{0}^T & \boldsymbol{0}^T & (\boldsymbol{n}^1)^T & \boldsymbol{0}^T \end{bmatrix} \tag{4.54}$$

depends linearly on the configuration vector. Accordingly, the revolute pair is characterized by the 17 constraints summarized in the vector of constraints given in Eq. (4.47) with the corresponding 17×24 constraint Jacobian given in Eq. (4.48). According to Betsch & Leyendecker [11], the 12×7 external null space matrix, which is necessary for the calculation of the null space matrix $\boldsymbol{P}$ via the formula in Eq. (4.49), can be written as

$$\boldsymbol{P}_{\text{ext}}(\boldsymbol{q}) = \begin{bmatrix} \boldsymbol{I}_3 & \boldsymbol{0}_3 & \boldsymbol{0} \\ \boldsymbol{0}_3 & \boldsymbol{I}_3 & \boldsymbol{0} \\ \boldsymbol{I}_3 & \boldsymbol{\rho}^2 \hat{-} \boldsymbol{\rho}^1 & \boldsymbol{\rho}^2 \times \boldsymbol{n}^1 \\ \boldsymbol{0}_3 & \boldsymbol{I}_3 & \boldsymbol{n}^1 \end{bmatrix} \tag{4.55}$$

At this point, all vectors and matrices needed for the formulation of a revolute pair are given. Similar to the spatial rigid body, a discrete reduction process can be applied also to the revolute pair as an example of a lower kinematic pair. The discrete reduction process consists of the premultiplication by the discrete null space matrix and the reparametrization of the unknowns. A detailed elaboration of the discrete reduction process for lower kinematic pairs can be found in Betsch & Leyendecker [11].

Incorporation of control torques and forces In the following, a few results regarding the control input for the revolute pair depicted in Fig. 4.4 will be assembled. In the case of the revolute pair treated in this section, the control vector consists of forces $\boldsymbol{u}_\varphi \in \mathbb{R}^3$ and torques $\boldsymbol{u}_\theta \in \mathbb{R}^3$ acting on the first body of the revolute pair. Additionally, a torque u_α is acting between the two bodies in the revolute joint about the rotation axis specified by the unit vector $\boldsymbol{n}^1$. Assuming $\boldsymbol{u} = (\boldsymbol{u}_{\boldsymbol{\varphi}}, \boldsymbol{u}_{\boldsymbol{\theta}}, u_\alpha)$ as control vector, the work of the control forces for this fully actuated revolute pair is given by Eq. (4.13). To obtain the redundant control forces $\boldsymbol{B}(\boldsymbol{q})^T \boldsymbol{u} \in \mathbb{R}^{24}$, which are work-conjugated to the redundant velocities $\boldsymbol{v} \in \mathbb{R}^{24}$, a suitable transformation matrix $\boldsymbol{B} \in \mathbb{R}^{24 \times 7}$ has to be calculated.

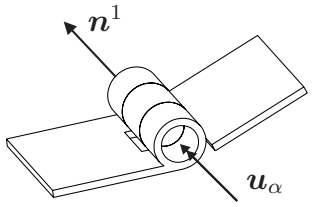

Figure 4.4.: Revolute pair: Control input

As in the case of a single rigid body, a transformation matrix has to fulfil the defining condition between the null space matrix and the transformation matrix given in Eq. (3.10). For the present actuation of the revolute pair, the mentioned transformation matrix takes the form

$$\boldsymbol{B}(\boldsymbol{q})^T = \boldsymbol{P}_{\mathrm{int}}(\boldsymbol{q}) \begin{bmatrix} \boldsymbol{I}_3 & \boldsymbol{0}_3 & \boldsymbol{0}_3 & \boldsymbol{0}_3 \\ \boldsymbol{0}_3 & \frac{1}{2}\boldsymbol{I}_3 & \boldsymbol{0}_3 & \boldsymbol{0}_3 \\ \boldsymbol{0}_3 & \boldsymbol{0}_3 & \boldsymbol{I}_3 & \boldsymbol{0}_3 \\ \boldsymbol{0}_3 & \boldsymbol{0}_3 & \boldsymbol{0}_3 & \frac{1}{2}\boldsymbol{I}_3 \end{bmatrix} \begin{bmatrix} \boldsymbol{I}_3 & \boldsymbol{0}_3 & \boldsymbol{0} \\ \boldsymbol{0}_3 & \boldsymbol{I}_3 & -\boldsymbol{n}^1 \\ \boldsymbol{0}_3 & \boldsymbol{0}_3 & \boldsymbol{0} \\ \boldsymbol{0}_3 & \boldsymbol{0}_3 & \boldsymbol{n}^1 \end{bmatrix} \tag{4.56}$$

Notice that the first two matrices on the right-hand side of Eq. (4.56) already arise for two spatial rigid bodies which are nonconnected. Furthermore, the third matrix in Eq. (4.56) does not yield differences in comparison to the case of single rigid bodies in space for the input of those forces $\boldsymbol{u}_\varphi \in \mathbb{R}^3$ and torques $\boldsymbol{u}_\theta \in \mathbb{R}^3$, which are acting solely on the first body. A difference arises through the last column of the third matrix. Particularly, the control torque u_α acting between the two bodies in the revolute joint will be incorporated by use of the unit vector $\boldsymbol{n}^1$ specifying the rotation axis of the revolute joint. To check the defining condition for the transformation matrix given in Eq. (3.10), first the arising relation for the corresponding internal null space matrices will be calculated, that is

$$\begin{bmatrix} \boldsymbol{I}_3 & \boldsymbol{0}_3 & \boldsymbol{0}_3 & \boldsymbol{0}_3 \\ \boldsymbol{0}_3 & \frac{1}{2}\boldsymbol{I}_3 & \boldsymbol{0}_3 & \boldsymbol{0}_3 \\ \boldsymbol{0}_3 & \boldsymbol{0}_3 & \boldsymbol{I}_3 & \boldsymbol{0}_3 \\ \boldsymbol{0}_3 & \boldsymbol{0}_3 & \boldsymbol{0}_3 & \frac{1}{2}\boldsymbol{I}_3 \end{bmatrix} \boldsymbol{P}_{\mathrm{int}}(\boldsymbol{q})^T \boldsymbol{P}_{\mathrm{int}}(\boldsymbol{q}) = \boldsymbol{I}_{12} \tag{4.57}$$

Therein, the orthogonality property for the directors given in Eq. (4.16) has been employed. At this point, the relation between the external components of the null space matrix and the transformation matrix has still to be checked. Therefore,

$$\begin{bmatrix} \boldsymbol{I}_3 & \boldsymbol{0}_3 & \boldsymbol{0} \\ \boldsymbol{0}_3 & \boldsymbol{I}_3 & -\boldsymbol{n}^1 \\ \boldsymbol{0}_3 & \boldsymbol{0}_3 & \boldsymbol{0} \\ \boldsymbol{0}_3 & \boldsymbol{0}_3 & \boldsymbol{n}^1 \end{bmatrix}^T \begin{bmatrix} \boldsymbol{I}_3 & \boldsymbol{0}_3 & \boldsymbol{0} \\ \boldsymbol{0}_3 & \boldsymbol{I}_3 & \boldsymbol{0} \\ \boldsymbol{I}_3 & \hat{-\boldsymbol{\rho}^1} & \boldsymbol{\rho}^2 \times \boldsymbol{n}^1 \\ \boldsymbol{0}_3 & \boldsymbol{I}_3 & \boldsymbol{n}^1 \end{bmatrix} = \begin{bmatrix} \boldsymbol{I}_3 & \boldsymbol{0}_3 & \boldsymbol{0} \\ \boldsymbol{0}_3 & \boldsymbol{I}_3 & \boldsymbol{0} \\ \boldsymbol{0}^T & \boldsymbol{0}^T & \boldsymbol{n}^1 \cdot \boldsymbol{n}^1 \end{bmatrix} \tag{4.58}$$

where the basic unit length property of the unit vector given by

$$\boldsymbol{n}^1 \cdot \boldsymbol{n}^1 = 1 \tag{4.59}$$

will be applied. Thus, the defining condition given in Eq. (3.10) is fulfilled in the continuous case. Again, the transformation matrix maps the generalized control forces and torques $\boldsymbol{u} \in \mathbb{R}^7$ to the corresponding redundant ones $\boldsymbol{B}(\boldsymbol{q})^T\boldsymbol{u} \in \mathbb{R}^{24}$, which are needed for the formulation of the equations of motion in Eq. (3.1).

Incorporation of linear viscous friction Below, results concerning the incorporation of linear viscous friction for a revolute pair will be illustrated. Assuming

$$\boldsymbol{K} = \operatorname{diag}(\boldsymbol{k}_{\boldsymbol{\varphi}}, \boldsymbol{k}_{\boldsymbol{\theta}}, k_\alpha) \tag{4.60}$$

as matrix consisting of the damping constants, which belong to the translational friction forces $\boldsymbol{a}_{\boldsymbol{\varphi}}$, the rotational friction forces $\boldsymbol{a}_{\boldsymbol{\theta}}$ and the friction force in the revolute joint a_α, on its diagonal. Then, the dissipation for the revolute pair is given by Eq. (4.18), where Eq. (3.9) has been employed. For that purpose, the necessary transformation matrix has been introduced in Eq. (4.56). As shown in the last paragraph, the relation between the null space matrix and the transformation matrix given in Eq. (3.10) is fulfilled. Finally, similar observations as those of the rigid body can be stated for the revolute pair.

Consistent incorporation of the controls and linear viscous friction Concerning the transition to the discrete setting, observations similar to those given at the end of Section 4.1 can be stated. Here again, a special evaluation of the transformation matrix is necessary.

Remember that the unit vector property given in Eq. (4.59) is to be valid. Using a direct midpoint evaluation of the transformation matrix, the mentioned relation does not hold, that is

$$(\boldsymbol{n}^1)_{k+\frac{1}{2}} \cdot (\boldsymbol{n}^1)_{k+\frac{1}{2}} \neq 1 \tag{4.61}$$

Hence, a contravariant evaluation of the transformation matrix will again be applied. Therewith, the relation given by

$$(\boldsymbol{n}^1)^{k+\frac{1}{2}} \cdot (\boldsymbol{n}^1)_{k+\frac{1}{2}} = 1 \tag{4.62}$$

is valid. Consequently, the defining condition for the transformation matrix given in Eq. (3.28) is fulfilled in the discrete case.

Continuous and discrete balance laws Next, the fundamental mechanical balance laws for the revolute pair will be elaborated. As a first mechanical balance law, the balance of linear momentum can be mentioned, which states that the time derivative of the linear momentum is equal to the sum of the resulting forces $\tilde{\boldsymbol{u}}_{\boldsymbol{\varphi}}$ and the constant gravitational forces $(m^1 + m^2)\, g\, \boldsymbol{e}_2$. The generalized forces $\tilde{\boldsymbol{u}} \in \mathbb{R}^7$ therefore have to be calculated by Eq. (4.19) with the present quantities. The corresponding discrete balance law for linear momentum can be achieved in a straightforward way as for the rigid body by application of the resulting discrete forces $\tilde{\boldsymbol{u}}_{\boldsymbol{\varphi}_{k,k+1}}$ calculated by Eq. (4.36). Additionally, the balance law for angular momentum will be treated for the revolute pair. The latter is given by

$$\frac{d}{dt}\boldsymbol{J} = \boldsymbol{\varphi}^1 \times (\tilde{\boldsymbol{u}}_{\boldsymbol{\varphi}} + m^1 g\, \boldsymbol{e}_2) + \boldsymbol{\varphi}^2 \times (m^2 g\, \boldsymbol{e}_2) + \boldsymbol{X}(\boldsymbol{q}^1)^T\, \tilde{\boldsymbol{u}}_{\boldsymbol{\theta}} + \tilde{u}_\alpha \boldsymbol{n}^1 - \tilde{u}_\alpha \boldsymbol{n}^1 \tag{4.63}$$

with the total angular momentum of the kinematic pair $\boldsymbol{J}$ given as sum of the individual angular momenta of the involved rigid bodies. While the constant

gravitational forces cause torques for both involved rigid bodies, the resulting force $\tilde{\boldsymbol{u}}_{\boldsymbol{\varphi}}$ causes only a torque for the first body. The resulting torque $\tilde{u}_\alpha$, which is acting between the two bodies in the revolute joint, causes torques about the axis $\boldsymbol{n}^1$ on both rigid bodies with opposite sign. Notice that the change in angular momentum is zero, if only the resulting joint torque $\tilde{u}_\alpha$ acts on the system. As in the case of the spatial rigid body, the orthogonality of the directors is mandatory for achieving the balance of angular momentum. Furthermore, the discrete balance law of angular momentum for the present revolute pair takes the form

$$\begin{aligned}\frac{1}{h}(\boldsymbol{J}_{k+1}-\boldsymbol{J}_k) &= \boldsymbol{\varphi}^1_{k+\frac{1}{2}} \times (\tilde{\boldsymbol{u}}_{\boldsymbol{\varphi}_{k,k+1}} + m^1 g\, \boldsymbol{e}_2) + \boldsymbol{\varphi}^2_{k+\frac{1}{2}} \times (m^2 g\, \boldsymbol{e}_2) \\ &\quad + \boldsymbol{X}((\boldsymbol{q}^1)_{k+\frac{1}{2}}, (\boldsymbol{q}^1)^{k+\frac{1}{2}})^T\, \tilde{\boldsymbol{u}}_{\boldsymbol{\theta}_{k,k+1}} + \tilde{u}_{\alpha_{k,k+1}} (\boldsymbol{n}^1)^{k+\frac{1}{2}} - \tilde{u}_{\alpha_{k,k+1}} (\boldsymbol{n}^1)^{k+\frac{1}{2}}\end{aligned} \tag{4.64}$$

with the difference quotient as approximation of the time derivative and the discrete resulting controls $\tilde{\boldsymbol{u}}_{k,k+1} = (\tilde{\boldsymbol{u}}_{\boldsymbol{\varphi}_{k,k+1}}, \tilde{\boldsymbol{u}}_{\boldsymbol{\theta}_{k,k+1}}, \tilde{u}_{\alpha_{k,k+1}})$. Notice again that the special evaluation of the matrix given in Eq. (4.34) is mandatory for achieving the discrete balance of angular momentum. Concerning the balance of energy, Eq. (4.21) for the continuous case and Eq. (4.39) for the discrete case are crucial also for the revolute pair. Of course, both involved rigid bodies have to be taken into account in the kinetic and the potential energy. For the work of the control forces and the dissipation the transformation matrix introduced in Eq. (4.56) has to be employed for the present revolute pair.

Prismatic pair

Multibody systems may also contain prismatic joints. Consequently, the basics for the prismatic pair depicted in Fig. 4.5 will be given below.

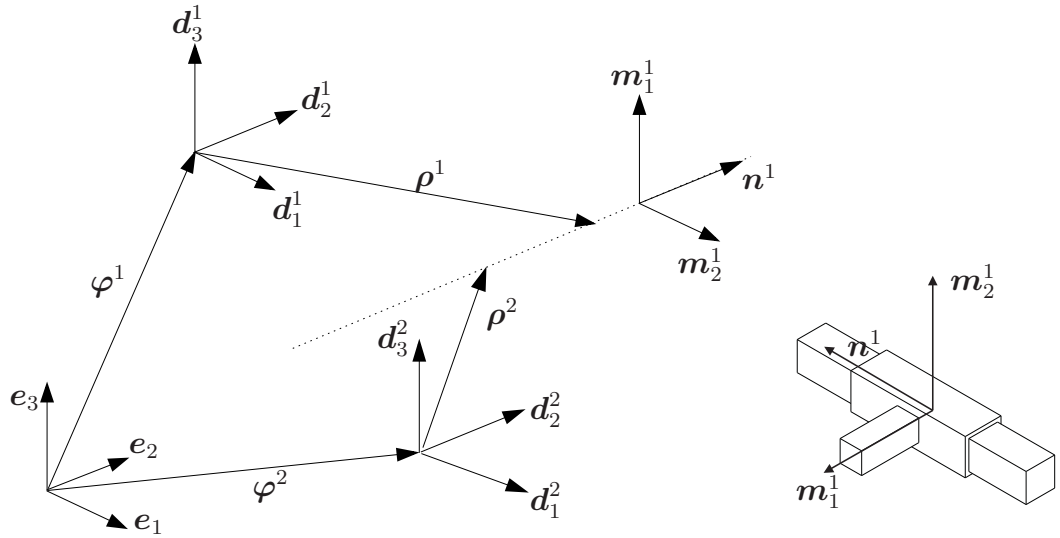

Figure 4.5.: Prismatic pair

For the introduction of prismatic joints, 5 additional constraint functions of the form

$$\boldsymbol{\Phi}_{\text{ext}}(\boldsymbol{q}) = \begin{bmatrix} \boldsymbol{m}_1^1 \cdot (\boldsymbol{\varphi}^2 - \boldsymbol{\varphi}^1 + \boldsymbol{\rho}^2 - \boldsymbol{\rho}^1) \\ \boldsymbol{m}_2^1 \cdot (\boldsymbol{\varphi}^2 - \boldsymbol{\varphi}^1 + \boldsymbol{\rho}^2 - \boldsymbol{\rho}^1) \\ \boldsymbol{d}_1^1 \cdot \boldsymbol{d}_2^2 - \mu_1 \\ \boldsymbol{d}_2^1 \cdot \boldsymbol{d}_3^2 - \mu_2 \\ \boldsymbol{d}_3^1 \cdot \boldsymbol{d}_1^2 - \mu_3 \end{bmatrix} \tag{4.65}$$

are necessary, where the unit vector $\boldsymbol{n}^1$ in Eq. (4.52) is fixed at the first body and specifies the translation axis. Additionally, the vectors

$$\boldsymbol{m}_\alpha^1 = \sum_{i=1}^{3} (m_\alpha^1)_i \, \boldsymbol{d}_i^1 \ , \ \alpha = 1, 2 \tag{4.66}$$

will be introduced, such that $\{\boldsymbol{m}_1^1, \boldsymbol{m}_2^1, \boldsymbol{n}^1\}$ constitute a right-handed orthogonal frame. The location of the joint on each body is again characterized by the vectors $\boldsymbol{\rho}^\alpha$ given in Eq. (4.53). Additionally, the constants μ_1, μ_2, and μ_3 need to be consistent. Furthermore, the corresponding 5×24 linear constraint Jacobian reads

$$\boldsymbol{G}_{\text{ext}}(\boldsymbol{q}) = \begin{bmatrix} -(\boldsymbol{m}_1^1)^T & \boldsymbol{G}_{11}^T & \boldsymbol{G}_{12}^T & \boldsymbol{G}_{13}^T & (\boldsymbol{m}_1^1)^T & \rho_1^2(\boldsymbol{m}_1^1)^T & \rho_2^2(\boldsymbol{m}_1^1)^T & \rho_3^2(\boldsymbol{m}_1^1)^T \\ -(\boldsymbol{m}_2^1)^T & \boldsymbol{G}_{21}^T & \boldsymbol{G}_{22}^T & \boldsymbol{G}_{23}^T & (\boldsymbol{m}_2^1)^T & \rho_1^2(\boldsymbol{m}_2^1)^T & \rho_2^2(\boldsymbol{m}_2^1)^T & \rho_3^2(\boldsymbol{m}_2^1)^T \\ \boldsymbol{0}^T & (\boldsymbol{d}_2^2)^T & \boldsymbol{0}^T & \boldsymbol{0}^T & \boldsymbol{0}^T & \boldsymbol{0}^T & (\boldsymbol{d}_1^1)^T & \boldsymbol{0}^T \\ \boldsymbol{0}^T & \boldsymbol{0}^T & (\boldsymbol{d}_3^2)^T & \boldsymbol{0}^T & \boldsymbol{0}^T & \boldsymbol{0}^T & \boldsymbol{0}^T & (\boldsymbol{d}_2^1)^T \\ \boldsymbol{0}^T & \boldsymbol{0}^T & \boldsymbol{0}^T & (\boldsymbol{d}_1^2)^T & \boldsymbol{0}^T & (\boldsymbol{d}_3^1)^T & \boldsymbol{0}^T & \boldsymbol{0}^T \end{bmatrix} \tag{4.67}$$

where

$$\boldsymbol{G}_{\alpha i}(\boldsymbol{q}) = (m_\alpha^1)_i \, (\boldsymbol{\varphi}^2 - \boldsymbol{\varphi}^1 + \boldsymbol{\rho}^2 - \boldsymbol{\rho}^1) - \rho_i^1 \boldsymbol{m}_\alpha^1 \tag{4.68}$$

Accordingly, the prismatic pair is characterized by the 17 constraints summarized in the vector of constraints given in Eq. (4.47) with the corresponding 17×24 constraint Jacobian given in Eq. (4.48). According to Betsch & Leyendecker [11], the 12×7 external null space matrix, which is necessary for the calculation of the null space matrix $\boldsymbol{P}$ via the formula in Eq. (4.49), can be written as

$$\boldsymbol{P}_{\text{ext}}(\boldsymbol{q}) = \begin{bmatrix} \boldsymbol{I}_3 & \boldsymbol{0}_3 & \boldsymbol{0} \\ \boldsymbol{0}_3 & \boldsymbol{I}_3 & \boldsymbol{0} \\ \boldsymbol{I}_3 & \boldsymbol{\varphi}^1 \hat{-} \boldsymbol{\varphi}^2 & \boldsymbol{n}^1 \\ \boldsymbol{0}_3 & \boldsymbol{I}_3 & \boldsymbol{0} \end{bmatrix} \tag{4.69}$$

At this point, all vectors and matrices needed for the formulation of a prismatic pair are introduced. Again, a discrete reduction process can be employed by the premultiplication of the discrete null space matrix and the reparametrization of the unknowns. Further details on the discrete reduction process can be found in Betsch & Leyendecker [11].

Incorporation of control torques and forces Below, some results regarding the control input for the prismatic pair depicted in Fig. 4.6 will be assembled. In

the case of a fully actuated prismatic pair, the control vector consists of forces $\boldsymbol{u}_\varphi \in \mathbb{R}^3$ and torques $\boldsymbol{u}_\theta \in \mathbb{R}^3$ acting on the first body and a force u_r acting between the two bodies along the translation axis specified by the unit vector $\boldsymbol{n}^1$. Assuming $\boldsymbol{u} = (\boldsymbol{u}_{\boldsymbol{\varphi}}, \boldsymbol{u}_{\boldsymbol{\theta}}, u_r)$ as control vector, the work of the control forces for this fully actuated prismatic pair is given by Eq. (4.13). As in the case of the revolute pair, to obtain the redundant control forces $\boldsymbol{B}(\boldsymbol{q})^T\boldsymbol{u} \in \mathbb{R}^{24}$, which are work-conjugated to the redundant velocities $\boldsymbol{v} \in \mathbb{R}^{24}$, a suitable transformation matrix $\boldsymbol{B} \in \mathbb{R}^{24\times 7}$ has to be calculated.

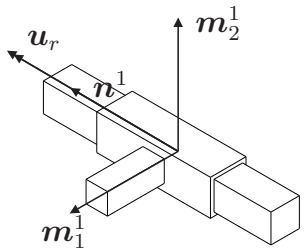

Figure 4.6.: Prismatic pair: Control input

A transformation matrix has to fulfil the defining condition between the null space matrix and the transformation matrix given in Eq. (3.10). In the present case of a fully actuated prismatic pair, a suitable transformation matrix is given by

$$\boldsymbol{B}(\boldsymbol{q})^T = \boldsymbol{P}_{\text{int}}(\boldsymbol{q}) \begin{bmatrix} \boldsymbol{I}_3 & \boldsymbol{0}_3 & \boldsymbol{0}_3 & \boldsymbol{0}_3 \\ \boldsymbol{0}_3 & \frac{1}{2}\boldsymbol{I}_3 & \boldsymbol{0}_3 & \boldsymbol{0}_3 \\ \boldsymbol{0}_3 & \boldsymbol{0}_3 & \boldsymbol{I}_3 & \boldsymbol{0}_3 \\ \boldsymbol{0}_3 & \boldsymbol{0}_3 & \boldsymbol{0}_3 & \frac{1}{2}\boldsymbol{I}_3 \end{bmatrix} \begin{bmatrix} \boldsymbol{I}_3 & \boldsymbol{0}_3 & -\boldsymbol{n}^1 \\ \boldsymbol{0}_3 & \boldsymbol{I}_3 & (\boldsymbol{\varphi}^1 - \boldsymbol{\varphi}^2) \times \boldsymbol{n}^1 \\ \boldsymbol{0}_3 & \boldsymbol{0}_3 & \boldsymbol{n}^1 \\ \boldsymbol{0}_3 & \boldsymbol{0}_3 & \boldsymbol{0} \end{bmatrix} \tag{4.70}$$

The decisive difference in comparison to the revolute pair arises through the last column of the third matrix on the right-hand side of Eq. (4.70). Remember that in the revolute pair, the last column of the third matrix in Eq. (4.56) contains the unit vector $\boldsymbol{n}^1$ specifying the rotation axis of the revolute joint. In the present prismatic pair, the mentioned column is necessary for the incorporation of the force u_r acting between the two bodies along the translation axis specified by the unit vector $\boldsymbol{n}^1$. Notice that a resulting torque acting on the prismatic pair is induced by the component $(\boldsymbol{\varphi}^1 - \boldsymbol{\varphi}^2) \times \boldsymbol{n}^1$, if the actuated prismatic joint is located away from the centers of mass of the two bodies. To check the defining condition for the transformation matrix given in Eq. (3.10), firstly a relation for the internal null space matrices given in Eq. (4.57) has to be checked. This has been done already for the revolute pair. Secondly, the relation between the external components of the null space matrix and the transformation matrix has to be checked, that is

$$\begin{bmatrix} \boldsymbol{I}_3 & \boldsymbol{0}_3 & -\boldsymbol{n}^1 \\ \boldsymbol{0}_3 & \boldsymbol{I}_3 & (\boldsymbol{\varphi}^1 - \boldsymbol{\varphi}^2) \times \boldsymbol{n}^1 \\ \boldsymbol{0}_3 & \boldsymbol{0}_3 & \boldsymbol{n}^1 \\ \boldsymbol{0}_3 & \boldsymbol{0}_3 & \boldsymbol{0} \end{bmatrix}^T \begin{bmatrix} \boldsymbol{I}_3 & \boldsymbol{0}_3 & \boldsymbol{0} \\ \boldsymbol{0}_3 & \boldsymbol{I}_3 & \boldsymbol{0} \\ \boldsymbol{I}_3 & \boldsymbol{\varphi}^1 \hat{-} \boldsymbol{\varphi}^2 & \boldsymbol{n}^1 \\ \boldsymbol{0}_3 & \boldsymbol{I}_3 & \boldsymbol{0} \end{bmatrix} = \begin{bmatrix} \boldsymbol{I}_3 & \boldsymbol{0}_3 & \boldsymbol{0} \\ \boldsymbol{0}_3 & \boldsymbol{I}_3 & \boldsymbol{0} \\ \boldsymbol{0}^T & \boldsymbol{0}^T & \boldsymbol{n}^1 \cdot \boldsymbol{n}^1 \end{bmatrix} \tag{4.71}$$

where the basic unit length property of the unit vector given by Eq. (4.59) will be employed. Thus, the defining condition given in Eq. (3.10) is fulfilled in the continuous case. Once again, the transformation matrix maps the generalized control forces and torques $\boldsymbol{u} \in \mathbb{R}^7$ to the corresponding redundant ones $\boldsymbol{B}(\boldsymbol{q})^T \boldsymbol{u} \in \mathbb{R}^{24}$, which are needed for the formulation of the equations of motion in Eq. (3.1).

Incorporation of linear viscous friction In the following, the incorporation of linear viscous friction will also be elaborated for a prismatic pair. Assuming

$$\boldsymbol{K} = \operatorname{diag}(\boldsymbol{k}_{\boldsymbol{\varphi}}, \boldsymbol{k}_{\boldsymbol{\theta}}, k_r) \tag{4.72}$$

as matrix consisting of the damping constants belonging to the already introduced translational and rotational friction forces $\boldsymbol{a}_{\boldsymbol{\varphi}}$ respectively $\boldsymbol{a}_{\boldsymbol{\theta}}$, as well as the friction force in the prismatic joint a_r, on its diagonal. Then, the dissipation for the prismatic pair is given by Eq. (4.18), where Eq. (3.9) has been applied. In the end, similar observations as those of the revolute pair can be stated.

Consistent incorporation of the controls and linear viscous friction Observations, totally similar to those for the revolute pair given in Section 4.2, can be stated concerning the consistent incorporation of control forces and torques, as well as linear viscous friction.

Continuous and discrete balance laws Regarding the fundamental mechanical balance laws for the prismatic pair, mainly the differences to the revolute pair will be mentioned. The balance law of linear momentum for the prismatic pair takes completely the same form as for the revolute pair. Furthermore, the balance law of angular momentum for the prismatic pair is given by

$$\begin{aligned} \frac{d}{dt}\boldsymbol{J} = \boldsymbol{\varphi}^1 \times (\tilde{\boldsymbol{u}}_{\boldsymbol{\varphi}} + m^1 g\, \boldsymbol{e}_2) + \boldsymbol{\varphi}^2 \times (m^2 g\, \boldsymbol{e}_2) + \boldsymbol{X}(\boldsymbol{q}^1)^T\, \tilde{\boldsymbol{u}}_{\boldsymbol{\theta}} \\ + \tilde{u}_r(\boldsymbol{\varphi}^1 - \boldsymbol{\varphi}^2) \times \boldsymbol{n}^1 - \tilde{u}_r(\boldsymbol{\varphi}^1 - \boldsymbol{\varphi}^2) \times \boldsymbol{n}^1 \end{aligned} \tag{4.73}$$

The resulting force $\tilde{u}_r$, which arises in the last two terms of Eq. (4.73) and acts between the two bodies in the prismatic joint, causes torques about the axis given by $(\boldsymbol{\varphi}^1 - \boldsymbol{\varphi}^2) \times \boldsymbol{n}^1$ on both rigid bodies with opposite sign. As for the revolute pair, the change in angular momentum is zero, if only the joint force $\tilde{u}_r$ acts on the system. Once again, the orthogonality property of the directors has to be fulfilled for obtaining the balance of angular momentum. Additionally, the discrete balance law of angular momentum for the present prismatic pair takes the form

$$\begin{aligned} \frac{1}{h}(\boldsymbol{J}_{k+1} - \boldsymbol{J}_k) = \boldsymbol{\varphi}^1_{k+\frac{1}{2}} \times (\tilde{\boldsymbol{u}}_{\boldsymbol{\varphi}_{k,k+1}} + m^1 g\, \boldsymbol{e}_2) + \boldsymbol{\varphi}^2_{k+\frac{1}{2}} \times (m^2 g\, \boldsymbol{e}_2) \\ + \boldsymbol{X}((\boldsymbol{q}^1)_{k+\frac{1}{2}}, (\boldsymbol{q}^1)^{k+\frac{1}{2}})^T\, \tilde{\boldsymbol{u}}_{\boldsymbol{\theta}_{k,k+1}} \\ + \tilde{u}_{r_{k,k+1}}(\boldsymbol{\varphi}^1_{k+\frac{1}{2}} - \boldsymbol{\varphi}^2_{k+\frac{1}{2}}) \times (\boldsymbol{n}^1)^{k+\frac{1}{2}} - \tilde{u}_{r_{k,k+1}}(\boldsymbol{\varphi}^1_{k+\frac{1}{2}} - \boldsymbol{\varphi}^2_{k+\frac{1}{2}}) \times (\boldsymbol{n}^1)^{k+\frac{1}{2}} \end{aligned} \tag{4.74}$$

with the difference quotient as approximation of the time derivative and the discrete resulting controls $\tilde{\boldsymbol{u}}_{k,k+1} = (\tilde{\boldsymbol{u}}_{\boldsymbol{\varphi}_{k,k+1}}, \tilde{\boldsymbol{u}}_{\boldsymbol{\theta}_{k,k+1}}, \tilde{u}_{r_{k,k+1}})$. Notice again that the special evaluation of the matrix given in Eq. (4.34) is required for achieving the discrete balance of angular momentum. Concerning the balance of energy, the transformation matrix for the prismatic pair given in Eq. (4.70) has to be used instead of the one given in Eq. (4.56) necessary for the revolute pair.

4.3. Consistent incorporation of control torques

Inspired by space telescopes such as the Hubble telescope, whose change in orientation is induced by spinning rotors, a multibody system consisting of a main body and three rotors will be analyzed. In this section, the algorithmic consistency of angular momentum of the introduced incorporation of control torques and forces will be demonstrated. Additionally, it will be demonstrated that the newly devised method yields good approximations for the kinetic energy, even for large time step sizes. Later in Section 6.3, this example, which has been introduced in Leyendecker et al. [77] in the context of optimal control, will here also be employed within optimal control. In contrast to Leyendecker et al. [77], where a variational integrator has been applied, here, the present EM-scheme will be employed.

Rotationless formulation The rigid body with rotors depicted in Fig. 4.7 consists of a main body, which is connected to three rotors by revolute joints. For clarity reasons, the inertial frame $\{\boldsymbol{e}_1, \boldsymbol{e}_2, \boldsymbol{e}_3\}$ and the position vectors $\boldsymbol{\varphi}^i$ for $i = 0, ..., 3$ have been neglected in Fig. 4.7. The vectors $\boldsymbol{\rho}_i^2$ denoting the location of the revolute joints on the rotors are equal to zero for $i = 1, 2, 3$. Furthermore, the necessary vectors and matrices can be obtained by following the procedure specified earlier in this chapter. Those are the configuration vector $\boldsymbol{q} \in \mathbb{R}^{48}$, the velocity vector $\boldsymbol{v} \in \mathbb{R}^{48}$ and the mass matrix $\boldsymbol{M} \in \mathbb{R}^{48\times48}$. The vector of constraints for the nine degree of freedom system $\boldsymbol{\Phi} \in \mathbb{R}^{39}$ consists of 24 internal constraints due to the rigidity and 15 external ones due to the three revolute pairs. Consequently, a corresponding constraint Jacobian $\boldsymbol{G} \in \mathbb{R}^{39\times48}$ is necessary. Due to the revolute joints, the rotation of one rotor relative to the main body is feasible around an axis which is fixed in the main body and goes through its center. Only the rotors can be actuated by control torques, that is

$$\boldsymbol{u} = \begin{bmatrix} \boldsymbol{0}_{1\times6} & u_1 & u_2 & u_3 \end{bmatrix}^T \tag{4.75}$$

Additionally, linear viscous friction can only act in the three revolute joints, thus the matrix $\boldsymbol{K}$ consisting of the damping constants reads

$$\boldsymbol{K} = \operatorname{diag}(\boldsymbol{0}_{6\times1}, k_1, k_2, k_3) \tag{4.76}$$

The control input as well as the incorporation of linear viscous friction will be done by the transformation matrix $\boldsymbol{B} \in \mathbb{R}^{9\times48}$. Finally, a null space matrix

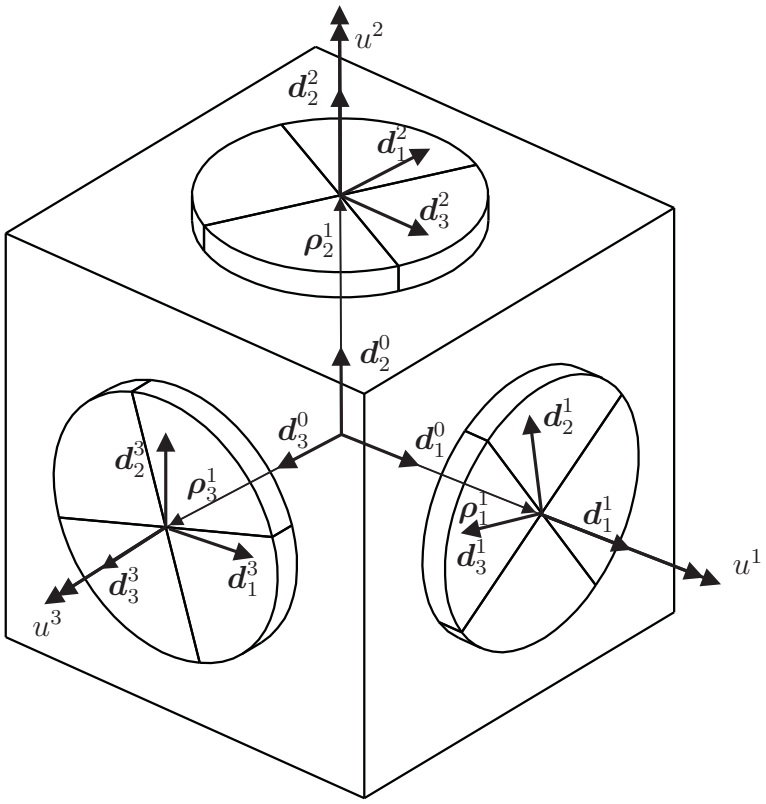

Figure 4.7.: Satellite

$\boldsymbol{P} \in \mathbb{R}^{48\times 9}$ can be used for calculating valid redundant initial velocities $\boldsymbol{v}_0 \in \mathbb{R}^{48}$ from the corresponding generalized ones $\boldsymbol{\nu}_0 \in \mathbb{R}^9$. The consistent evaluation is primarily important for the BEM, hence only the BEM without any reduction process will be employed.

Numerical example: Satellite In the following, the importance of the consistent incorporation of control torques will be shown within the example of the satellite. The mass and geometric properties of the spacecraft are summarized in Table 4.1. Therein, l_i is the distance between the center of mass of rotor i to

body	m	$\mathcal{E}_1$	$\mathcal{E}_2$	$\mathcal{E}_3$	l
0	1005.3096	89.3609	201.0619	357.4434	
1	424.1150	8.8357	106.0288	106.0288	0.9167
2	424.1150	106.0288	8.8357	106.0288	1.25
3	424.1150	106.0288	106.0288	8.8357	1.5833

Table 4.1.: Inertia and geometric data for the Rigid body with rotors.

the center of mass of the main body. Furthermore, it is assumed that there is no

friction acting in the revolute joints between the base body and the three reaction wheels, thus $k_i = 0$ for $i = 1, 2, 3$. To show the importance of the consistent incorporation of the controls, a simulation or forward dynamics problem of the satellite with constant joint-torques $u_i = 200$ for $i = 1, 2, 3$ will be investigated.

In the numerical simulation, the 3-component of the total angular momentum and the total kinetic energy of the multibody system will be observed. The corresponding results for the case of consistent incorporation of control torques will be denoted by J_3^{kontra} for the 3-component of the total angular momentum and T^{kontra} for the total kinetic energy. For comparison, a straightforward midpoint evaluation of the transformation matrix will be applied. In this case, the related results will be denoted by J_3^{kov} respectively T^{kov}.

A number of N time steps is used to resolve the time interval with $t_0 = 0$ and $t_f = 5$. The arising subintervals all have the size $h = \frac{t_f}{N}$. As visible in the right diagram of Fig. 4.8, the 3-component of the total angular momentum J_3^{kontra} stays constant all time, even for large time step sizes. Hence, algorithmic consistency of the total angular momentum is valid. The case of simple midpoint evaluation yields a totally different behaviour, to state more precisely, J_3^{kov} does not stay constant. Thus, the balance law for angular momentum is violated. As expected, the discretization error can be decreased by decreasing the time step size h. Analogous observations can be done concerning the total kinetic energy depicted in the left diagram of Fig. 4.8. While T^{kontra} does hardly change, if the time steps are refined, this is in severe contrast to T^{kov}. In particular, using only $N = 5$ time steps in the consistent case already leads to a very good approximation of the kinetic energy.

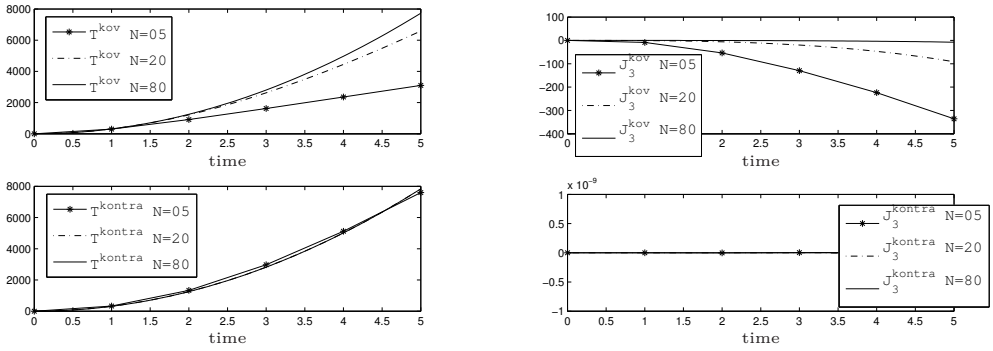

Figure 4.8.: Nonconsistent (top) and consistent (bottom) incorporation of control torques: 1. Resulting kinetic energy (Left). 2. Resulting angular momentum (Right).

4.4. Consistent incorporation of linear viscous friction

In this section, the algorithmic consistency of angular momentum of the present incorporation of linear viscous friction will be demonstrated. Additionally, it will be demonstrated that the newly devised approach yields good approximations for the kinetic energy, even for large time step sizes. Again, the satellite introduced in Section 4.3 will be employed as an example.

Numerical example: Satellite In the following, the importance of the consistent incorporation of linear viscous friction will be demonstrated within the example of the satellite. The mass and geometric properties of the spacecraft are again those of Table 4.1. It is assumed that there is friction acting in the revolute joints between the base body and the three reaction wheels. The corresponding damping constants are given by $k_i = 100$ for $i = 1, 2, 3$. In contrast to the case of incorporation of control torques, the consistent evaluation is important for both the BEM and the REM. However, only the BEM without any reduction process will be employed. To show the importance of the consistency, a simulation or forward dynamics problem of the satellite with an initial velocity described by generalized velocity

$$\boldsymbol{\nu}_0 = \begin{bmatrix} 0 & 0 & 0 & 0.2 & 0.3 & 0.4 & 1 & 2 & 3 \end{bmatrix}^T \tag{4.77}$$

and zero joint-torques $u_i = 0$ for $i = 1, 2, 3$ will be investigated. Finally, the redundant initial velocity $\boldsymbol{v}_0$, corresponding to the generalized one $\boldsymbol{\nu}_0$, will be calculated using the null space matrix $\boldsymbol{P}$.

Similar investigations as those of Section 4.3 will be performed. The arising results are depicted in Fig. 4.9. Identical comments as those of Section 4.3 can be stated.

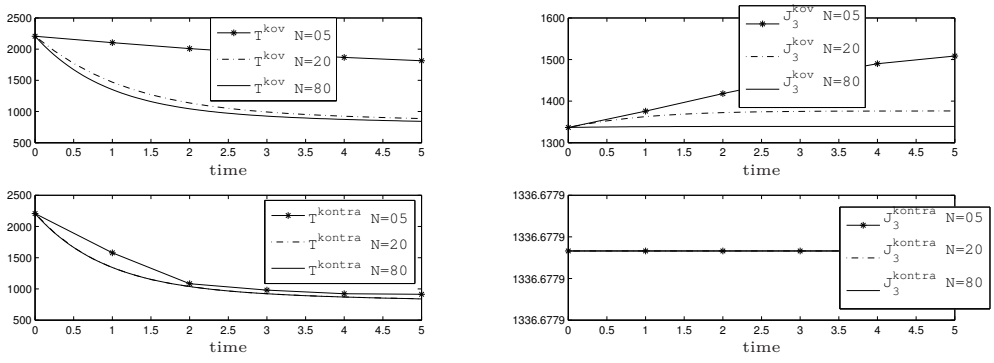

Figure 4.9.: Nonconsistent (top) and consistent (bottom) incorporation of linear viscous friction: 1. Resulting kinetic energy (Left). 2. Resulting angular momentum (Right).

5. Alternative rigid body formulation: Quaternions

Unit quaternions (or Euler parameters) are known to be well-suited for the singularity-free description of finite rotations. Previously, unit quaternions have been used for the formulation of the equations of motion in the pioneering works by Nikravesh [85], Haug [62] and the references cited therein. In these works (see also Wendlandt & Marsden [106], O'Reilly & Varadi [87] and Rabier & Rheinboldt [90]) the orientation of a single rigid body is specified by a quaternion, which is subjected to the unit length constraint.

In the aforementioned works the Lagrange equations of motion have been used. In this connection, the quaternion form of the kinetic energy is commonly obtained from the standard expression in terms of the angular velocity vector and the classical inertia tensor. Consequently, the 4×4 mass matrix of the quaternion formulation is singular in general. In the present work, the approach originally introduced in Betsch & Siebert [12] will be employed for the derivation of a nonsingular mass matrix. Therein, a size reduction from the formulation of the equations of motion with directors introduced in Section 4.1 (see also Vallee et al. [101], Betsch & Steinmann [16] and Leimkuhler & Reich [71]) will be performed. The present approach makes possible the straightforward transition to the Hamilton equations of motion in terms of quaternions. This is in contrast to previous works by Maciejewski [78] and Morton [82] (see also Arribas et al. [3] and Borri et al. [30]), where undetermined inertia terms have been introduced in order to set up the quaternion-based Hamilton equations of motion.

In the present work, the quaternion-based Hamilton equations of motion serve as starting point for the design of an energy-momentum conserving time-stepping scheme, which has been recently derived in Betsch & Siebert [12]. Energy-momentum schemes are well-known for their advantageous numerical stability properties (see, for example, Gonzalez & Simo [54]). It is worth mentioning that the majority of previous works aiming at the design of conserving schemes for rigid body dynamics relies on the discretization of the classical Euler equations (see, e.g., Simo & Wong [97], Lens et al. [74], Krysl [67] and Romero [91]).

The present energy-momentum conserving time-stepping scheme based on the Hamilton equations of motion described with quaternions will be tested within a steady precession of a gyro top as numerical example. Finally, concluding remarks regarding the application of quaternions for the formulation of rigid body dynamics and the problematic extension to flexible multibody dynamics within

an energy-momentum scheme will be given. Furthermore, it will be stated that the quaternion formulation will not serve as basis for the formulation of optimal control problems in Chapters 6, 7 and 8 due to the mentioned problems.

5.1. Basics of quaternions

Below, the essential properties of quaternions needed for the rest of this chapter will be given. More background on this topic can be found in Altmann [2] and Kuipers [68].

A quaternion $\mathbb{q} \in \mathbb{R}^4$ consists of a scalar part $q_0 \in \mathbb{R}$ and a vector part $\boldsymbol{q} \in \mathbb{R}^3$, thus

$$\mathbb{q} = \begin{bmatrix} q_0 \\ \boldsymbol{q} \end{bmatrix} \tag{5.1}$$

The orientation of rigid bodies in space can be specified by a subgroup of the quaternions, which is the group of quaternions with unit length given by

$$S^3 = \{\mathbb{q} \in \mathbb{R}^4 \,|\, |\mathbb{q}| = 1\} \tag{5.2}$$

As previously done in Chou [39] and Kuipers [68] a matrix representation of quaternions will be chosen in the following. Accordingly, the product of two quaternions is defined by

$$\mathbb{q} \circ \mathbb{p} = \boldsymbol{Q}_l(\mathbb{q})\, \mathbb{p} = \boldsymbol{Q}_r(\mathbb{p})\, \mathbb{q} \tag{5.3}$$

where the 4×4 matrices $\boldsymbol{Q}_l$ and $\boldsymbol{Q}_r$ are given by

$$\begin{aligned} \boldsymbol{Q}_l(\mathbb{q}) &= \begin{bmatrix} \mathbb{q} & \boldsymbol{E}_2(\mathbb{q})^T \end{bmatrix} = q_0\, \boldsymbol{I}_4 + \overset{+}{\boldsymbol{q}} \\ \boldsymbol{Q}_r(\mathbb{q}) &= \begin{bmatrix} \mathbb{q} & \boldsymbol{E}_1(\mathbb{q})^T \end{bmatrix} = q_0\, \boldsymbol{I}_4 + \bar{\boldsymbol{q}} \end{aligned} \tag{5.4}$$

In this connection, the 3×4 matrices

$$\begin{aligned} \boldsymbol{E}_1(\mathbb{q}) &= \begin{bmatrix} -\boldsymbol{q} & q_0 \boldsymbol{I}_3 + \hat{\boldsymbol{q}} \end{bmatrix} \\ \boldsymbol{E}_2(\mathbb{q}) &= \begin{bmatrix} -\boldsymbol{q} & q_0 \boldsymbol{I}_3 - \hat{\boldsymbol{q}} \end{bmatrix} \end{aligned} \tag{5.5}$$

as well as the 4×4 skew-symmetric matrices

$$\begin{aligned} \overset{+}{\boldsymbol{q}} &= \begin{bmatrix} 0 & -\boldsymbol{q}^T \\ \boldsymbol{q} & \hat{\boldsymbol{q}} \end{bmatrix} \\ \bar{\boldsymbol{q}} &= \begin{bmatrix} 0 & -\boldsymbol{q}^T \\ \boldsymbol{q} & -\hat{\boldsymbol{q}} \end{bmatrix} \end{aligned} \tag{5.6}$$

have to be introduced.

Introducing rotations described with unit quaternions, one may start with the Euler-Theorem, which states that a rotation can be specified by a rotation axis

given by an unit vector $\boldsymbol{n} \in \mathbb{R}^3$ and a rotation angle $\theta \in \mathbb{R}$. Furthermore, the corresponding rotation vector $\boldsymbol{\theta} \in \mathbb{R}^3$ is given by $\boldsymbol{\theta} = \theta\, \boldsymbol{n}$. The related unit quaternion $\mathbb{q} \in S^3$ can be calculated by application of the exponential map $\exp_{S^3} : \mathbb{R}^3 \to S^3$ via the formula

$$\mathbb{q} = \exp_{\mathsf{S}^3} \begin{bmatrix} 0 \\ \frac{1}{2}\boldsymbol{\theta} \end{bmatrix} = \begin{bmatrix} \cos\left(\frac{\theta}{2}\right) \\ \sin\left(\frac{\theta}{2}\right) \boldsymbol{n} \end{bmatrix} \tag{5.7}$$

The exponential map can also be written in matrix form, that is

$$\boldsymbol{Q}_l(\mathbb{q}) = \exp_{O(4)} \left(\frac{1}{2} \overset{+}{\boldsymbol{\theta}} \right) = \cos\left(\frac{\theta}{2}\right) \boldsymbol{I}_4 + \sin\left(\frac{\theta}{2}\right) \overset{+}{\boldsymbol{n}} \tag{5.8}$$

Additionally, the rotation matrix can be obtained by use of

$$\boldsymbol{R}(\mathbb{q}) = \boldsymbol{E}_1(\mathbb{q})\, \boldsymbol{E}_2(\mathbb{q})^T \tag{5.9}$$

where the map $\boldsymbol{R} : S^3 \to SO(3)$ is often called the Euler-Rodrigues parametrization (see, for example, Marsden & Ratiu [79]). Differentiating Eq. (5.9) with respect to time yields the spatial and the convective angular velocity given by

$$\begin{aligned} \boldsymbol{\Omega} &= 2\, \boldsymbol{E}_2(\mathbb{q}) \dot{\mathbb{q}} \\ \boldsymbol{\omega} &= 2\, \boldsymbol{E}_1(\mathbb{q}) \dot{\mathbb{q}} \end{aligned} \tag{5.10}$$

The verification of the above given formulas in Eq. (5.7), Eq. (5.9) and Eq. (5.10) can be found in Betsch & Siebert [12].

5.2. Rigid body dynamics

In the following, a rigid body formulation in terms of quaternions will be introduced. This can be achieved by performing a size reduction of the rigid body formulation specified in Chapter 4. To this end, the connection between the quaternions $\mathbb{q} \in S^3 \subset \mathbb{R}^4$ and the directors summed up in the vector $\boldsymbol{q} \in Q_{\text{free}} \subset \mathbb{R}^9$ will be given. Thereby, only the rotational part of the configuration vector will be considered. Following the procedure elaborated in Betsch & Siebert [12], a mapping $\boldsymbol{f} : S^3 \to Q_{\text{free}}$ can be introduced, such that

$$\boldsymbol{q} = \boldsymbol{f}(\mathbb{q}) = \frac{1}{2}\, \boldsymbol{P}(\mathbb{q})\, \mathbb{q} \tag{5.11}$$

where the 9×4 matrix $\boldsymbol{P}(\mathbb{q})$ is given by

$$\boldsymbol{P}(\mathbb{q}) = \begin{bmatrix} 2\, \boldsymbol{E}_1(\mathbb{q})\, \bar{\boldsymbol{e}}_1 \\ 2\, \boldsymbol{E}_1(\mathbb{q})\, \bar{\boldsymbol{e}}_2 \\ 2\, \boldsymbol{E}_1(\mathbb{q})\, \bar{\boldsymbol{e}}_3 \end{bmatrix} \tag{5.12}$$

Differentiating Eq. (5.11) with respect to time yields the relation between the director-velocity and the quaternion-velocity given by

$$\dot{\boldsymbol{q}} = D\boldsymbol{f}(\mathbb{q})\,\dot{\mathbb{q}} = \boldsymbol{P}(\mathbb{q})\,\dot{\mathbb{q}} \tag{5.13}$$

hence the matrix $\boldsymbol{P}$ can be seen as null space matrix for the connection between directors and quaternions.

Now the kinetic energy of the rigid body can be written in terms of quaternions. Inserting Eq. (5.13) into Eq. (3.4) yields

$$T(\mathbb{q}, \dot{\mathbb{q}}) = \frac{1}{2}\,\dot{\mathbb{q}} \cdot \boldsymbol{M}_4(\mathbb{q})\,\dot{\mathbb{q}} \tag{5.14}$$

where the reduced, configuration-dependent 4×4 mass matrix is given by

$$\boldsymbol{M}_4(\mathbb{q}) = \boldsymbol{P}(\mathbb{q})^T\,\boldsymbol{M}_9\,\boldsymbol{P}(\mathbb{q}) \tag{5.15}$$

By application of Eq. (4.5), in the following the convective inertia tensor will be employed instead of the convective Euler tensor. Following the procedure illustrated in Betsch & Siebert [12], another representation of the mass matrix $\boldsymbol{M}_4$ can be achieved by introducing the extended convective inertia matrix

$$\boldsymbol{\mathcal{J}}_4 = \begin{bmatrix} \mathcal{J}_0 & \boldsymbol{0}^T \\ \boldsymbol{0} & \boldsymbol{\mathcal{J}} \end{bmatrix} \tag{5.16}$$

where $\mathcal{J}_0 = \frac{1}{2}\mathrm{tr}\boldsymbol{\mathcal{J}}$. Then the mass matrix $\boldsymbol{M}_4$ can be written in the alternative form

$$\boldsymbol{M}_4(\mathbb{q}) = 4\,\boldsymbol{Q}_l(\mathbb{q})\,\boldsymbol{\mathcal{J}}_4\,\boldsymbol{Q}_l(\mathbb{q})^T \tag{5.17}$$

The last representation of $\boldsymbol{M}_4$ is especially useful for calculating the inverse given by

$$\boldsymbol{M}_4(\mathbb{q})^{-1} = \frac{1}{4}\,\boldsymbol{Q}_l(\mathbb{q})\,\boldsymbol{\mathcal{J}}_4^{-1}\,\boldsymbol{Q}_l(\mathbb{q})^T \tag{5.18}$$

The inverse is necessary later for the transition to the Hamiltonian formulation of the equations of motion.

In the next step, the angular momentum of the rigid body introduced in Eq. (4.8) will be provided in terms of quaternions. In the present case of a pure rotational motion, the angular momentum assumes the form

$$\boldsymbol{J} = \frac{1}{2}\,\boldsymbol{E}_1(\mathbb{q})\,\boldsymbol{M}_4(\mathbb{q})\,\dot{\mathbb{q}} \tag{5.19}$$

Again, the details of the derivation can be found in Betsch & Siebert [12].

5.3. Hamilton equations of motion

The next aim is a Hamiltonian formulation of rigid body dynamics in terms of quaternions. To perform the transition to the Hamiltonian framework, the quaternion momentum will be introduced through

$$\mathbb{p} = \nabla_{\dot{\mathbb{q}}} T(\mathbb{q}, \dot{\mathbb{q}}) = \boldsymbol{M}_4(\mathbb{q})\, \dot{\mathbb{q}} \tag{5.20}$$

Inserting

$$\dot{\mathbb{q}} = \boldsymbol{M}_4(\mathbb{q})^{-1}\, \mathbb{p} \tag{5.21}$$

into Eq. (5.14) for the kinetic energy yields

$$T(\mathbb{q}, \mathbb{p}) = \frac{1}{2}\, \mathbb{p} \cdot \boldsymbol{M}_4(\mathbb{q})^{-1}\, \mathbb{p} \tag{5.22}$$

For later use, alternative representations of the kinetic energy will be supplied. After a short calculation, the relation

$$T(\mathbb{q}, \mathbb{p}) = \frac{1}{8}\, \mathbb{q} \cdot \boldsymbol{Q}_l(\mathbb{p})\, \boldsymbol{\mathcal{J}}_4^{-1}\, \boldsymbol{Q}_l(\mathbb{p})^T\, \mathbb{q} \tag{5.23}$$

can be achieved (see Betsch & Siebert [12]). Next, the augmented Hamilton function will be introduced by the equation

$$H_\gamma(\mathbb{q}, \mathbb{p}) = T(\mathbb{q}, \mathbb{p}) + V(\mathbb{q}) + \gamma\, \Phi(\mathbb{q}) \tag{5.24}$$

Here, it has been tacitly assumed that the external loads can be derived from a potential function $V(\mathbb{q})$. Moreover, $\Phi : \mathbb{R}^4 \to \mathbb{R}$ denotes a constraint function given by

$$\Phi(\mathbb{q}) = \frac{1}{2}(\mathbb{q} \cdot \mathbb{q} - 1) \tag{5.25}$$

Now the Hamiltonian form of the equations governing the rotational motion of a rigid body can be written as

$$\begin{aligned} \dot{\mathbb{q}} &= \nabla_{\mathbb{p}} H_\gamma(\mathbb{q}, \mathbb{p}) \\ \dot{\mathbb{p}} &= -\nabla_{\mathbb{q}} H_\gamma(\mathbb{q}, \mathbb{p}) \\ 0 &= \Phi(\mathbb{q}) \end{aligned} \tag{5.26}$$

Accordingly, the equations of motion assume the form of differential-algebraic equations (DAEs). Note that the algebraic constraint equation given in Eq. $(5.26)_3$ ensures that $\mathbb{q} \in S^3 \subset \mathbb{R}^4$. With regard to Eqs. (5.22) and (5.23) the differential part of the DAEs can also be written as

$$\begin{aligned} \dot{\mathbb{q}} &= \frac{1}{4}\, \boldsymbol{Q}_l(\mathbb{q})\, \boldsymbol{\mathcal{J}}_4^{-1}\, \boldsymbol{Q}_l(\mathbb{q})^T\, \mathbb{p} \\ \dot{\mathbb{p}} &= -\frac{1}{4}\, \boldsymbol{Q}_l(\mathbb{p})\, \boldsymbol{\mathcal{J}}_4^{-1}\, \boldsymbol{Q}_l(\mathbb{p})^T\, \mathbb{q} - \nabla V(\mathbb{q}) - \gamma\, \mathbb{q} \end{aligned} \tag{5.27}$$

It can be shown easily that the configuration-level constraint in Eq. (5.25) implies a hidden constraint on the momentum level. Correspondingly, the phase space coordinates $(\mathbb{q}, \mathbb{p})$ are constrained to lie on the manifold

$$P = \{(\mathbb{q}, \mathbb{p}) \in \mathbb{R}^4 \times \mathbb{R}^4 \,|\, \mathbb{q} \cdot \mathbb{q} = 1\,,\ \mathbb{q} \cdot \mathbb{p} = 0\} \tag{5.28}$$

see Betsch & Siebert [12] for a verification.

Rotational invariance and conservation of angular momentum It can be verified that the augmented Hamilton function of the free rigid body is invariant under rotations (see Betsch & Siebert [12] for the details). In particular, the constraint $\Phi(\mathbb{q})$ and the kinetic energy $T(\mathbb{q}, \mathbb{p})$ are invariant under the group S^3 acting by rotations on $(\mathbb{q}, \mathbb{p})$. Rotational invariance implies that

$$\begin{aligned} \Phi(\mathbb{q}^\sharp) &= \Phi(\mathbb{q}) \\ T(\mathbb{q}^\sharp, \mathbb{p}^\sharp) &= T(\mathbb{q}, \mathbb{p}) \end{aligned} \tag{5.29}$$

where

$$\begin{aligned} \mathbb{q}^\sharp &= \boldsymbol{Q}_l(\mathbb{r})\, \mathbb{q} \\ \mathbb{p}^\sharp &= \left(\boldsymbol{Q}_l(\mathbb{r})^T\right)^{-1} \mathbb{p} = \boldsymbol{Q}_l(\mathbb{r})\, \mathbb{p} \end{aligned} \tag{5.30}$$

for $\mathbb{r} \in S^3$. To verify the invariance of the kinetic energy, the proof of the invariance property of the quaternion product given by

$$\boldsymbol{Q}_l(\mathbb{q}^\sharp)^T\, \mathbb{p}^\sharp = \boldsymbol{Q}_l(\mathbb{q})^T\, \mathbb{p} \tag{5.31}$$

is required. For the free rigid body, the above invariance properties imply rotational invariance of the augmented Hamilton function, that is

$$H_\gamma\left(\exp_{O(4)}\left(\frac{\epsilon}{2}\overset{+}{\boldsymbol{\xi}}\right)\mathbb{q}\,,\, \exp_{O(4)}\left(\frac{\epsilon}{2}\overset{+}{\boldsymbol{\xi}}\right)\mathbb{p}\right) = H_\gamma(\mathbb{q}, \mathbb{p}) \tag{5.32}$$

for $\epsilon \in \mathbb{R}$ and $\boldsymbol{\xi} \in \mathbb{R}^3$. Here, the exponential map $\exp_{O(4)} : \mathbb{R}^3 \to O(4)$ is given by Eq. (5.8). The last equation leads to

$$\begin{aligned} \left.\frac{d}{d\epsilon}\right|_{\epsilon=0} H_\gamma\left(\exp_{O(4)}\left(\frac{\epsilon}{2}\overset{+}{\boldsymbol{\xi}}\right)\mathbb{q}\,,\, \exp_{O(4)}\left(\frac{\epsilon}{2}\overset{+}{\boldsymbol{\xi}}\right)\mathbb{p}\right) &= 0 \\ \frac{1}{2}\nabla_{\mathbb{q}} H_\gamma(\mathbb{q}, \mathbb{p}) \cdot \overset{+}{\boldsymbol{\xi}}\, \mathbb{q} + \frac{1}{2}\nabla_{\mathbb{p}} H_\gamma(\mathbb{q}, \mathbb{p}) \cdot \overset{+}{\boldsymbol{\xi}}\, \mathbb{p} &= 0 \end{aligned} \tag{5.33}$$

Rotational invariance of the augmented Hamilton function can be linked to the conservation of a momentum map $\boldsymbol{J} \in \mathbb{R}^3$. To see this, consider $J_\xi(\mathbb{q}, \mathbb{p}) = \boldsymbol{J}(\mathbb{q}, \mathbb{p}) \cdot \boldsymbol{\xi}$ and

$$\frac{d}{dt} J_\xi(\mathbb{q}, \mathbb{p}) = -\nabla_{\mathbb{p}} J_\xi(\mathbb{q}, \mathbb{p}) \cdot \nabla_{\mathbb{q}} H_\gamma(\mathbb{q}, \mathbb{p}) + \nabla_{\mathbb{q}} J_\xi(\mathbb{q}, \mathbb{p}) \cdot \nabla_{\mathbb{p}} H_\gamma(\mathbb{q}, \mathbb{p}) \tag{5.34}$$

Comparison of the last equation with Eq. $(5.33)_2$ leads to the conclusion that $J_\xi(\mathbb{q}, \mathbb{p})$ is a first integral, if the following conditions are satisfied:

$$\begin{aligned} \nabla_{\mathbb{p}} J_\xi(\mathbb{q}, \mathbb{p}) &= \frac{1}{2}\overset{+}{\boldsymbol{\xi}}\, \mathbb{q} \\ \nabla_{\mathbb{q}} J_\xi(\mathbb{q}, \mathbb{p}) &= -\frac{1}{2}\overset{+}{\boldsymbol{\xi}}\, \mathbb{p} \end{aligned} \tag{5.35}$$

The above equations can be solved by choosing

$$J_\xi(\mathbb{q}, \mathbb{p}) = \frac{1}{2}\, \mathbb{p} \cdot \overset{+}{\boldsymbol{\xi}}\, \mathbb{q} = \frac{1}{2}\, \mathbb{p} \cdot \boldsymbol{E}_1(\mathbb{q})^T \boldsymbol{\xi} \tag{5.36}$$

Consequently, the momentum map associated with rotational invariance of the system under consideration is given by

$$\boldsymbol{J}(\mathbb{q},\mathbb{p}) = \frac{1}{2}\,\boldsymbol{E}_1(\mathbb{q})\,\mathbb{p} \tag{5.37}$$

and thus is identical to the spatial angular momentum in Eq. (5.19).

A similar procedure has been applied in Marsden & Ratiu [79] for the derivation the common spatial angular momentum for particles.

Introduction of invariants Due to the rotational invariance of the kinetic energy $T(\mathbb{q},\mathbb{p})$, it is possible to reparametrize the kinetic energy in terms of appropriate invariants. The formulation with invariants is necessary for the conserving numerical discretization of the equations of motion. With regard to Eq. (5.31), invariants are given by

$$\boldsymbol{\pi}(\mathbb{q},\mathbb{p}) = \boldsymbol{Q}_l(\mathbb{q})^T\,\mathbb{p} \tag{5.38}$$

By application of those invariants, the kinetic energy can be written as

$$T(\mathbb{q},\mathbb{p}) = \tilde{T}\left(\boldsymbol{\pi}(\mathbb{q},\mathbb{p})\right) = \frac{1}{8}\,\boldsymbol{\pi}(\mathbb{q},\mathbb{p})\cdot\boldsymbol{\mathcal{J}}_4^{-1}\,\boldsymbol{\pi}(\mathbb{q},\mathbb{p}) \tag{5.39}$$

In anticipation of the conserving time discretization it is required to recast the differential part of the DAEs in Eq. (5.26) in terms of the invariants in Eq. (5.38). Accordingly, by application of Eq. (5.24), the Hamilton equations of motion in Eq. (5.26) can be written in the form

$$\begin{aligned}
\dot{\mathbb{q}} &= \left(\frac{\partial\boldsymbol{\pi}}{\partial\mathbb{p}}\right)^T\nabla\tilde{T}(\boldsymbol{\pi}) \\
\dot{\mathbb{p}} &= -\left(\frac{\partial\boldsymbol{\pi}}{\partial\mathbb{q}}\right)^T\nabla\tilde{T}(\boldsymbol{\pi}) - \nabla V(\mathbb{q}) - \gamma\,\nabla\Phi(\mathbb{q})
\end{aligned} \tag{5.40}$$

or alternatively

$$\begin{aligned}
\dot{\mathbb{q}} &= \frac{1}{4}\,\boldsymbol{Q}_l(\mathbb{q})\,\boldsymbol{\mathcal{J}}_4^{-1}\,\boldsymbol{\pi}(\mathbb{q},\mathbb{p}) \\
\dot{\mathbb{p}} &= -\frac{1}{4}\,\boldsymbol{Q}_l(\mathbb{p})\,\boldsymbol{\mathcal{J}}_4^{-1}\,\boldsymbol{\pi}(\mathbb{q},\mathbb{p}) - \nabla V(\mathbb{q}) - \gamma\,\mathbb{q}
\end{aligned} \tag{5.41}$$

Of course, the above equations are equivalent to those in Eq. (5.27).

5.4. Conserving discretization

Below, the time discretization of the DAEs given in Eq. (5.26) will be performed. To this end, the conserving one-step method due to Gonzalez [53], which fits into the framework of the mixed Galerkin method (specifically the mG(1) method) developed by Betsch & Steinmann [17], will be applied. Let the phase space

coordinates $(\mathfrak{q}_k, \mathfrak{p}_k) \in P$ at time t_k along with the step size h be given. Then approximations of the quantities $(\mathfrak{q}_{k+1}, \mathfrak{p}_{k+1}) \in \mathbb{R}^4 \times \mathbb{R}^4$ and $\gamma_{k,k+1} \in \mathbb{R}$ at time t_{k+1} follow from the scheme

$$\begin{aligned} \mathfrak{q}_{k+1} - \mathfrak{q}_k &= h\, \overline{\nabla}_{\mathfrak{p}} H_\gamma \left(\mathfrak{q}_k, \mathfrak{p}_k, \mathfrak{q}_{k+1}, \mathfrak{p}_{k+1} \right) \\ \mathfrak{p}_{k+1} - \mathfrak{p}_k &= -h\, \overline{\nabla}_{\mathfrak{q}} H_\gamma \left(\mathfrak{q}_k, \mathfrak{p}_k, \mathfrak{q}_{k+1}, \mathfrak{p}_{k+1} \right) \\ 0 &= \Phi(\mathfrak{q}_{k+1}) \end{aligned} \tag{5.42}$$

Here, $\overline{\nabla}_{\mathfrak{q}}$ and $\overline{\nabla}_{\mathfrak{p}}$ denote discrete derivatives in the sense of Gonzalez [52]. In particular, the scheme in Eq. (5.42) assumes the form

$$\begin{aligned} \mathfrak{q}_{k+1} - \mathfrak{q}_k &= \frac{h}{8} \boldsymbol{Q}_l(\mathfrak{q}_{k+\frac{1}{2}})\, \boldsymbol{\mathcal{J}}_4^{-1}\, [\boldsymbol{\pi}_k + \boldsymbol{\pi}_{k+1}] \\ \mathfrak{p}_{k+1} - \mathfrak{p}_k &= -\frac{h}{8} \boldsymbol{Q}_l(\mathfrak{p}_{k+\frac{1}{2}})\, \boldsymbol{\mathcal{J}}_4^{-1}\, [\boldsymbol{\pi}_k + \boldsymbol{\pi}_{k+1}] - h\, \overline{\nabla} V \left(\mathfrak{q}_k, \mathfrak{q}_{k+1} \right) \\ &\quad - h\, \gamma_{k,k+1}\, \mathfrak{q}_{k+\frac{1}{2}} \\ 0 &= \frac{1}{2} \left(\mathfrak{q}_{k+1} \cdot \mathfrak{q}_{k+1} - 1 \right) \end{aligned} \tag{5.43}$$

where the abbreviations

$$\boldsymbol{\pi}_k = \boldsymbol{\pi} \left(\mathfrak{q}_k, \mathfrak{p}_k \right) \qquad \text{and} \qquad \boldsymbol{\pi}_{k+1} = \boldsymbol{\pi} \left(\mathfrak{q}_{k+1}, \mathfrak{p}_{k+1} \right) \tag{5.44}$$

have been employed. Moreover, for the present purposes it suffices to choose $\overline{\nabla} V \left(\mathfrak{q}_k, \mathfrak{q}_{k+1} \right) = \nabla V \left(\mathfrak{q}_{k+\frac{1}{2}} \right)$. Note that the first two equations in Eq. (5.43) can be viewed as discrete counterparts of those in Eq. (5.41).

By design, the scheme given in Eq. (5.43) conserves both angular momentum and energy. In addition to that, the configuration-level constraint as well as the momentum-level constraint are satisfied also in the discrete case, that is $(\mathfrak{q}_{k+1}, \mathfrak{p}_{k+1}) \in P$ (see Betsch & Siebert [12] for a verification of both statements).

Implementation The scheme in Eq. (5.43) constitutes a system of nine nonlinear algebraic equations for the determination of $\mathfrak{q}_{k+1}, \mathfrak{p}_{k+1} \in \mathbb{R}^4$ and $\gamma_{k,k+1} \in \mathbb{R}$. Application of Newton's method leads to a generalized saddle point system, which has to be solved in each iteration. The solution of saddle point systems can be circumvented by eliminating the Lagrange-multiplier $\gamma_{k,k+1}$ from Eq. $(5.43)_2$. This task can be accomplished by applying the discrete null space method originally developed in Betsch [9] and Betsch & Leyendecker [11]. To achieve a first size reduction of the algebraic system in Eq. (5.43), use will be made of the 4×3 discrete null space matrix

$$\boldsymbol{P} \left(\mathfrak{q}_{k+\frac{1}{2}} \right) = \boldsymbol{E}_2 \left(\mathfrak{q}_{k+\frac{1}{2}} \right)^T \tag{5.45}$$

Premultiplication of Eq. $(5.43)_2$ by the transpose of the discrete null space matrix given in Eq. (5.45) yields

$$\begin{aligned} &\boldsymbol{P}\left(\mathfrak{q}_{k+\frac{1}{2}}\right)^T\left\{\mathbb{p}_{k+1}-\mathbb{p}_k\right\} \\ &=-\frac{h}{8}\,\boldsymbol{P}\left(\mathfrak{q}_{k+\frac{1}{2}}\right)^T\left\{\boldsymbol{Q}_l(\mathbb{p}_{k+\frac{1}{2}})\,\boldsymbol{\mathcal{J}}_4^{-1}\,[\boldsymbol{\pi}_k+\boldsymbol{\pi}_{k+1}]\right\}-h\,\boldsymbol{P}\left(\mathfrak{q}_{k+\frac{1}{2}}\right)^T\nabla V\left(\mathfrak{q}_{k+\frac{1}{2}}\right) \end{aligned} \tag{5.46}$$

Thus, the discrete constraint force is annihilated. Secondary, the reparametrization of the unknowns will be performed, that is

$$\mathfrak{q}_{k+1}(\boldsymbol{\theta})=\exp_{\mathsf{S}^3}\begin{bmatrix}0\\ \frac{1}{2}\,\boldsymbol{\theta}\end{bmatrix}\circ\mathfrak{q}_k \tag{5.47}$$

where the exponential map has been introduced in Eq. (5.7). Accordingly, the four original unknowns $\mathfrak{q}_{k+1}\in\mathbb{R}^4$ are replaced by $\boldsymbol{\theta}\in\mathbb{R}^3$, which plays the role of an incremental rotation vector. Note that the unit length constraint is identically satisfied by employing the reparametrization. To summarize, application of the discrete null space method leads to the reduced system of seven nonlinear algebraic equations consisting of Eq. $(5.43)_1$ and Eq. (5.46). In these equations $\mathfrak{q}_{k+1}$ is expressed in terms of $\boldsymbol{\theta}\in\mathbb{R}^3$ via the reparametrization in Eq. (5.47). The system of seven equations can be solved iteratively by applying Newton's method. Further details of the implementation can be found in Betsch & Siebert [12].

5.5. Steady precession of a gyro top

The numerical example deals with a heavy symmetrical top (see Fig. 5.1), which has originally been applied in Betsch & Leyendecker [11] within a director-based EM-scheme. In Betsch & Siebert [12], the results of the director-based EM-scheme have been compared with the newly developed EM-scheme based on quaternions. The corresponding results will be given in the following. Additionally, in the aforementioned work, the two EM-schemes have been compared with a quaternion-based variational integrator specified in Betsch & Siebert [12] and a momentum conserving scheme due to Simo & Wong [97]. With regard to the accuracy, the results of the two last-mentioned integrators lie between those of the two EM-schemes and thus will be neglected in the following.

Numerical experiments One point on the symmetry axis of the top is fixed to the origin of the inertial frame $\{\boldsymbol{e}_1,\boldsymbol{e}_2,\boldsymbol{e}_3\}$. The shape of the top is assumed to be a cone with height $H=0.1$ and radius $r=0.05$. The total mass of the top is given by $m=\frac{1}{3}\,\rho\,\pi\,r^2\,H$, where the mass density is assumed to be $\rho=2700$. The principal moments of inertia relative to the center of mass are given by $\bar{\mathcal{J}}_1=\bar{\mathcal{J}}_2=\frac{3\,m}{80}\,(4\,r^2+H^2)$ and $\bar{\mathcal{J}}_3=\frac{3\,m}{10}\,r^2$. The principal values of the convective inertia tensor relative to the point of attachment follow from

$$\mathcal{J}_1=\bar{\mathcal{J}}_1+m\,l^2\quad\text{and}\quad\mathcal{J}_3=\bar{\mathcal{J}}_3 \tag{5.48}$$

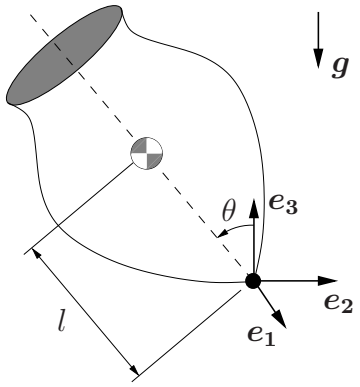

Figure 5.1.: Symmetrical top

where $l = \frac{3}{4} H$ denotes the distance between the center of mass and the origin. Gravity is acting on the top such that the potential energy function is given by

$$V(\mathbb{q}) = m\, g\, l\, \boldsymbol{d_3}(\mathbb{q}) \cdot \boldsymbol{e_3} \tag{5.49}$$

where $\boldsymbol{d_3}(\mathbb{q}) = \boldsymbol{R}(\mathbb{q})\, \boldsymbol{e_3}$ and $g = 9.81$ denotes the gravitational acceleration. A straightforward calculation applying the formulas given in Betsch & Siebert [12] yields the corresponding gradient. The initial configuration of the top $\mathbb{q}_0$ is specified by the unit vector $\boldsymbol{n}_0 = \boldsymbol{e}_1$ and the rotation angle $\theta_0 = \frac{\pi}{3}$ via the formula in Eq. (5.7). In order to provide an analytical reference solution, the case of precession with no nutation will be considered. Let θ be the angle of nutation, ω_p the precession rate and ω_s the spin rate. Specifically, the initial values will be chosen as

$$\theta = \theta_0 \quad \text{and} \quad \omega_p = 10 \tag{5.50}$$

The condition for steady precession is given by (see, for example, Moon [81, Section 5.3])

$$\omega_s = \frac{m\, g\, l}{\mathcal{J}_3\, \omega_p} + \frac{\mathcal{J}_1 - \mathcal{J}_3}{\mathcal{J}_3}\, \omega_p\, \cos\theta \tag{5.51}$$

Accordingly, application of the formula

$$\boldsymbol{\omega}_0 = \omega_p \boldsymbol{e_3} + \omega_s \boldsymbol{d_3} \tag{5.52}$$

yields the initial angular velocity vector.

In the present example both the total energy and the 3-component of the angular momentum vector are first integrals of the motion. The newly developed quaternion-based energy-momentum scheme does indeed conserve these quantities, independent of the step size. This is illustrated in the first diagram of Fig. 5.2 for a time step size of $h = 0.01$.

To evaluate the accuracy of the two EM-schemes, next the numerical results will be compared with the analytical reference solution. To this end, the position vector of the center of mass given by

$$\boldsymbol{\varphi} = l\, \boldsymbol{d}_3 = x\, \boldsymbol{e}_1 + y\, \boldsymbol{e}_2 + z\, \boldsymbol{e}_3 \tag{5.53}$$

In the case of steady precession, the center of mass of the top has to move on a circular trajectory in the plane $z = z(0) = l\,\cos(\theta_0)$. Accordingly, the analytical reference solution is given by

$$\boldsymbol{\varphi}_{\text{ref}} = l\,\sin(\theta_0)\sin(\omega_p t)\,\boldsymbol{e}_1 - l\,\sin(\theta_0)\cos(\omega_p t)\,\boldsymbol{e}_2 + l\,\cos(\theta_0)\,\boldsymbol{e}_3 \tag{5.54}$$

In the third and the forth diagrams of Fig. 5.2 the numerical results are compared with the analytical solutions. In particular, the results of both the quaternion-based and the director-based (see Betsch & Steinmann [16]) energy-momentum integrators are depicted for $h = 0.01$. While both integrators converge to the analytical solution, the director-based integrator yields a higher accuracy for a prescribed step size. This can also be seen from the log-log plot of the configuration error depicted in the second diagram of Fig. 5.2. Here, the relative error has been calculated via the formula

$$e = \frac{|\boldsymbol{\varphi}_{\text{ref}} - \boldsymbol{\varphi}|}{|\boldsymbol{\varphi}_{\text{ref}}|} \tag{5.55}$$

at $t = 1$.

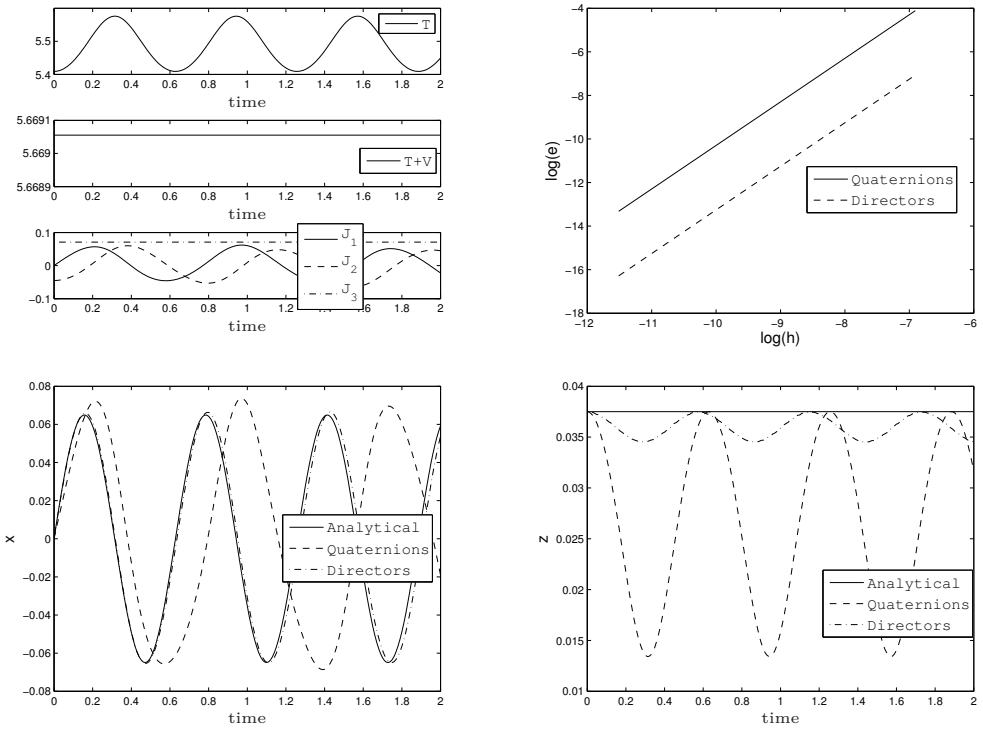

Figure 5.2.: Steady precession of a gyro top: 1. Conservation of the total energy and the 3-component of the angular momentum ($h = 0.01$). 2. Relative error at $t = 1s$ for the motion of the center of mass. 3.+4. Comparison between the numerical and the analytical solutions for the coordinates x and z of the center of mass ($h = 0.01$).

5.6. Concluding remarks on quaternions

In the past, quaternions have been preferred by virtue of their lower degree of redundancy (see Nikravesh [85], Haug [62]). However, it has been demonstrated that the quaternion formulation exhibits a higher degree of nonlinearity in comparison to the one with directors. This is basically due to the configuration dependent mass matrix. Furthermore, it has been experienced numerically that the quaternion formulation of rigid body dynamics is not faster than the formulation with the directors, despite its lower degree of redundancy. Concerning the accuracy, the EM-scheme based on quaternions can compete with other time-stepping schemes (see Betsch & Siebert [12]). Finally, quaternions may be applied for rigid body dynamics, but do not seem to be advantageous in comparison to directors, which lead to a strikingly simple formulation of the equations of motion.

Concerning the assembly of several rigid bodies in a multibody system, some constitutive words have to be said. First of all, the number of constraints needed for describing the kinematic joints do not depend on the choice of rotational parameters. Secondly, the formulation of external constraints exhibits a higher degree of nonlinearity in the quaternion formulation. Hence, the quaternion formulation does not have advantages in comparison to the director formulation within the extension of rigid body dynamics to multibody dynamics consisting of rigid components. Additionally, problems arise regarding the energy-momentum conserving discretization. The external constraints due to the lower kinematic pairs described in Betsch & Leyendecker [11] are partially specified with scalar products. The constraints that are not quadratic can be described with quadratic invariants. Hence, those constraints can be discretized in an energy and angular momentum conserving way. Other external constraints are specified as composition of linear and quadratic terms. The discretization of those constraints within the quaternion-based energy-momentum scheme turns out to be cumbersome.

Finally, apart from the issue of algorithmic energy-momentum conservation, the quaternions may have some benefits in flexible multibody dynamics. Works concerning the formulation of flexible multibody components like geometrically exact Cosserat rods were recently published (see, for example, Lang et al. [70] and Celledoni & Säfström [38]). Anyhow, the striking simplicity of the director formulation enables its wide applicability in flexible multibody dynamics (see, for example, Betsch & Steinmann [18], Leyendecker et al. [76] and Betsch et al. [10]). In this work, the quaternions will not be the redundant coordinates of choice in the following Chapters 6 and 7.

6. Optimal control with equations of motion in ODE-form

In the current chapter the topics of Chapters 2, 3, and 4 will be combined for the development of an energy and angular momentum consistent direct transcription method for the solution of optimal control problems in multibody dynamics. As described in Chapter 2, a direct transcription (or collocation) method is based on discretizing the underlying equations of motion and incorporating them into the cost function with Lagrange-multipliers to get the corresponding augmented cost function. To calculate the discrete necessary conditions of optimality, the derivatives of the discrete augmented cost function have to be provided either analytically or, at least, numerically. In direct transcription the arising system of equations is of huge size, but has a sparse structure. The procedure necessary for direct transcription is illustrated in detail for example in Betts [22].

The dynamics of the mechanical system will be described by use of the rotationless formulation, which facilitates the application of an energy-momentum consistent integration scheme. As described in Chapters 3 and 4, the corresponding equations of motion in a first step take the form of differential-algebraic equations of index 3. Subsequently, the equations will be reduced by application of the discrete null space method with nodal reparametrization (see Betsch & Leyendecker [11] for further details). Additionally, equations of motion based on generalized (or minimal) coordinates will be employed in connection with a midpoint scheme. While in the first case, the algebraic constraints arising in the continuous setting will be eliminated in the discrete setting, in the second case, the equations of motion are in purely differential form from the outset.

Different kinds of consistent integrators have been applied within optimal control problems in multibody dynamics in recent works. In Bottasso & Croce [31] an energy consistent direct transcription method has been elaborated for the solution of optimal control problems. In contrast to this, a variational integrator has been employed for the formulation of the forward dynamics in Leyendecker et al. [77] and Ober–Blöbaum et al. [86]. The arising methods, referred to as DMOC for unconstrained mechanical systems and DMOCC for constrained mechanical systems, are angular momentum consistent, but not energy consistent. An optimal control method which is based on direct transcription and an energy and angular momentum consistent discretization of the equations of motion can be found in the recent work of Betsch et al. [13] (see also Siebert & Betsch [94]).

6.1. Optimal control formulation: Direct transcription

The task that will be treated in this chapter, is minimizing the control effort which is necessary for moving a multibody system from a specific initial configuration into a specific final one. To solve such an optimal control problem, formulations of the cost function, the state vectors, boundary conditions for the configuration and the velocity, and a description of the solution procedure are required. For that purpose, some general informations which are independent from the differing numerical examples introduced later, will be given below.

Cost function For the aforementioned problem the integral costs needed for Eq. (2.3) are equal to the control effort which is to be minimized. This control effort will be specified by the quadratic function

$$\mathcal{L}(\boldsymbol{u}) = \frac{1}{2}\,\boldsymbol{u} \cdot \boldsymbol{u} \tag{6.1}$$

to be inserted into the cost function in Eq. (2.3) with the control vector $\boldsymbol{u}$ consisting of all generalized control forces and torques. While the formulation of the corresponding discrete cost function can be done in a straightforward way as described in Section 2.2, the extension to the discrete augmented cost function is much more challenging and will be detailed later within the different numerical examples.

Composition of the state vectors To achieve proper formulations of the augmented cost function in Eq. (2.5) and the discrete analogon in Eq. (2.15), some words have to be said about the composition of the state vectors $\boldsymbol{x}$. In the generalized coordinates formulation the state vector will be built up with the generalized configuration $\tilde{\boldsymbol{q}}$ and the generalized velocity $\tilde{\boldsymbol{v}}$, thus $\boldsymbol{x} = (\tilde{\boldsymbol{q}}, \tilde{\boldsymbol{v}})$. In contrast to that, only the vector of local coordinates $\boldsymbol{\theta}$ is used in the REM (see Chapter 3). The velocity will be obtained by the update process described in Eq. (3.33). Accordingly, the corresponding formula for the state vector reads $\boldsymbol{x} = \boldsymbol{\theta}$. While incremental rotations are widely-used in forward dynamics, which is due to the involved prevention of arising singularities, absolute rotations will be preferred for the optimal control problems treated in this work. This will be done for two reasons. Firstly, the use of absolute rotations has benefits concerning the boundary conditions on configuration level outlined in the next paragraph. In particular, the angles can be used directly without use of a representation by a sum, which would be necessary if incremental rotations are used. Secondly, the application of incremental rotations would require the calculation of more complicated gradients, because, in that case, every configuration vector depends on every preceding incremental angle. The arising gradients then have a lower-diagonal structure instead of a diagonal structure, thus are much less sparse.

Boundary conditions on configuration and velocity level As mentioned in the last paragraph, absolute rotations will be applied in the REM. This enables a direct formulation of the final conditions on configuration level. The application of incremental rotations would require final conditions on configuration level exhibiting an additive structure. While the final conditions on configuration level differ in the varying examples in this chapter, the ones on velocity level are each time equal to zero. In particular, rest-to-rest maneuvers will be considered in this chapter. In the generalized coordinates formulation, the latter gives rise to final conditions of the form

$$\boldsymbol{\psi}(\boldsymbol{x}_N) = \begin{bmatrix} \tilde{\boldsymbol{q}}_N - \tilde{\boldsymbol{q}}_f \\ \tilde{\boldsymbol{v}}_N - \tilde{\boldsymbol{v}}_f \end{bmatrix} \tag{6.2}$$

On the other hand, the final conditions in the REM take the form

$$\boldsymbol{\psi}(\boldsymbol{x}_N) = \begin{bmatrix} \boldsymbol{\theta}_N - \boldsymbol{\theta}_f \\ \boldsymbol{B}(\boldsymbol{q}_N)\boldsymbol{v}_N - \boldsymbol{B}(\boldsymbol{q}_f)\boldsymbol{v}_f \end{bmatrix} \tag{6.3}$$

where, according to Eq. (3.9), $\boldsymbol{B}$ maps the redundant velocity $\boldsymbol{v}$ to the corresponding generalized one $\boldsymbol{\nu}$. It is worth mentioning that the second part of Eq. (6.3) yields final conditions of the form $\boldsymbol{\nu}_N = \boldsymbol{\nu}_f$, which are not equivalent to the ones given by $\boldsymbol{v}_N = \boldsymbol{v}_f$. In particular, the zero final conditions on velocity level $\boldsymbol{\nu}_N = \boldsymbol{0}$ necessary for the rest-to-rest maneuvers treated in this chapter, do not automatically yield zero redundant velocities at the end, that is $\boldsymbol{v}_N = \boldsymbol{0}$. This is due to the fact that the redundant velocities do not lie on the correct manifold in the time discretization points. The reduced final conditions on velocity level given by the second part of Eq. (6.3) will be applied due to some benefits. Firstly, the reduced velocity boundary conditions yield better results than the redundant velocity boundary conditions. This is due to the fact that the reduced velocities do lie on the correct manifold in the time discretization points. Secondly, more important, the reduced final conditions on velocity level do not form a redundant set of equations, which sometimes produce a bad numerical convergence behaviour. In other words, the final conditions on velocity level fulfil the so-called 'linear independence constraint qualification' (see, for example, Diehl [41]). Obviously, the kinetic energy, which will be calculated with Eq. (3.4), is equal to zero at the beginning of the motion due to the chosen starting velocity $\boldsymbol{v}_0 = \boldsymbol{0}$, but typically not exactly equal to zero at the end of the motion. However, the kinetic energy at the final time obtained by Eq. (3.4) converges to zero for vanishing time step sizes.

Solution procedure Following the procedure described in Chapter 2, the discrete cost function, the boundary conditions on configuration and velocity level as well as the discrete equations of motion, which will be detailed subsequently within the differing numerical examples, are required for the discrete augmented cost function in Eq. (2.15). The discrete augmented cost function serves as basis for the direct transcription methods used in this chapter. While the necessary derivatives for the solution process may be calculated by use of numerical

difference methods, a fast solution procedure strongly depends on analytically calculated derivatives. If all first- and second-order derivatives of the discrete augmented cost function can be calculated analytically, the discrete necessary conditions of optimality can be calculated completely and, additionally, solved with a fast and efficient solution procedure. In the 3-link manipulator example, the first-order derivatives will be provided for both schemes. Details of the corresponding implementation will be given in Appendix A. The solution of the optimal control problem will be calculated by use of the SQP solver fmincon in MATLAB with provided gradients. It is worth mentioning that the calculation of the discrete necessary conditions of optimality by application of the procedure described in Appendix A yields similar results. Concerning the satellite as three-dimensional example, all derivatives will be calculated by use of the SQP solver fmincon in MATLAB, i.e. the corresponding gradients will not be provided. Consequently, the necessary calculation time for the solution of the optimal control problem is of huge size.

6.2. 3-link manipulator

The first example is the three degree of freedom planar robotic manipulator depicted in Fig. 6.1. While an underactuated version of the 3-link manipulator was previously applied as example for trajectory tracking problems (Betsch et al. [20]), here, the manipulator is fully actuated. In particular, an optimal movement of the manipulator for a rest-to-rest maneuver with given boundary conditions for the configuration will be calculated.

Rotationless formulation with reduction Each of the three robot arms will be modeled as planar rigid bodies, which makes possible the use of a simplified version of the rigid body kinematics given in Chapter 4. The vector of redundant coordinates $\boldsymbol{q} \in \mathbb{R}^{18}$ is built up by

$$\boldsymbol{q}^i = \begin{bmatrix} \boldsymbol{\varphi}^i \\ \boldsymbol{d}_1^i \\ \boldsymbol{d}_2^i \end{bmatrix} \tag{6.4}$$

for each of the three rigid bodies $i = 1, 2, 3$. Furthermore, the mass matrix $\boldsymbol{M} \in \mathbb{R}^{18\times 18}$ consists of the matrices pertaining to the planar rigid bodies

$$\boldsymbol{M}^i = \begin{bmatrix} m^i \boldsymbol{I}_2 & \boldsymbol{0}_2 & \boldsymbol{0}_2 \\ \boldsymbol{0}_2 & \mathcal{E}_1^i \boldsymbol{I}_2 & \boldsymbol{0}_2 \\ \boldsymbol{0}_2 & \boldsymbol{0}_2 & \mathcal{E}_2^i \boldsymbol{I}_2 \end{bmatrix} \tag{6.5}$$

Since the potential energy is given by

$$V(\boldsymbol{q}) = \sum_{i=1}^{3} m^i g \, \boldsymbol{\varphi}^i \cdot \boldsymbol{e}_2 \tag{6.6}$$

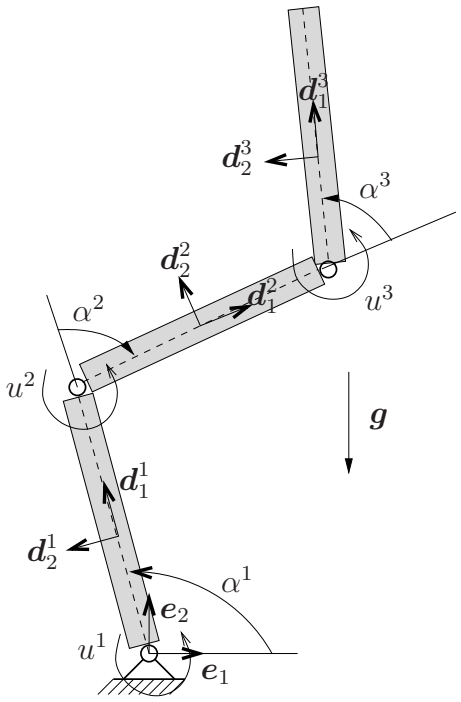

Figure 6.1.: 3-link manipulator

the corresponding gradient $\nabla_{\boldsymbol{q}} V \in \mathbb{R}^{18}$ is constant. Here, the vector of constraints $\boldsymbol{\Phi} \in \mathbb{R}^{15}$ consists of the internal ones due to rigidity

$$\boldsymbol{\Phi}_{\text{int}}(\boldsymbol{q}^i) = \begin{bmatrix} \frac{1}{2}(\boldsymbol{d}_1^i \cdot \boldsymbol{d}_1^i - 1) \\ \frac{1}{2}(\boldsymbol{d}_2^i \cdot \boldsymbol{d}_2^i - 1) \\ \boldsymbol{d}_1^i \cdot \boldsymbol{d}_2^i \end{bmatrix} \tag{6.7}$$

and the external ones due to the three revolute joints

$$\boldsymbol{\Phi}_{\text{ext}}(\boldsymbol{q}) = \begin{bmatrix} -\boldsymbol{\varphi}^1 + \dfrac{l_1}{2}\boldsymbol{d}_1^1 \\ -\boldsymbol{\varphi}^2 + l_1\boldsymbol{d}_1^1 + \dfrac{l_2}{2}\boldsymbol{d}_1^2 \\ -\boldsymbol{\varphi}^3 + l_1\boldsymbol{d}_1^1 + l_2\boldsymbol{d}_1^2 + \dfrac{l_3}{2}\boldsymbol{d}_1^3 \end{bmatrix} \tag{6.8}$$

The present 3-link manipulator can be regarded as open kinematic chain. A way for calculating null space matrices for kinematic chains has been proposed in Betsch & Leyendecker [11]. Following the procedure described in that work, one of the possible null space matrices for the elimination of the corresponding

constraint Jacobian $\boldsymbol{G} = \nabla_{\boldsymbol{q}} \boldsymbol{\Phi}$ is given by

$$\boldsymbol{P}(\boldsymbol{q}) = \begin{bmatrix} \frac{l_1}{2}\boldsymbol{d}_2^1 & \boldsymbol{0} & \boldsymbol{0} \\ \boldsymbol{d}_2^1 & \boldsymbol{0} & \boldsymbol{0} \\ -\boldsymbol{d}_1^1 & \boldsymbol{0} & \boldsymbol{0} \\ (l_1\boldsymbol{d}_2^1 + \frac{l_2}{2}\boldsymbol{d}_2^2) & \frac{l_2}{2}\boldsymbol{d}_2^2 & \boldsymbol{0} \\ \boldsymbol{d}_2^2 & \boldsymbol{d}_2^2 & \boldsymbol{0} \\ -\boldsymbol{d}_1^2 & -\boldsymbol{d}_1^2 & \boldsymbol{0} \\ (l_1\boldsymbol{d}_2^1 + l_2\boldsymbol{d}_2^2 + \frac{l_3}{2}\boldsymbol{d}_2^3) & (l_2\boldsymbol{d}_2^2 + \frac{l_3}{2}\boldsymbol{d}_2^3) & \frac{l_3}{2}\boldsymbol{d}_2^3 \\ \boldsymbol{d}_2^3 & \boldsymbol{d}_2^3 & \boldsymbol{d}_2^3 \\ -\boldsymbol{d}_1^3 & -\boldsymbol{d}_1^3 & -\boldsymbol{d}_1^3 \end{bmatrix} \tag{6.9}$$

Control torques $\boldsymbol{u} = (u_1, u_2, u_3)$ are employed at the base of the first link and the joints between the links one and two and the links two and three. The joint angles $\boldsymbol{\alpha} = (\alpha_1, \alpha_2, \alpha_3)$ are used as relative coordinates in the REM. The work of the control forces can be calculated by Eq. (4.13) with the transformation matrix $\boldsymbol{B}$ fulfilling the equation

$$\boldsymbol{B}(\boldsymbol{q})\, \boldsymbol{P}(\boldsymbol{q}) = \boldsymbol{I}_3 \tag{6.10}$$

The formulation of the REM does not make necessary a control input with the transformation matrix $\boldsymbol{B}$, due to similar observations as the ones at the end of Chapter 4. Nevertheless, the calculation of the work of the control forces with Eq. (4.13) requires $\boldsymbol{B}$. Additionally, the transformation matrix is necessary for the incorporation of joint-friction. Taking into account the rotation axes $\boldsymbol{n}^i = \boldsymbol{e}_3$ for $i = 1, 2, 3$, the transformation matrix for the 3-link manipulator takes the form

$$\boldsymbol{B}(\boldsymbol{q})^T = \frac{1}{2} \begin{bmatrix} \boldsymbol{0} & \boldsymbol{0} & \boldsymbol{0} \\ -\hat{\boldsymbol{d}}_1^1\, \boldsymbol{e}_3 & \hat{\boldsymbol{d}}_1^1\, \boldsymbol{e}_3 & \boldsymbol{0} \\ -\hat{\boldsymbol{d}}_2^1\, \boldsymbol{e}_3 & \hat{\boldsymbol{d}}_2^1\, \boldsymbol{e}_3 & \boldsymbol{0} \\ \boldsymbol{0} & \boldsymbol{0} & \boldsymbol{0} \\ \boldsymbol{0} & -\hat{\boldsymbol{d}}_1^2\, \boldsymbol{e}_3 & \hat{\boldsymbol{d}}_1^2\, \boldsymbol{e}_3 \\ \boldsymbol{0} & -\hat{\boldsymbol{d}}_2^2\, \boldsymbol{e}_3 & \hat{\boldsymbol{d}}_2^2\, \boldsymbol{e}_3 \\ \boldsymbol{0} & \boldsymbol{0} & \boldsymbol{0} \\ \boldsymbol{0} & \boldsymbol{0} & -\hat{\boldsymbol{d}}_1^3\, \boldsymbol{e}_3 \\ \boldsymbol{0} & \boldsymbol{0} & -\hat{\boldsymbol{d}}_2^3\, \boldsymbol{e}_3 \end{bmatrix} \tag{6.11}$$

where the last components of the vectors resulting from the cross-products are automatically zero and thus will be neglected in the given planar multibody system.

For the transition to the energy and angular momentum consistent discrete setting, the contravariant evaluated transformation matrix $\boldsymbol{B}$ is necessary. While the proceeding for the calculation has been given in Section 4.1 for a single rigid body in space, now the same will be presented for the planar manipulator with its three revolute joints. In a first step, discrete rotation matrices will be calculated from the covariant directors for each of the three rigid bodies, that is

$$\boldsymbol{R}_{k+\frac{1}{2}} = \begin{bmatrix} (\boldsymbol{d}_1)_{k+\frac{1}{2}} & (\boldsymbol{d}_2)_{k+\frac{1}{2}} \end{bmatrix} \tag{6.12}$$

In a second step, discrete rotation matrices consisting of contravariant directors will be calculated by application of the formula

$$\boldsymbol{R}^{k+\frac{1}{2}} = \boldsymbol{R}_{k+\frac{1}{2}}^{-T} \tag{6.13}$$

Finally, for each of the three rigid bodies, the contravariant directors can be obtained by

$$\left[(\boldsymbol{d}^1)^{k+\frac{1}{2}} \quad (\boldsymbol{d}^2)^{k+\frac{1}{2}}\right] = \boldsymbol{R}^{k+\frac{1}{2}} \tag{6.14}$$

Notice that the upper index, at this point, denotes the contravariance of the directors, not the number of the rigid body. A total number of six contravariant directors have to be calculated that way and inserted into Eq. (6.11) to obtain the contravariant evaluated transformation matrix $\boldsymbol{B}(\boldsymbol{q}^{k+\frac{1}{2}})$.

In the case of the 3-link manipulator, the function $\boldsymbol{f}$, which has to be inserted into Eq. (2.1), takes the form of Eq. (3.20) with the matrices given in this section. Finally, the transition to the discrete setting can be done straightforwardly as described in Section 3.2.

Generalized coordinates formulation Alternatively to the redundant coordinates described before, the 3-link manipulator can also be specified by the three generalized coordinates

$$\tilde{\boldsymbol{q}} = \begin{bmatrix}\alpha_1 & \alpha_2 & \alpha_3\end{bmatrix}^T \tag{6.15}$$

where $\alpha_1, \alpha_2, \alpha_3$ are the joint angles. As described in Section 3.3, the necessary matrices can be derived by reduction from the redundant formulation by use of the null space matrix $\boldsymbol{P}$. For that purpose, the relation between the generalized and the redundant coordinates is given by

$$\boldsymbol{q} = \boldsymbol{q}(\tilde{\boldsymbol{q}}) = \begin{bmatrix}\boldsymbol{F}^1 & \boldsymbol{F}^2 & \boldsymbol{F}^3\end{bmatrix}^T \tag{6.16}$$

with

$$\begin{aligned}
\boldsymbol{F}^1 &= \begin{bmatrix}\frac{l_1}{2}c_1 & \frac{l_1}{2}s_1 & c_1 & s_1 & -s_1 & c_1\end{bmatrix} \\
\boldsymbol{F}^2 &= \begin{bmatrix}(l_1c_1 + \frac{l_2}{2}c_{12}) & (l_1s_1 + \frac{l_2}{2}s_{12}) & c_{12} & s_{12} & -s_{12} & c_{12}\end{bmatrix} \\
\boldsymbol{F}^3 &= \begin{bmatrix}(l_1c_1 + l_2c_{12} + \frac{l_3}{2}c_{123}) & (l_1s_1 + l_2s_{12} + \frac{l_3}{2}s_{123}) & c_{123} & s_{123} & -s_{123} & c_{123}\end{bmatrix}
\end{aligned} \tag{6.17}$$

In Eq. (6.17), the abbreviations $c_i = \cos(\alpha_i)$, $c_{ij} = \cos(\alpha_i + \alpha_j)$, and $c_{ijk} = \cos(\alpha_i + \alpha_j + \alpha_k)$ are used. Analogous ones are used for the sinus function. Eq. (6.9), together with Eq. (6.16) can be used for the derivation of a null space matrix $\boldsymbol{P}(\tilde{\boldsymbol{q}})$, which then takes the form

$$\boldsymbol{P}(\tilde{\boldsymbol{q}}) = \begin{bmatrix}\boldsymbol{F}^1_{,\alpha_1} & \boldsymbol{F}^2_{,\alpha_1} & \boldsymbol{F}^3_{,\alpha_1} \\ \boldsymbol{F}^1_{,\alpha_2} & \boldsymbol{F}^2_{,\alpha_2} & \boldsymbol{F}^3_{,\alpha_2} \\ \boldsymbol{F}^1_{,\alpha_3} & \boldsymbol{F}^2_{,\alpha_3} & \boldsymbol{F}^3_{,\alpha_3}\end{bmatrix}^T \tag{6.18}$$

with

$$
\begin{aligned}
\boldsymbol{F}^1_{,\alpha_1} &= \begin{bmatrix} -\frac{l_1}{2}s_1 & \frac{l_1}{2}c_1 & -s_1 & c_1 & -c_1 & -s_1 \end{bmatrix} \\
\boldsymbol{F}^2_{,\alpha_1} &= \begin{bmatrix} (-l_1 s_1 - \frac{l_2}{2}s_{12}) & (l_1 c_1 + \frac{l_2}{2}c_{12}) & -s_{12} & c_{12} & -c_{12} & -s_{12} \end{bmatrix} \\
\boldsymbol{F}^2_{,\alpha_2} &= \begin{bmatrix} -\frac{l_2}{2}s_{12} & \frac{l_2}{2}c_{12} & -s_{12} & c_{12} & -c_{12} & -s_{12} \end{bmatrix} \\
\boldsymbol{F}^3_{,\alpha_1} &= \begin{bmatrix} (-l_1 s_1 - l_2 s_{12} - \frac{l_3}{2}s_{123}) & (l_1 c_1 + l_2 c_{12} + \frac{l_3}{2}c_{123}) & -s_{123} & c_{123} & -c_{123} & -s_{123} \end{bmatrix} \\
\boldsymbol{F}^3_{,\alpha_2} &= \begin{bmatrix} (-l_2 s_{12} - \frac{l_3}{2}s_{123}) & (l_2 c_{12} + \frac{l_3}{2}c_{123}) & -s_{123} & c_{123} & -c_{123} & -s_{123} \end{bmatrix} \\
\boldsymbol{F}^3_{,\alpha_3} &= \begin{bmatrix} -\frac{l_3}{2}s_{123} & \frac{l_3}{2}c_{123} & -s_{123} & c_{123} & -c_{123} & -s_{123} \end{bmatrix}
\end{aligned}
\tag{6.19}
$$

and the vanishing components $\boldsymbol{F}^1_{,\alpha_2} = \boldsymbol{F}^1_{,\alpha_3} = \boldsymbol{F}^2_{,\alpha_3} = \boldsymbol{0}$. Furthermore, the matrix $\dot{\boldsymbol{P}}(\tilde{\boldsymbol{q}}, \tilde{\boldsymbol{v}})$ containing the time derivatives of the components of $\boldsymbol{P}(\tilde{\boldsymbol{q}})$ takes the form

$$
\dot{\boldsymbol{P}}(\tilde{\boldsymbol{q}}, \tilde{\boldsymbol{v}}) = \begin{bmatrix} \dot{\boldsymbol{F}}^1_{,\alpha_1} & \dot{\boldsymbol{F}}^2_{,\alpha_1} & \dot{\boldsymbol{F}}^3_{,\alpha_1} \\ \dot{\boldsymbol{F}}^1_{,\alpha_2} & \dot{\boldsymbol{F}}^2_{,\alpha_2} & \dot{\boldsymbol{F}}^3_{,\alpha_2} \\ \dot{\boldsymbol{F}}^1_{,\alpha_3} & \dot{\boldsymbol{F}}^2_{,\alpha_3} & \dot{\boldsymbol{F}}^3_{,\alpha_3} \end{bmatrix}^T \tag{6.20}
$$

with

$$
\begin{aligned}
\dot{\boldsymbol{F}}^1_{,\alpha_1} &= \begin{bmatrix} -\frac{l_1}{2}v_1 c_1 & -\frac{l_1}{2}v_1 s_1 & -v_1 c_1 & -v_1 s_1 & v_1 s_1 & -v_1 c_1 \end{bmatrix} \\
\dot{\boldsymbol{F}}^2_{,\alpha_1} &= \begin{bmatrix} -v_1(l_1 c_1 + \frac{l_2}{2}c_{12}) - \frac{l_2}{2}v_2 c_{12} \\ -v_1(l_1 s_1 + \frac{l_2}{2}s_{12}) - \frac{l_2}{2}v_2 s_{12} \\ -v_1 c_{12} - v_2 c_{12} \\ -v_1 s_{12} - v_2 s_{12} \\ v_1 s_{12} + v_2 s_{12} \\ -v_1 c_{12} - v_2 c_{12} \end{bmatrix}^T \quad \dot{\boldsymbol{F}}^2_{,\alpha_2} = \begin{bmatrix} -\frac{l_2}{2}v_1 c_{12} - \frac{l_2}{2}v_2 c_{12} \\ -\frac{l_2}{2}v_1 s_{12} - \frac{l_2}{2}v_2 s_{12} \\ -v_1 c_{12} - v_2 c_{12} \\ -v_1 s_{12} - v_2 s_{12} \\ v_1 s_{12} + v_2 s_{12} \\ -v_1 c_{12} - v_2 c_{12} \end{bmatrix}^T \\
\dot{\boldsymbol{F}}^3_{,\alpha_1} &= \begin{bmatrix} -v_1(l_1 c_1 + l_2 c_{12} + \frac{l_3}{2}c_{123}) - v_2(l_2 c_{12} + \frac{l_3}{2}c_{123}) - \frac{l_3}{2}v_3 c_{123} \\ -v_1(l_1 s_1 + l_2 s_{12} + \frac{l_3}{2}s_{123}) - v_2(l_2 s_{12} + \frac{l_3}{2}s_{123}) - \frac{l_3}{2}v_3 s_{123} \\ -v_1 c_{123} - v_2 c_{123} - v_3 c_{123} \\ -v_1 s_{123} - v_2 s_{123} - v_3 s_{123} \\ v_1 s_{123} + v_2 s_{123} + v_3 s_{123} \\ -v_1 c_{123} - v_2 c_{123} - v_3 c_{123} \end{bmatrix}^T \\
\dot{\boldsymbol{F}}^3_{,\alpha_2} &= \begin{bmatrix} -v_1(l_2 c_{12} + \frac{l_3}{2}c_{123}) - v_2(l_2 c_{12} + \frac{l_3}{2}c_{123}) - \frac{l_3}{2}v_3 c_{123} \\ -v_1(l_2 s_{12} + \frac{l_3}{2}s_{123}) - v_2(l_2 s_{12} + \frac{l_3}{2}s_{123}) - \frac{l_3}{2}v_3 s_{123} \\ -v_1 c_{123} - v_2 c_{123} - v_3 c_{123} \\ -v_1 s_{123} - v_2 s_{123} - v_3 s_{123} \\ v_1 s_{123} + v_2 s_{123} + v_3 s_{123} \\ -v_1 c_{123} - v_2 c_{123} - v_3 c_{123} \end{bmatrix}^T \\
\dot{\boldsymbol{F}}^3_{,\alpha_3} &= \begin{bmatrix} -\frac{l_3}{2}v_1 c_{123} - \frac{l_3}{2}v_2 c_{123} - \frac{l_3}{2}v_3 c_{123} \\ -\frac{l_3}{2}v_1 s_{123} - \frac{l_3}{2}v_2 s_{123} - \frac{l_3}{2}v_3 s_{123} \\ -v_1 c_{123} - v_2 c_{123} - v_3 c_{123} \\ -v_1 s_{123} - v_2 s_{123} - v_3 s_{123} \\ v_1 s_{123} + v_2 s_{123} + v_3 s_{123} \\ -v_1 c_{123} - v_2 c_{123} - v_3 c_{123} \end{bmatrix}^T
\end{aligned}
\tag{6.21}
$$

and the vanishing components $\dot{\boldsymbol{F}}^1_{,\alpha_2} = \dot{\boldsymbol{F}}^1_{,\alpha_3} = \dot{\boldsymbol{F}}^2_{,\alpha_3} = \boldsymbol{0}$. The three velocities v_1, v_2, and v_3 therein are the components of the generalized velocity vector $\tilde{\boldsymbol{v}} = (\dot{\alpha}_1, \dot{\alpha}_2, \dot{\alpha}_3)$. Finally, the transformation matrix $\boldsymbol{B}(\tilde{\boldsymbol{q}})$ can be calculated by use of Eq. (6.11) together with Eq. (6.16). Alternatively, the relation in Eq. (6.10) can be employed directly. At this point, all matrices are provided for the function given in Eq. (3.37) to be inserted into the continuous augmented cost function given in Eq. (2.5). Here again, the transition to the discrete setting has been done by applying the midpoint rule, which yields the Eq. (3.40).

Numerical experiments The mass and geometric properties of the 3-link manipulator are summarized in Table 6.1. The total time of the movement is $t_f = 3$.

body	m	$\mathcal{E}_1$	$\mathcal{E}_2$	l	$\boldsymbol{\alpha}_0$	$\boldsymbol{\alpha}_f$
1	30	1.225	143.3027	7	$\frac{\pi}{2}$	$\frac{\pi}{2}$
2	25	1.0208	88.0208	6	$-\frac{\pi}{2}$	0
3	10	0.4083	60.2083	8	$\frac{\pi}{2}$	0

Table 6.1.: Inertia and geometric data for the 3-link manipulator.

The system starts and ends at rest. For both formulations the starting point $\boldsymbol{q}_0$ was taken as initial guess for the configuration for all times $\boldsymbol{q}_k, k = 1, ..., N$. Both the generalized coordinates formulation with midpoint evaluation and the REM work for large time step sizes. In this example, the chosen time step size was $h = \frac{t_f}{N}$ with $N = 20$.

Two different problems for the optimal control of the 3-link manipulator will be treated. In the first version, the third component of the control vector is enforced to be nonnegative. This makes necessary the incorporation of the inequality constraint $u_3 \geq 0$. In the second version it is assumed that linear viscous damping is acting in the three revolute joints of the manipulator. The corresponding damping constants are given by $k_i = 300$ for $i = 1, 2, 3$.

Finally, snapshots for the optimal movement are given in Fig. 6.2 for the 3-link manipulator with limited control and in Fig. 6.3 for the 3-link manipulator with linear viscous friction. Further numerical results for both cases are given in Fig. 6.4 and Fig. 6.5. Furthermore, the basic conservation property of the system is given as sum of the total energy $T + V$ and the work of the control forces W in the first case (see Fig. 6.4) and as sum of the total energy $T + V$, the work of the control forces W and the dissipation D due to the linear viscous friction in the second case (see Fig. 6.5).

6.3. Satellite

Here again, the spacecraft which has been introduced in Section 4.3, will be investigated. In contrast to Section 4.3, where a forward dynamics problem of

Figure 6.2.: Optimal control of a 3-link manipulator with limited control ($N = 20$): Snapshots for the optimal movement at $t \in \{0, 0.75, 1.5, 2.25, 3\}$ for REM.

Figure 6.3.: Optimal control of a 3-link manipulator with linear viscous friction ($N = 20$): Snapshots for the optimal movement at $t \in \{0, 0.75, 1.5, 2.25, 3\}$ for REM.

the satellite has been studied with application of the BEM, here, an optimal control problem will be analyzed. For that purpose, the REM will serve as basis for the formulation of the equations of motion. Formerly, this example was used in Leyendecker et al. [77] within optimal control. In contrast to the aforementioned work, where a variational scheme was applied for the numerical integration, here, the EM-scheme will be employed. Additionally, the results will be compared with those of a formulation of the equations of motion in terms of Euler angles. Special attention will be concentrated on the consistency properties of the EM-scheme, that is the consistency of total angular momentum and the consistency of total energy.

Rotationless formulation with reduction Based on the rotationless formulation of the rigid body with rotors described in Section 4.3, the subsequent reduction process has to be specified. The constraint Jacobian $\boldsymbol{G} \in \mathbb{R}^{39\times 48}$ can be eliminated by the null space matrix $\boldsymbol{P} \in \mathbb{R}^{48\times 9}$. In addition to the six relative coordinates for the description of the movement of the main body, the three additional coordinates $\boldsymbol{\alpha} = (\alpha^1, \alpha^2, \alpha^3)$ are necessary for specifying the orientation of the rotors relative to the main body. Thus, the total vector of relative coordinates $\boldsymbol{\theta}$ consists of nine components. Furthermore, the work of the control forces can be calculated by Eq. (4.13) with the transformation matrix $\boldsymbol{B}$ fulfilling the equation

$$\boldsymbol{B}(\boldsymbol{q})\,\boldsymbol{P}(\boldsymbol{q}) = \boldsymbol{I}_9 \tag{6.22}$$

Notice that in the REM, the constant identity matrix $\boldsymbol{I}_9$ can be used directly for the control input. In the case of the satellite, the function $\boldsymbol{f}$, which has to be inserted into Eq. (2.1), takes the form of Eq. (3.20) with zero potential energy and the matrices mentioned before.

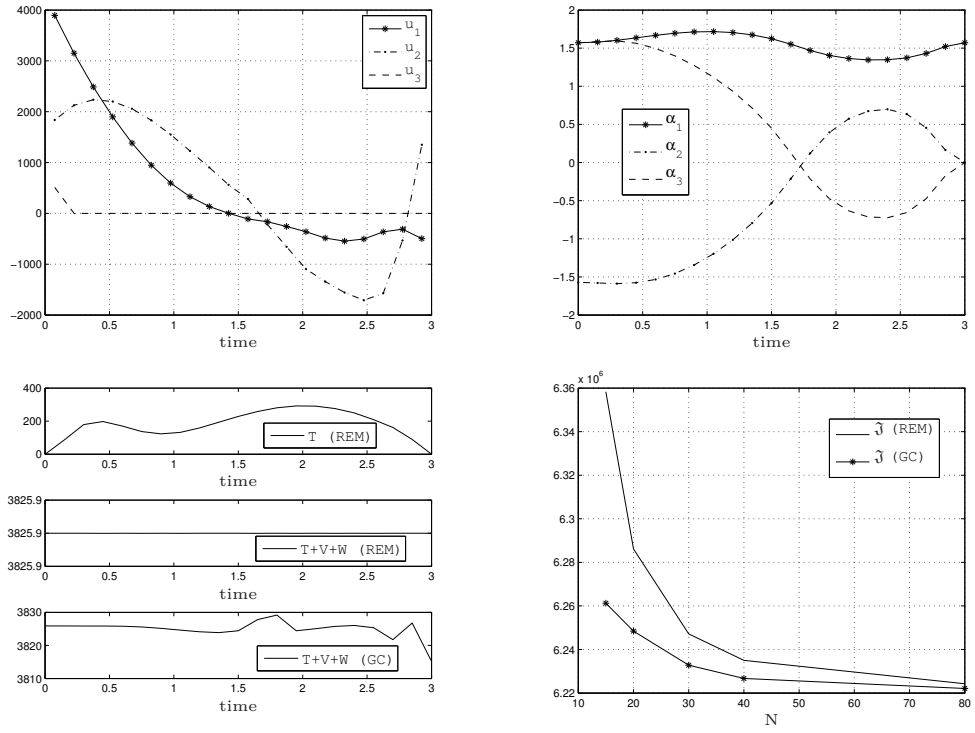

Figure 6.4.: Optimal control of a 3-link manipulator with limited control ($N = 20$): 1. Resulting torques for REM. 2. Resulting angles for REM. 3. Resulting kinetic energy for REM and energy consistency for both schemes. 4. Convergence of the total costs for both schemes.

Generalized coordinates formulation The rigid body with rotors can also be described by the vector of generalized coordinates

$$\tilde{\boldsymbol{q}} = \begin{bmatrix} \boldsymbol{\varphi}^T & \Phi & \Theta & \Psi & \boldsymbol{\alpha}^T \end{bmatrix}^T \tag{6.23}$$

where $\boldsymbol{\varphi}$ is the position vector for the center of mass of the main body. The Euler angles Φ, Θ, and Ψ together with a 3-1-3 rotation convention are used for describing the orientation of the main body. Additionally the angles $\alpha^i, i = 1, 2, 3$ are again used to specify the orientation of the rotors relative to the main body. Concerning the main body, the relation between generalized coordinates and redundant coordinates is given by

$$\boldsymbol{q}^0 = \boldsymbol{q}^0(\tilde{\boldsymbol{q}}) = \begin{bmatrix} \boldsymbol{\varphi} \\ \boldsymbol{d}_1^0 \\ \boldsymbol{d}_2^0 \\ \boldsymbol{d}_3^0 \end{bmatrix} = \begin{bmatrix} \boldsymbol{\varphi} \\ \cos\Psi\cos\Phi - \sin\Psi\cos\Theta\sin\Phi \\ \sin\Psi\cos\Phi + \cos\Psi\cos\Theta\sin\Phi \\ \sin\Theta\sin\Phi \\ -\cos\Psi\sin\Phi - \sin\Psi\cos\Theta\cos\Phi \\ -\sin\Psi\sin\Phi + \cos\Psi\cos\Theta\cos\Phi \\ \sin\Theta\cos\Phi \\ \sin\Psi\sin\Theta \\ -\cos\Psi\sin\Theta \\ \cos\Theta \end{bmatrix} \tag{6.24}$$

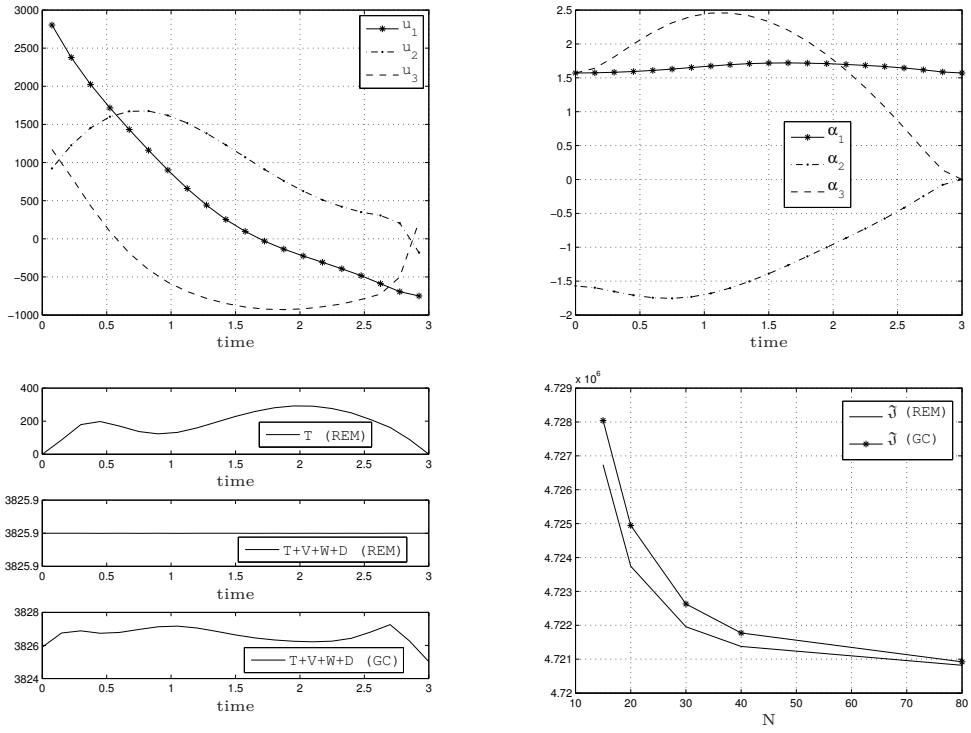

Figure 6.5.: Optimal control of a 3-link manipulator with linear viscous friction ($N = 20$): 1. Resulting torques for REM. 2. Resulting angles for REM. 3. Resulting kinetic energy for REM and energy consistency for both schemes. 4. Convergence of the total costs for both schemes.

For the three rotors, the relations are given by

$$\boldsymbol{q}^1 = \boldsymbol{q}^1(\tilde{\boldsymbol{q}}) = \begin{bmatrix} \boldsymbol{\varphi} + l_1\, \boldsymbol{d}_1^0 \\ \boldsymbol{d}_1^0 \\ \boldsymbol{d}_2^0 \cos\alpha^1 + \boldsymbol{d}_3^0 \sin\alpha^1 \\ -\boldsymbol{d}_2^0 \sin\alpha^1 + \boldsymbol{d}_3^0 \cos\alpha^1 \end{bmatrix} \tag{6.25}$$

$$\boldsymbol{q}^2 = \boldsymbol{q}^2(\tilde{\boldsymbol{q}}) = \begin{bmatrix} \boldsymbol{\varphi} + l_2\, \boldsymbol{d}_2^0 \\ \boldsymbol{d}_1^0 \cos\alpha^2 - \boldsymbol{d}_3^0 \sin\alpha^2 \\ \boldsymbol{d}_2^0 \\ \boldsymbol{d}_1^0 \sin\alpha^2 + \boldsymbol{d}_3^0 \cos\alpha^2 \end{bmatrix} \tag{6.26}$$

and

$$\boldsymbol{q}^3 = \boldsymbol{q}^3(\tilde{\boldsymbol{q}}) = \begin{bmatrix} \boldsymbol{\varphi} + l_3\, \boldsymbol{d}_3^0 \\ \boldsymbol{d}_1^0 \cos\alpha^3 + \boldsymbol{d}_2^0 \sin\alpha^3 \\ -\boldsymbol{d}_1^0 \sin\alpha^3 + \boldsymbol{d}_2^0 \cos\alpha^3 \\ \boldsymbol{d}_3^0 \end{bmatrix} \tag{6.27}$$

Eqs. (6.24), (6.25), (6.26), (6.27), together with the null space matrix $\boldsymbol{P}$, described by redundant coordinates, are necessary for the derivation of the null space matrix $\boldsymbol{P}(\tilde{\boldsymbol{q}})$. At this point, an explicit representation of the null space

matrix $\boldsymbol{P}(\tilde{\boldsymbol{q}})$, the matrix $\dot{\boldsymbol{P}}(\tilde{\boldsymbol{q}})$ as well as the transformation matrix $\boldsymbol{B}(\tilde{\boldsymbol{q}})$ will be renounced. While the null space matrix already takes a large shape, the corresponding time derivatives yield a much larger shape for $\dot{\boldsymbol{P}}(\tilde{\boldsymbol{q}})$. Hence, the analytical calculation of $\dot{\boldsymbol{P}}(\tilde{\boldsymbol{q}})$ necessitates the use of a computer algebra system such as Maple or the Symbolic Math Toolbox in MATLAB. Finally, the function $\boldsymbol{f}$ to be inserted into the continuous augmented cost function in Eq. (2.5) takes the form of Eq. (3.37) with zero gravity. Again, the midpoint rule will be applied for the transition to the discrete setting given in Eq. (3.40).

Numerical experiments The mass and geometric properties of the satellite are again those of Table 4.1. When applying the REM, the reorientation maneuver of the main body is enforced through the boundary conditions for the configuration $(\boldsymbol{\varphi}_0^0, \boldsymbol{\theta}_0^0, \boldsymbol{\alpha}_0) = (\mathbf{0}, \mathbf{0}, \mathbf{0})$ at $t_0 = 0$ and $\boldsymbol{\theta}_f^0 = \frac{\pi}{\sqrt{14}}(1, 2, 3)$ at $t_f = 5$. The orientation of the rotors and the position of the main body at the final time will not be enforced through the boundary conditions. When applying the Euler angles as generalized coordinates, the well-known problem of singularities has to be taken into account. A value of zero for the second Euler angle Θ has to be avoided. Using $(\Phi_0, \Theta_0, \Psi_0) = (2, 2, 2)$ as starting orientation and $(\Phi_f, \Theta_f, \Psi_f) = (4.7543, 1.6598, 0.7074)$ as final orientation for the main body leads to a singularity-free movement, which is equivalent the one achieved with the REM. Here again, a rest-to-rest maneuver will be investigated, thus $\boldsymbol{v}_0 = \boldsymbol{v}_f = \mathbf{0}$.

Two different versions of the satellite will be treated. While in the first one it is assumed that there is neither damping nor any limitation for the controls, in the second one it is assumed that there is linear viscous damping in the revolute joints between the base body and the three rotors. The corresponding damping constants are assumed to be $k_i = 100$ for $i = 1, 2, 3$.

Snapshots for the optimal movement of the rigid body with rotors are given in Fig. 6.6 for the frictionless case and in Fig. 6.7 for the friction-afflicted case. Further numerical results for both cases are given in Fig. 6.8 and Fig. 6.9. Due to the absence of gravity in the space craft maneuver, a basic conservation property is the sum of the kinetic energy T and the work of the control forces W for the frictionless satellite (see Fig. 6.8) and the sum of the kinetic energy T, the work of the control forces W and the dissipation D for the friction-afflicted satellite (see Fig. 6.9). An additional consistency property for this multibody system is the conservation of total angular momentum. Notice that the application of the REM leads to the desired consistency properties, the same is not valid for the formulation with Euler angles. Finally, the total costs in the REM are always higher than those in the Euler angles formulation. The latter seems to result from the errors in the REM arising from the midpoint evaluation of the comprised directors. As mentioned earlier in this thesis, the orthogonality constraints for the directors are fulfilled in the time nodes, but not in the midpoints of each time interval. The error is particularly high, if the multibody system contains

fast rotating components, which is the case in the present example. A way for circumventing this problem has been approached in the recent work Becker [8].

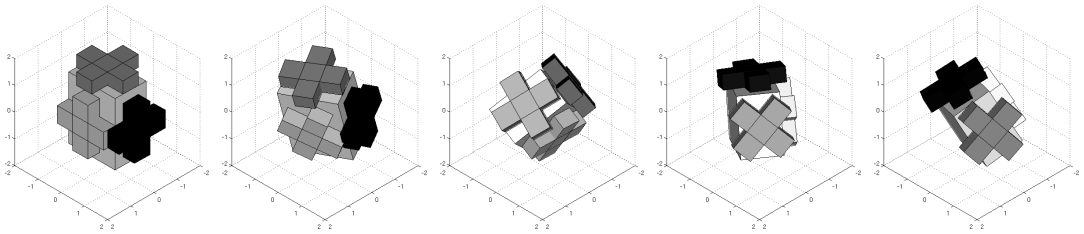

Figure 6.6.: Optimal control of a Satellite ($N = 20$): Snapshots for the optimal movement at $t \in \{0, 1.25, 2.5, 3.75, 5\}$ for REM.

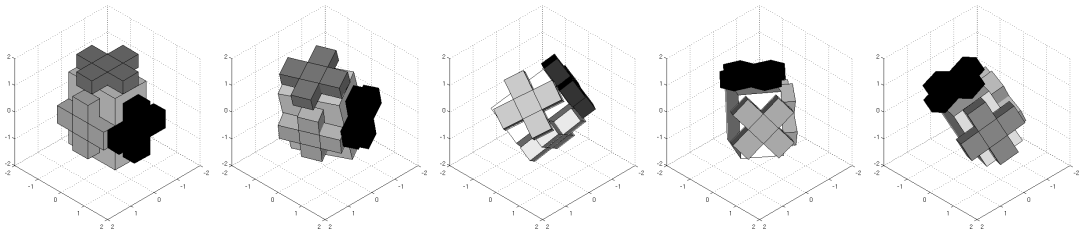

Figure 6.7.: Optimal control of a Satellite with linear viscous friction ($N = 20$): Snapshots for the optimal movement at $t \in \{0, 1.25, 2.5, 3.75, 5\}$ for REM.

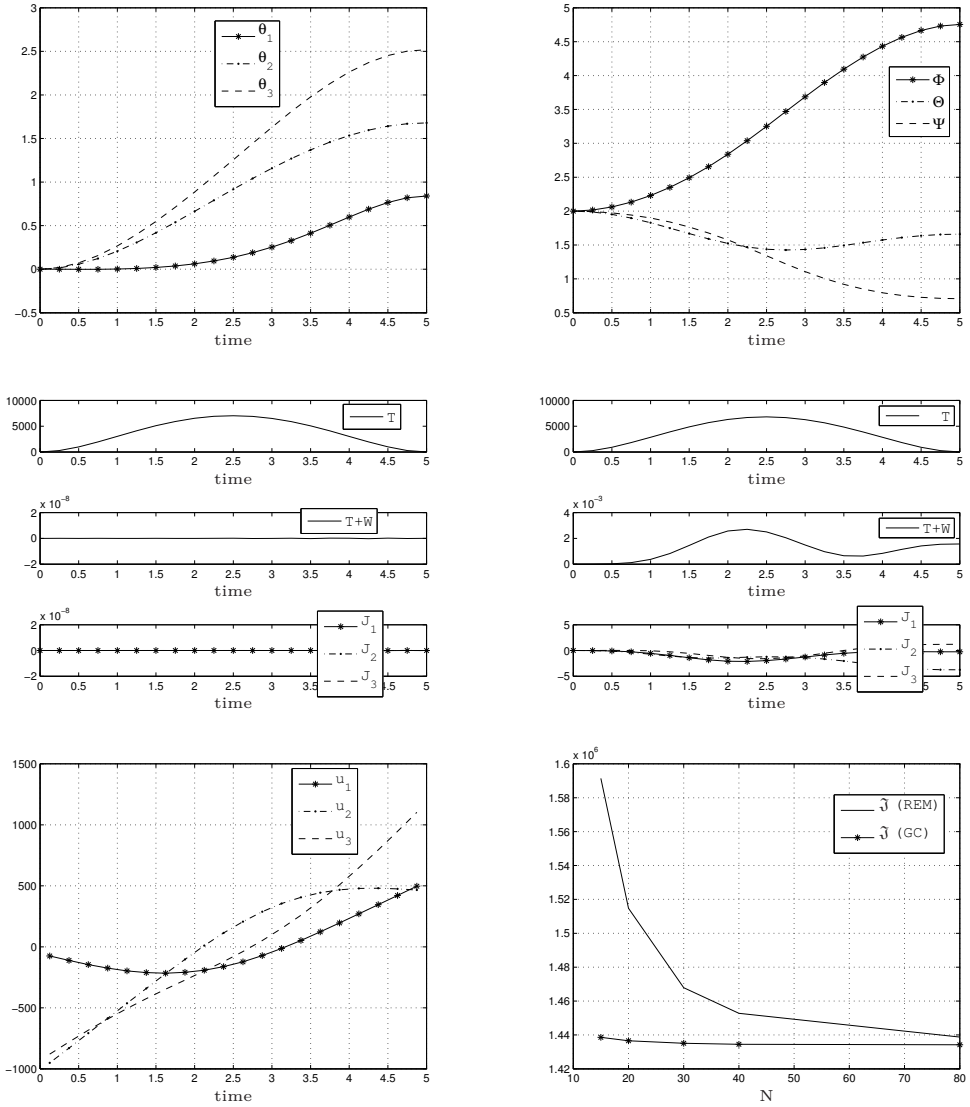

Figure 6.8.: Optimal control of a Satellite ($N = 20$): 1. Orientation of the main body for REM (left) and GC (right). 2. Resulting energies and angular momentum for REM (left) and GC (right). 3. Resulting torques for REM (Results for the generalized coordinates formulation are similar). 4. Convergence of the total costs for both schemes.

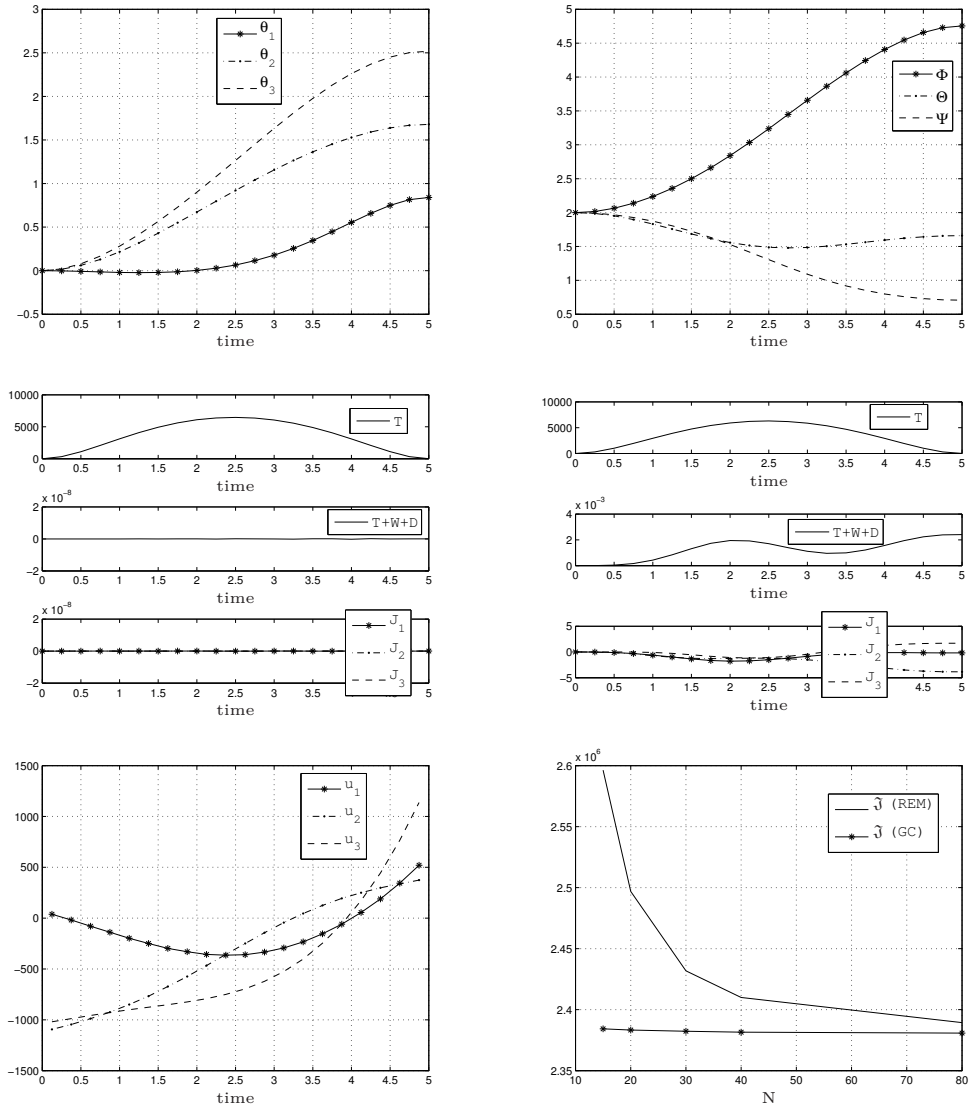

Figure 6.9.: Optimal control of a Satellite with linear viscous friction ($N = 20$): 1. Orientation of the main body for REM (left) and GC (right). 2. Resulting energies and angular momentum for REM (left) and GC (right). 3. Resulting torques for REM (Results for the generalized coordinates formulation are similar). 4. Convergence of the total costs for both schemes.

7. Optimal control with equations of motion in DAE-form

Equations of motions in form of differential-algebraic equations (DAEs) are widely-used, especially in flexible multibody dynamics. Particularly, the rotationless formulation based on natural coordinates (see, for example, Garcia de Jalon [46]) is closely linked to DAEs. However, only few works are concerned with optimal control of multibody systems described that way. Notable exceptions are the works of Bottasso and co-workers [32, 31], von Schwerin [102], and Kraus et el. [65] focussed on real multibody systems as well as the more theoretical ones of Kunkel & Mehrmann [69], Gerdts [48, 49], Gerdts & Kunkel [50], and Müller [83, 84].

In the current chapter the nonreduced equations of motion, which basically contain constraints, will serve as basis for the formulation of the optimal control problem. Consequently, the optimal control method is based on equations of motion in form of DAEs of index 3. The equations of motion will be discretized by use of the basic energy-momentum scheme introduced earlier in Chapter 3. In direct transcription methods based on the mentioned scheme the arising gradients needed for building up the discrete necessary conditions of optimality are of enormous size, but have a very sparse structure. Hence, a fast solution of the corresponding equations requires the utilization of efficient solvers for sparse matrices. Additionally, a meaningful choice of an initial guess to start the iteration process for solving the nonlinear equations turns out to be mandatory.

Below, the recently developed DAE-based approach will be employed within two representative examples. On the one hand, the optimal control of an underactuated overhead crane as an example of a point mass system will be investigated. In addition to that, the 3-link robot manipulator introduced earlier in Chapter 6 will be explored. Therein, the orientation of the involved three rigid bodies will be specified using directors, which necessitates the rotationless rigid body formulation including kinematic pairs introduced in Chapter 4. Finally, the results of the DAE-based numerical examples will be compared with those achieved by the ODE-based approaches illustrated in Chapter 6.

7.1. Optimal control formulation: Direct transcription

As in the last chapter, the control effort which is necessary for moving a multibody system from a specific initial configuration into a specific final one, will be minimized. While the quadratic function to be inserted into the cost function is of identical form as in Eq. (6.1), the formulation of the state vectors and the description of the solution procedure have to be treated in this chapter once again. Additionally, variable forms of the boundary conditions for the configuration and the velocity are needed in the differing examples of the current chapter.

Composition of the state vector To achieve proper formulations of the augmented cost function in Eq. (2.5) and the discrete analogon in Eq. (2.15), the composition of the state vector $\boldsymbol{x}$ is of decisive importance. In the BEM the state vector $\boldsymbol{x}$ may be built up with the configuration vector $\boldsymbol{q}$, the velocity vector $\boldsymbol{v}$, and the vector of Lagrange-multipliers $\boldsymbol{\gamma}$, thus $\boldsymbol{x} = (\boldsymbol{q}, \boldsymbol{v}, \boldsymbol{\gamma})$. This version will be applied in Section 7.3 within the 3-link manipulator as example. Alternatively, a reduced version of the state vector $\boldsymbol{x}$ only consisting of the configuration vector $\boldsymbol{q}$ and the vector of Lagrange-multipliers $\boldsymbol{\gamma}$ may be applied. The corresponding velocity vector can be obtained by the update process described in Eq. (3.33). The reduced state vector $\boldsymbol{x} = (\boldsymbol{q}, \boldsymbol{\gamma})$ will be used in Section 7.2 within the overhead crane as example.

Solution procedure Following the procedure described in Chapter 2, the discrete cost function, the boundary conditions as well as the discrete equations of motion are required for the discrete augmented cost function in Eq. (2.15). Furthermore, a direct transcription method based on the discrete augmented cost function will be applied for the solution of the mechanical optimal control problems. Again, the calculation of the derivatives is of essential importance. It is worth mentioning that the derivatives of the discrete equations of motion in DAE-form can be calculated more easily than the ones in ODE-form. First-order derivatives can be provided without any difficulty even for three-dimensional multibody systems consisting of kinematic chains. Due to the simply structured discrete equations of motion, also second-order derivatives might be calculated and provided for the solution procedure. However, this will not be done in the numerical examples in the present chapter. Notice that for three-dimensional multibody systems consisting of kinematic chains described with the discrete equations of motion in ODE-form treated in Chapter 6, the calculation of the derivatives is much more challenging. The latter is valid already for the first-order derivatives. Details of the implementation for the 3-link manipulator as example will be given in Appendix B. As a general problem for the DAE-based optimal control formulation, the provision of a good initial guess has to be stated. A good initial guess is not only necessary to avoid finding local minima instead of global ones, but also for finding a trajectory that is feasible. The latter emerges

as one of the major problems for the DAE-based optimal control treated in this chapter. Finally, as in Chapter 6, the solution of the optimal control problem will be calculated by use of the SQP solver fmincon in MATLAB.

7.2. Overhead crane

Below, the underactuated overhead crane depicted in Fig. 7.1 as prototypical example of a mechanical point mass system will be considered. In previous works, this example was used within the framework of trajectory tracking for underactuated multibody systems (see, for example, Blajer & Kolodziejczyk [26]). In examples dealing with trajectory tracking, the point mass is required to follow a prescribed trajectory. In contrast to the examples in Chapter 6, the underactuated overhead crane does not make necessary the rigid body kinematics that has been introduced in Chapter 4. In the following, both the BEM and the REM will be compared with the commonly used generalized coordinates formulation within optimal control.

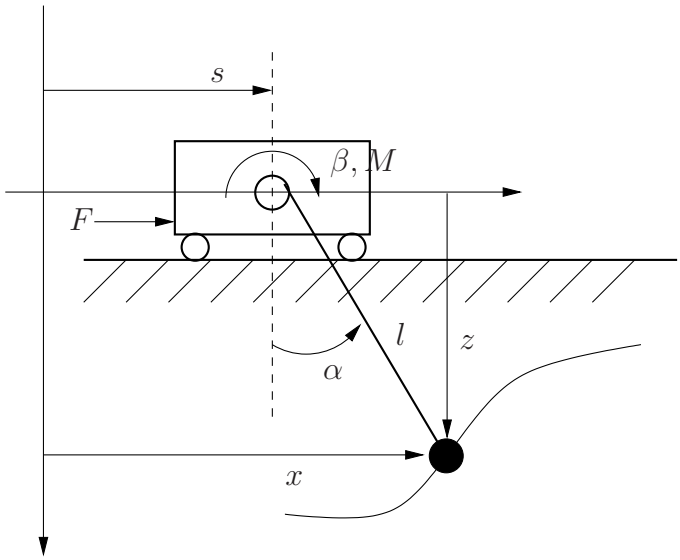

Figure 7.1.: Overhead Crane

Rotationless formulation with reduction Here, use will be made of four redundant coordinates for the three degree of freedom system, so that the problem will basically be specified by DAEs. The configuration vector then is given by

$$\boldsymbol{q} = \begin{bmatrix} s & \beta & x & z \end{bmatrix}^T \tag{7.1}$$

A basic property of the rotationless formulation is the constant and diagonal mass matrix. Here, the corresponding 4×4 mass matrix reads

$$\boldsymbol{M} = \mathrm{diag}(m_t, \mathcal{J}, m, m) \tag{7.2}$$

where m_t is the mass of the trolley, $\mathcal{J}$ the moment of inertia of the winch and m the mass of the load. Gravity is acting on the bodies, which yields the potential energy

$$V(\boldsymbol{q}) = -mg\,z \tag{7.3}$$

where g denotes the gravitational acceleration. In order to incorporate the effect of the rope properly, the holonomic constraint function

$$\Phi(\boldsymbol{q}) = (x-s)^2 + z^2 - r^2\beta^2 \tag{7.4}$$

has to be fulfilled. The formulation of the overhead crane within the BEM will be employed in this section and, additionally, will be compared with the REM as well as the generalized coordinates formulation.

Since the control forces $\boldsymbol{u} = (F, M)$ belong to the coordinates s and β, the work of the control forces can be calculated by Eq. (4.13) with the transformation matrix

$$\boldsymbol{B} = \begin{bmatrix} -\boldsymbol{I}_2 & \boldsymbol{0}_2 \end{bmatrix} \tag{7.5}$$

The work-conjugated coordinates s and β serve as redundant coordinates. Hence, the transformation matrix is constant, which is in difference to all other examples in this work. Furthermore, the null space matrix, which is necessary for the REM, reads

$$\boldsymbol{P}(\boldsymbol{q}) = \begin{bmatrix} 1 & 0 & 0 \\ 0 & z & 0 \\ 1 & 0 & -z \\ 0 & r^2\beta & x-s \end{bmatrix} \tag{7.6}$$

Now that all matrices needed for Eqs. (3.1) respectively (3.20) are derived the two formulations of the augmented cost function in Eq. (2.5) are complete. Finally, the transition to the discrete setting can be done straightforwardly as described in Section 3.2.

Generalized coordinates formulation One of the main goals of this work is the comparison between the above described EM-scheme and the well-known generalized coordinates formulation. For that purpose, the vector of generalized coordinates for the overhead crane

$$\tilde{\boldsymbol{q}} = \begin{bmatrix} s & l & \alpha \end{bmatrix}^T \tag{7.7}$$

will be introduced. The relation between the generalized coordinates and the redundant coordinates is given by

$$\boldsymbol{q} = \boldsymbol{q}(\tilde{\boldsymbol{q}}) = \begin{bmatrix} s & \frac{l}{r} & s + l\sin\alpha & l\cos\alpha \end{bmatrix}^T \tag{7.8}$$

Following the procedure specified in Section 3.3, a generalized coordinates formulation applicable for optimal control can be derived.

Boundary conditions on configuration and velocity level While in the numerical examples in Chapter 6 corresponding generalized velocities have been calculated by application of the transformation matrix $\boldsymbol{B}$ with Eq. (3.9), the same is not directly possible with the transformation matrix in the present example. In the present example, a possible reduction of the final conditions on velocity level would make necessary a different proceeding, which will not be carried out in this work. Within the rest-to-rest maneuver of the overhead crane as example the final conditions for the BEM will be chosen as

$$\boldsymbol{\psi}(\boldsymbol{x}_N) = \begin{bmatrix} \boldsymbol{q}_N - \boldsymbol{q}_f \\ \boldsymbol{v}_N - \boldsymbol{v}_f \end{bmatrix} \tag{7.9}$$

hence nonreduced boundary conditions both on configuration and on velocity level will be used. Consequently, the so-called 'linear independence constraint qualification' (see, for example, Diehl [41]) is not fulfilled for the final conditions. Nevertheless, no numerical problems have been experienced in the present three degree of freedom system. Finally, the nonreduced boundary conditions on velocity level will be applied also for the REM.

Numerical experiments The mass properties of the different bodies are given by $(m_t, \mathcal{J}, m) = (10, 0.1, 100)$, the radius of the winch is $r = 0.1$. Gravity is acting on the system with gravitational constant $g = 9.81$. While the boundary conditions on velocity level $\tilde{\boldsymbol{v}}_0$ and $\tilde{\boldsymbol{v}}_f$ for this rest-to-rest maneuver are zero, the ones on configuration level can be given by the vector of generalized coordinates $\tilde{\boldsymbol{q}}_0 = (0, 4, 0)$ at $t_0 = 0$ and $\tilde{\boldsymbol{q}}_f = (5, 1, 0)$ at $t_f = 3$. The corresponding redundant ones follow from Eq. (7.8).

Snapshots for the optimal movement of the overhead crane are given in Fig. 7.2. Furthermore, the consistency property, which will be checked within this example, is the sum of the total energy $T + V$ and the work of the control forces W. The total energy is consistent, if the BEM is applied (see Fig. 7.3). The curve of the coordinates, the controls and the kinetic energy are quite similar in the generalized coordinates formulation and in the BEM. Finally, the convergence of the total costs for the optimal movements are plotted in the last diagram of Fig. 7.3. Notice that the results for the BEM and the REM are equal.

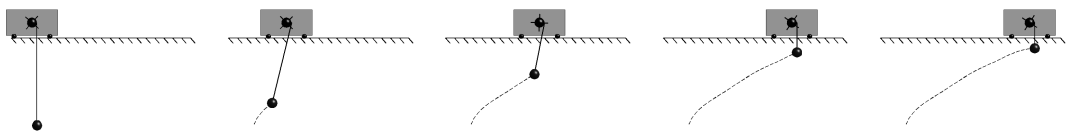

Figure 7.2.: Optimal control of an overhead crane ($N = 40$): Snapshots for the optimal movement at $t \in \{0, 0.75, 1.5, 2.25, 3\}$ for BEM.

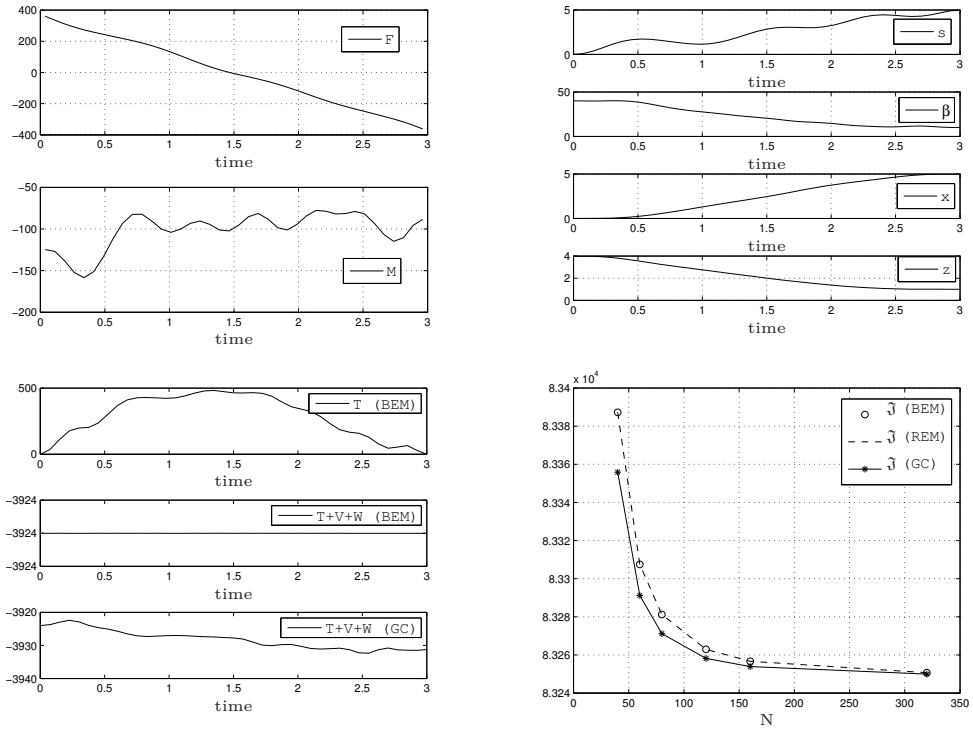

Figure 7.3.: Optimal control of an overhead crane ($N = 40$): 1. Resulting force and torque for BEM. 2. Resulting redundant coordinates for BEM. 3. Resulting kinetic energy for BEM and energy consistency for BEM and GC. 4. Convergence of the total costs for the three schemes.

7.3. 3-link manipulator

As previously in Section 6.2, the three degree of freedom planar robotic manipulator depicted in Fig. 6.1 will be applied as example for optimal control. An optimal movement of the manipulator for a rest-to-rest maneuver with given boundary conditions for the configuration will be calculated. In contrast to Section 6.2, here, the BEM will serve as basis for the formulation of the equations of motion. Additionally, the arising results will be compared with those of the REM and the generalized coordinates formulation. The required ingredients for the different formulations of the equations of motion have been provided in Section 6.2.

Boundary conditions on configuration and velocity level In the present example, the configuration vector $\boldsymbol{q}$, consisting of position vectors for the center of mass of each rigid body and the directors for describing the orientation, will be used in the BEM for the boundary conditions on configuration level. This has basic implications for the scope of these boundary conditions. While the enforcement of complete rotations is generally feasible if angles as relative coordinates are used as done in Chapter 6, the same is not valid for the present rotationless

formulation of the 3-link manipulator, whose orientation is described solely with directors. Nevertheless, the range of movement from the 3-link manipulator example of Section 6.2 can also be enforced in the numerical example of the present section. As a direct consequence of the use of the complete configuration vector for the boundary conditions, the vector of constraint functions $\boldsymbol{\Phi}(\boldsymbol{q}_N)$ at the final time t_N can be neglected in the present direct transcription method. Those constraints are automatically fulfilled due to the boundary conditions. Details of the implementation concerning that topic will be provided in Appendix B. As an alternative to the chosen proceeding, reduced boundary conditions on configuration level might be used in the present example. Corresponding angles, which are not directly available in the BEM, can be calculated by application of

$$\begin{aligned} \alpha_1 &= +\arccos(\boldsymbol{d}_1^1 \cdot \boldsymbol{e}_1) \\ \alpha_2 &= -\arccos(\boldsymbol{d}_1^2 \cdot \boldsymbol{d}_1^1) \\ \alpha_3 &= +\arccos(\boldsymbol{d}_1^3 \cdot \boldsymbol{d}_1^2) \end{aligned} \tag{7.10}$$

Obviously, the calculation of the gradients becomes more elaborated in that case. Additionally, the enforcement of complete rotations is still not possible due to the limited range of the angles calculated by Eq. (7.10). If the reduced boundary conditions on configuration level are used in the present direct transcription method, the constraints at the final time t_N have to be incorporated additionally. Furthermore, the reduced boundary condition on velocity level will be applied for the BEM in the current example. This is similar to the optimal control of the 3-link manipulator formulated with equations of motion in ODE-form from Chapter 6. Consequently, the whole set of final conditions in the BEM take the form

$$\boldsymbol{\psi}(\boldsymbol{x}_N) = \begin{bmatrix} \boldsymbol{q}_N - \boldsymbol{q}_f \\ \boldsymbol{B}(\boldsymbol{q}_N)\boldsymbol{v}_N - \boldsymbol{B}(\boldsymbol{q}_f)\boldsymbol{v}_f \end{bmatrix} \tag{7.11}$$

Hence, the 'linear independence constraint qualification' is not fulfilled for the final conditions on configuration level. Nevertheless, no numerical problems have been experienced in the present example.

Evolution of the discrete Hamiltonian In the present example, the evolution of the discrete Hamiltonian for the employed direct transcription method will be investigated. For this aim, the results of three different integrators, the BEM, the REM, and the generalized coordinates formulation with midpoint evaluation will be compared. In all cases, the discrete Hamiltonian can be calculated by Eq. (2.17), where the discrete Lagrange-multiplier $\bar{\boldsymbol{\lambda}}$ generally consists of the components $\boldsymbol{\lambda}^{\boldsymbol{q}}_{k,k+1}$, $\boldsymbol{\lambda}^{\boldsymbol{p}}_{k,k+1}$, and $\boldsymbol{\lambda}^{\boldsymbol{\Phi}}_{k+1}$. For ease of calculation, the function $\bar{\boldsymbol{f}}$ will be represented by use of the left hand sides of the discrete equations of motion in Eq. (2.16) in this paragraph. In the BEM the function $\bar{\boldsymbol{f}} \in \mathbb{R}^{18+18+15}$ is given by

$$\bar{\boldsymbol{f}}(\boldsymbol{x}_k, \boldsymbol{x}_{k+1}, \boldsymbol{x}_{k,k+1}, \boldsymbol{u}_{k,k+1}) = \begin{bmatrix} \frac{1}{h}(\boldsymbol{q}_{k+1} - \boldsymbol{q}_k) \\ \frac{1}{h}\boldsymbol{M}(\boldsymbol{v}_{k+1} - \boldsymbol{v}_k) \\ \boldsymbol{0} \end{bmatrix} \tag{7.12}$$

where the discrete Lagrange-multiplier in Eq. (2.17) is of the size $\bar{\boldsymbol{\lambda}} \in \mathbb{R}^{18+18+15}$. Furthermore, in the REM the function $\bar{\boldsymbol{f}} \in \mathbb{R}^{18+3+0}$ is of the form

$$\bar{\boldsymbol{f}}(\boldsymbol{x}_k, \boldsymbol{x}_{k+1}, \boldsymbol{u}_{k,k+1}) = \begin{bmatrix} \frac{1}{h}\left(\boldsymbol{q}_{k+1} - \boldsymbol{q}_k\right) \\ \frac{1}{h}\,\boldsymbol{P}(\boldsymbol{q}_{k+\frac{1}{2}})^T\,\boldsymbol{M}(\boldsymbol{v}_{k+1} - \boldsymbol{v}_k) \end{bmatrix} \tag{7.13}$$

where the discrete Lagrange-multiplier in Eq. (2.17) is of the size $\bar{\boldsymbol{\lambda}} \in \mathbb{R}^{18+3+0}$. Finally, in the generalized coordinates formulation the function $\bar{\boldsymbol{f}} \in \mathbb{R}^{3+3+0}$ reads

$$\bar{\boldsymbol{f}}(\boldsymbol{x}_k, \boldsymbol{x}_{k+1}, \boldsymbol{u}_{k,k+1}) = \begin{bmatrix} \frac{1}{h}\left(\tilde{\boldsymbol{q}}_{k+1} - \tilde{\boldsymbol{q}}_k\right) \\ \frac{1}{h}\,\tilde{\boldsymbol{M}}(\tilde{\boldsymbol{q}}_{k+\frac{1}{2}})\left(\tilde{\boldsymbol{v}}_{k+1} - \tilde{\boldsymbol{v}}_k\right) \end{bmatrix} \tag{7.14}$$

where the discrete Lagrange-multiplier in Eq. (2.17) is of the size $\bar{\boldsymbol{\lambda}} \in \mathbb{R}^{3+3+0}$. Notice that for the calculation of the discrete Hamiltonian in all of the three formulations, the velocity will not be eliminated in the equations of motion. Numerical experiments concerning the evolution of the discrete Hamiltonian for the direct transcription methods applied in this chapter and Chapter 6, will be done at the end of this section.

Evolution of the discrete Lagrange-multipliers Similar to the case of the velocities, a relation between the continuous Lagrange-multipliers in the BEM, contained in the vector $\boldsymbol{\lambda}^{\boldsymbol{p},BEM}$, and the corresponding ones in the REM, contained in $\boldsymbol{\lambda}^{\boldsymbol{p},REM}$, can be found for the present 3-link manipulator example. Starting point for the considerations are the continuous control equations as part of the necessary conditions of optimality introduced in Eq. (2.8). In contrast to the last paragraph, the required Hamiltonian will be represented by use of the right hand sides of the equations of motion in Eq. (2.6). Taking into account Eq. $(2.8)_3$, the continuous control equations in the REM take the form

$$\boldsymbol{0} = -\boldsymbol{u} - \boldsymbol{\lambda}^{\boldsymbol{p},REM} \tag{7.15}$$

By application of Eq. $(2.8)_3$, the corresponding equations in the BEM read

$$\boldsymbol{0} = -\boldsymbol{u} - \boldsymbol{B}(\boldsymbol{q})\,\boldsymbol{\lambda}^{\boldsymbol{p},BEM} \tag{7.16}$$

Combining Eq. (7.15) and Eq. (7.16) yields a relation between the continuous Lagrange-multipliers of the form

$$\boldsymbol{\lambda}^{\boldsymbol{p},REM} = \boldsymbol{B}(\boldsymbol{q})\,\boldsymbol{\lambda}^{\boldsymbol{p},BEM} \tag{7.17}$$

With regard to the content of the Chapters 3 and 4, the inverse calculation can be done by premultiplication of the continuous null space matrix $\boldsymbol{P}$ and application of Eq. (6.10). The latter yields

$$\boldsymbol{\lambda}^{\boldsymbol{p},BEM} = \boldsymbol{P}(\boldsymbol{q})\,\boldsymbol{\lambda}^{\boldsymbol{p},REM} \tag{7.18}$$

The above introduced relation between the continuous Lagrange-multipliers can be devolved to the corresponding discrete quantities. In the discrete case, starting

point for the considerations are the discrete control equations given in Eq. $(2.18)_3$ as third part of the discrete necessary conditions of optimality. While the discrete control equations in the REM take the form

$$\mathbf{0} = -\boldsymbol{u}_{k,k+1} - \boldsymbol{\lambda}^{\boldsymbol{p},REM}_{k,k+1} \tag{7.19}$$

the corresponding equations in the BEM read

$$\mathbf{0} = -\boldsymbol{u}_{k,k+1} - \boldsymbol{B}(\boldsymbol{q}^{k+\frac{1}{2}})\, \boldsymbol{\lambda}^{\boldsymbol{p},BEM}_{k,k+1} \tag{7.20}$$

Notice that the contravariant evaluated transformation matrix appears in the last equation. Combining Eq. (7.19) and Eq. (7.20) yield a relation between the discrete Lagrange-multipliers, which is given by

$$\boldsymbol{\lambda}^{\boldsymbol{p},REM}_{k,k+1} = \boldsymbol{B}(\boldsymbol{q}^{k+\frac{1}{2}})\, \boldsymbol{\lambda}^{\boldsymbol{p},BEM}_{k,k+1} \tag{7.21}$$

Following the procedure presented in the Chapters 3 and 4, the inverse calculation can be done by application of the discrete null space matrix, that is

$$\boldsymbol{\lambda}^{\boldsymbol{p},BEM}_{k,k+1} = \boldsymbol{P}(\boldsymbol{q}_{k+\frac{1}{2}})\, \boldsymbol{\lambda}^{\boldsymbol{p},REM}_{k,k+1} \tag{7.22}$$

Adequate numerical experiments will be performed at the end of the present section to demonstrate the validity of the given relations.

Finally, two additional statements will be given. Firstly, a transfer of the presented considerations to similarly formulated multibody systems seems to be possible. Secondly, the control equations in the generalized coordinates formulation take a similar form than those of the REM given in Eq. (7.15). In particular, the vector of Lagrange-multipliers $\boldsymbol{\lambda}^{\boldsymbol{p},REM}$ therein has simply to be replaced by $\boldsymbol{\lambda}^{\boldsymbol{p},GC}$.

Numerical experiments Again, the total time of the movement for the 3-link manipulator is $t_f = 3$. The system starts and ends at rest. For the BEM, the starting point $\boldsymbol{q}_0$ was taken as initial guess for the configuration for all times $\boldsymbol{q}_k, k = 1, ..., N$. This poor initial guess is sufficient for getting a solution for the optimal control problem. Again, the chosen time step size was $h = \frac{t_f}{N}$ with $N = 20$. It is assumed that there is neither damping in the joints of the multibody system, nor any limitations of the controls.

Snapshots for the optimal movement of the 3-link manipulator are given in Fig. 7.4. The numerical results for the optimal movement of the 3-link manipulator are presented in Fig. 7.5. Two different ways for the calculation of the control torques can be applied. Obviously, the control vector $\boldsymbol{u}$ can be used directly. As an alternative, the controls can be calculated by use of the contravariant evaluated transformation matrix and the Lagrange-multipliers by application of Eq. (7.20). As one can see in the first diagram, both versions yield the same results. The curves of the angles calculated by Eq. (7.10) coincide with those obtained by the REM or the generalized coordinates formulation. Furthermore,

the basic conservation property of the system is given as sum of the total energy $T + V$ and the work of the control forces W. In the last diagram of Fig. 7.5, the convergence of the total costs are plotted for all of the three formulations of the equations of motion, that is the BEM, the REM and the generalized coordinates formulation. Notice that the results for the BEM and the REM are exactly the same.

Finally, the curves of the discrete Hamiltonian for the applied direct transcription methods based on the BEM and the generalized coordinates formulation with employed midpoint rule have been depicted in Fig. 7.6. It can be recognized that conservation of the discrete Hamiltonian is only valid in the limit case of vanishing time step sizes. Furthermore, the BEM and the REM yield the same results for the discrete Hamiltonian. This can be seen in the left diagram of Fig. 7.6, where the discrete Hamiltonian for the REM has been added for $N = 10$.

Figure 7.4.: Optimal control of a 3-link manipulator ($N = 20$): Snapshots for the optimal movement at $t \in \{0, 0.75, 1.5, 2.25, 3\}$ for BEM.

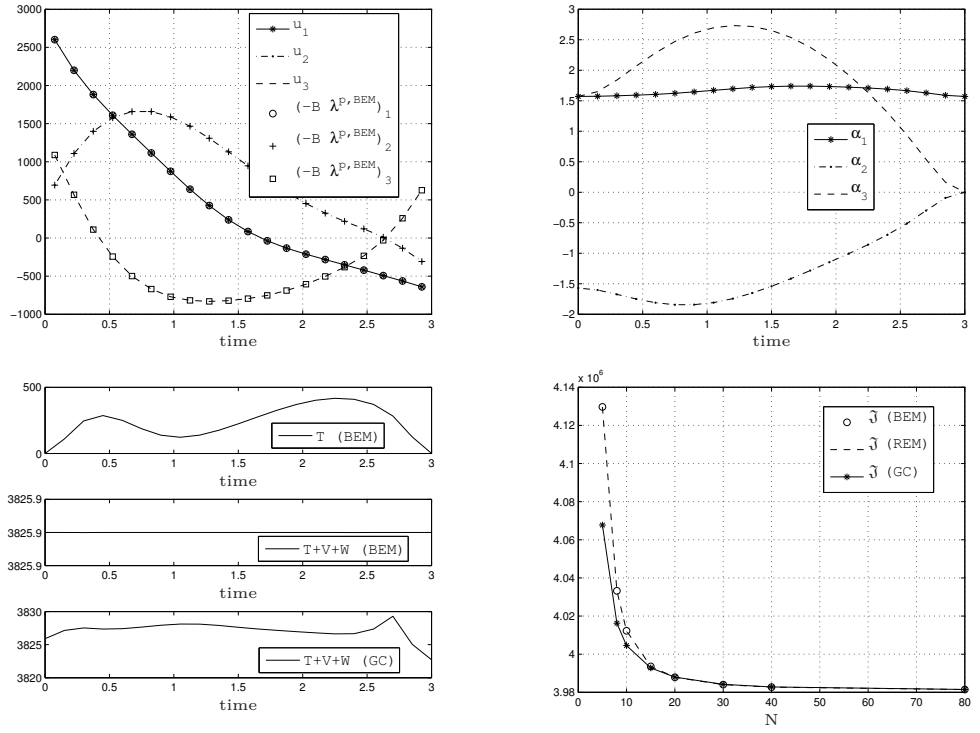

Figure 7.5.: Optimal control of a 3-link manipulator ($N = 20$): 1. Resulting torques for BEM. 2. Resulting angles for BEM. 3. Resulting kinetic energy for BEM and energy consistency for BEM and GC. 4. Convergence of the total costs for the three schemes.

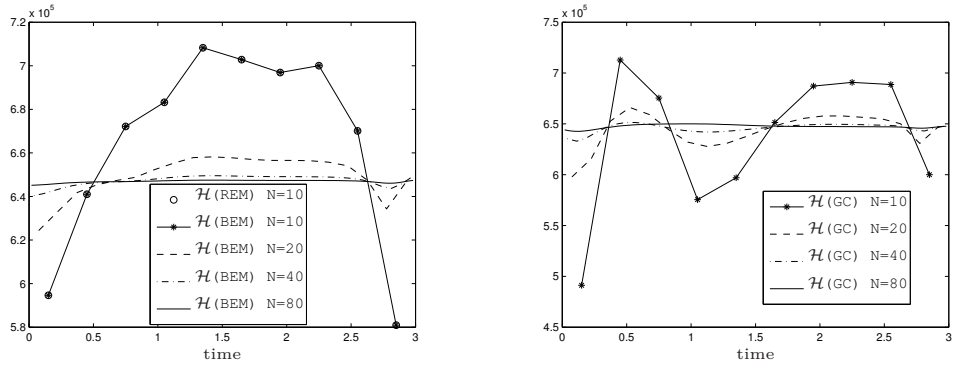

Figure 7.6.: Optimal control of a 3-link manipulator for the direct methods: 1. Convergence of the Hamiltonian for EM-schemes (Left). 2. Convergence of the Hamiltonian for GC (Right).

8. Hamiltonian conserving indirect optimal control method

In the past, a lot of effort has gone into the development of structure-preserving time-stepping schemes for forward dynamics problems. This is due to the superior numerical stability of these integrators. The complexity of these schemes strongly depends on the nonlinearity of the underlying equations of motion. If the kinetic energy of the system contains a constant mass matrix, then the Lagrangian and the Hamiltonian formalisms are equivalent. In general, the transition to the Hamilton equations of motion is required for the development of energy consistent schemes. It is well known that for maximally quadratic Hamilton functions, the midpoint rule is sufficient for the consistency of energy (see, for example, Wood [107]). For general nonlinear Hamilton functions, the midpoint rule looses energy consistency. In that case, a discrete derivative introduced in Gonzalez [53] is necessary. The discrete derivative can be seen as a consistent variant of the midpoint rule. Different approaches applying the discrete derivative have been introduced, see Gonzalez [53] for a specific second-order method and Groß et al. [57] for higher-order schemes. As a special case, the Greenspan formula introduced in Greenspan [55] can be mentioned, which can be applied for one-dimensional systems with general nonlinear potential functions.

Guided by previous developments in the design of energy-momentum integrators for forward dynamics problems, a Hamiltonian conserving indirect optimal control method will be introduced. For the state equations, a midpoint evaluation or a consistent variant thereof will be employed. Based on this specific discretization of the state equations, a discretization of the costate equations will be introduced which is based on the discrete derivative and which leads to the algorithmic conservation of the discrete Hamiltonian. As in the forward dynamics case, it can be expected that a Hamiltonian conserving method will yield superior numerical stability properties.

In the following sections, three mechanical multibody systems will be investigated within the newly developed Hamiltonian conserving indirect optimal control method. These are on the one hand a mathematical pendulum as an example for a system with one degree of freedom. Additionally, a particle in a three-dimensional gravitational field and the 3-link manipulator, introduced earlier in Section 6.2, will be treated as examples for systems with several degrees of freedom. Furthermore, a Hamiltonian formulation of the equations of motion will be used as basis. The discrete derivative will first be introduced for the forward dynamics problem for achieving energy consistency, as it has been done earlier

for example in Betsch & Steinmann [14]. Additionally, the discrete derivative will be applied for the discretization of the costate equations to achieve conservation of the discrete Hamiltonian. For simplicity it is assumed that the mechanical systems do not contain friction and that the controls as well as the angles are not limited.

8.1. Systems with one degree of freedom

In this section, the mathematical pendulum depicted in Fig. 8.1 will be investigated within the framework of optimal control. The pendulum serves as prototypical example of a mechanical system with one degree of freedom. As generalized coordinate, the angle $q \in \mathbb{R}$ will be used. The pendulum will be actuated by the control torque $u \in \mathbb{R}$.

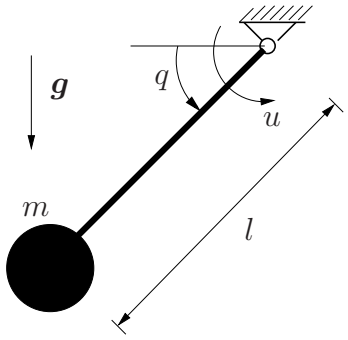

Figure 8.1.: Mathematical pendulum

Due to the constant mass matrix, there is no difference between the Lagrange equations of motion and the Hamilton equations of motion. However, the Hamiltonian formalism will be preferred in view of Section 8.2. An energy consistent time-stepping scheme based on the Greenspan formula introduced in Greenspan [55] will be applied for the formulation of the forward dynamics. Additionally, an indirect optimal control method, which conserves the underlying discrete Hamiltonian of the optimal control problem, will be introduced. For that purpose, a special discretization of the costate equations has to be employed, which is similar to the Greenspan formula applied for forward dynamics problems.

Consistent discretization of the equations of motion In the following, a discretization of the equations of motion for the mathematical pendulum which yields energy consistency will be illustrated. For that purpose, the kinetic and the potential energy has to be formulated using the generalized coordinate $q \in \mathbb{R}$ together with the momentum $p \in \mathbb{R}$. The kinetic and the potential energy for the one degree of freedom system are given by

$$T(p) = \frac{1}{2}(m\,l^2)^{-1} \cdot p^2 \tag{8.1}$$

respectively

$$V(q) = -m\,g\,l \cdot \sin q \tag{8.2}$$

Furthermore, the work of the control forces for the mathematical pendulum is given by

$$W = \int_{t_0}^{t} u \cdot (\,m\,l^2)^{-1} p\,dt \tag{8.3}$$

For the description of the dynamic behaviour, the Hamiltonian formulation of the equations of motion given by

$$\begin{aligned} \dot{q} &= (\,m\,l^2)^{-1}\,p \\ \dot{p} &= -\nabla_q V(q) - u \end{aligned} \tag{8.4}$$

will be preferred. The gradient of the potential energy for the mathematical pendulum is given by

$$\nabla_q V(q) = -m\,g\,l \cdot \cos q \tag{8.5}$$

Accordingly, the motion is described by a system of two first-order differential equations instead of one second-order differential equation, which would be the case for the Lagrange equations of motion. The discrete equations of motion take the form

$$\begin{aligned} \frac{1}{h}(q_{k+1} - q_k) &= (\,m\,l^2)^{-1} \cdot p_{k+\frac{1}{2}} \\ \frac{1}{h}(p_{k+1} - p_k) &= -\bar{\nabla}_q V(q_k, q_{k+1}) - u_{k,k+1} \end{aligned} \tag{8.6}$$

where the time derivative has been approximated with the difference quotient and a simple midpoint evaluation has been applied for the momentum in the first equation of the system. Furthermore, to achieve total energy consistency for a mechanical system described with one generalized coordinate, the discretization of the gradient of the potential has to be of the form

$$\bar{\nabla}_q V(q_k, q_{k+1}) = \frac{V(q_{k+1}) - V(q_k)}{q_{k+1} - q_k} \tag{8.7}$$

that is for the present example

$$\bar{\nabla}_q V(q_k, q_{k+1}) = -m\,g\,l \cdot \frac{\sin q_{k+1} - \sin q_k}{q_{k+1} - q_k} \tag{8.8}$$

The formula in Eq. (8.7) yields the well-known method of Greenspan introduced in Greenspan [55]. Two properties have to be fulfilled to obtain a discrete gradient which yields total energy consistency. On the one hand, the discrete gradient of the potential function has to satisfy the directionality property given by

$$\bar{\nabla}_q V(q_k, q_{k+1}) \cdot (q_{k+1} - q_k) = V(q_{k+1}) - V(q_k) \tag{8.9}$$

which is fulfilled for the formula in Eq. (8.7) by construction. On the other hand, the discrete gradient has to satisfy the consistency property, which means that the discrete gradient has to converge locally against the gradient of the potential function evaluated at the midpoint. Notice that total energy consistency is not

valid, if a simple midpoint evaluation of the gradient of the potential energy given by

$$\bar{\nabla}_q V(q_k, q_{k+1}) = \nabla_q V(q_{k+\frac{1}{2}}) \tag{8.10}$$

is employed. Finally, the discrete work of the control forces for the mathematical pendulum takes the form

$$W_k = h \cdot \sum_{i=0}^{k-1} u_{i,i+1} \cdot (m\, l^2)^{-1} p_{i+\frac{1}{2}} \tag{8.11}$$

Necessary conditions of optimality The task is minimizing the control effort which is necessary for moving the mathematical pendulum from an initial configuration into a final one. This control effort can be specified by the continuous quadratic function

$$\mathcal{L}(u) = \frac{1}{2}\, u \cdot u \tag{8.12}$$

to be inserted into the cost function in Eq. (2.3) with the control torque u. If the Hamilton equations of motion for the mathematical pendulum, introduced in Eq. (8.4), will be applied, the continuous Hamiltonian is given by

$$\mathcal{H} = -\mathcal{L}(u) + \begin{bmatrix} \lambda^q \\ \lambda^p \end{bmatrix} \cdot \begin{bmatrix} (m\, l^2)^{-1}\, p \\ -\nabla_q V(q) - u \end{bmatrix} \tag{8.13}$$

The Hamiltonian can be used for the derivation of the NCO, which, for this example, take the form

$$\begin{aligned} \dot{q} &= (m\, l^2)^{-1}\, p \\ \dot{p} &= -\nabla_q V(q) - u \\ \dot{\lambda}^q &= \nabla_{qq} V(q) \cdot \lambda^p \\ \dot{\lambda}^p &= -(m\, l^2)^{-1}\, \lambda^q \\ 0 &= u + \lambda^p \end{aligned} \tag{8.14}$$

where the second derivative of the potential energy for the present example is given by

$$\nabla_{qq} V(q) = m\, g\, l \cdot \sin q \tag{8.15}$$

Fulfilment of the NCO in Eq. (8.14) involves conservation of the Hamiltonian (see Section 2.1 for the proof).

Direct transcription approach The discrete counterpart of the continuous function introduced in Eq. (8.12), which has to be inserted into the discrete cost function in Eq. (2.14), is given by

$$\mathcal{L}(u_{k,k+1}) = \frac{1}{2}\, u_{k,k+1} \cdot u_{k,k+1} \tag{8.16}$$

where the discrete controls $u_{k,k+1}$ are assumed to be constant on every time interval. The discrete Hamiltonian for the present example reads

$$\mathcal{H}^d_{k,k+1} = -\mathcal{L}(u_{k,k+1}) + \begin{bmatrix} \lambda^q_{k,k+1} \\ \lambda^p_{k,k+1} \end{bmatrix} \cdot \begin{bmatrix} (m\,l^2)^{-1} \cdot p_{k+\frac{1}{2}} \\ -\bar{\nabla}_q V(q_k, q_{k+1}) - u_{k,k+1} \end{bmatrix} \tag{8.17}$$

and can be used for deriving the discrete necessary conditions of optimality (DNCO). This approach yields a direct transcription method. If the gradient of the potential energy will be evaluated in the midpoint using Eq. (8.10), the discrete necessary conditions of optimality take the form

$$\begin{aligned} \frac{1}{h}(q_{k+1} - q_k) &= (m\,l^2)^{-1} \cdot p_{k+\frac{1}{2}} \\ \frac{1}{h}(p_{k+1} - p_k) &= -\bar{\nabla}_q V(q_k, q_{k+1}) - u_{k,k+1} \\ \frac{1}{h}(\lambda^q_{k,k+1} - \lambda^q_{k-1,k}) &= \frac{1}{2}(\bar{\nabla}_{qq} V(q_k, q_{k+1}) \cdot \lambda^p_{k,k+1} + \bar{\nabla}_{qq} V(q_{k-1}, q_k) \cdot \lambda^p_{k-1,k}) \\ \frac{1}{h}(\lambda^p_{k,k+1} - \lambda^p_{k-1,k}) &= -(m\,l^2)^{-1} \cdot \frac{1}{2}(\lambda^q_{k,k+1} + \lambda^q_{k-1,k}) \\ 0 &= u_{k,k+1} + \lambda^p_{k,k+1} \end{aligned} \tag{8.18}$$

where the discrete second derivative of the potential energy is given by

$$\bar{\nabla}_{qq} V(q_k, q_{k+1}) = \nabla_{qq} V(q_{k+\frac{1}{2}}) \tag{8.19}$$

Notice that midpoint evaluation of the state equations leads to a trapezoidal evaluation of the costate equations. The application of the formula of Greenspan for the state equations within a direct transcription approach yields a more involved form of the costate equations, that will not be given here. However, the corresponding results can be calculated by the SQP solver fmincon in MATLAB. It will be demonstrated later that the direct transcription approach given above does not lead to a conserved discrete Hamiltonian.

Consistent discretization of the necessary conditions of optimality Alternatively, an indirect transcription approach leading to a conserved discrete Hamiltonian can be employed. For that purpose, the costate equations for this example will be discretized in the form

$$\begin{aligned} \frac{1}{h}(\lambda^q_{k,k+1} - \lambda^q_{k-1,k}) &= \bar{\nabla}_{qq} V(q_{k-1}, q_k, q_{k+1}) \cdot \frac{1}{2}(\lambda^p_{k,k+1} + \lambda^p_{k-1,k}) \\ \frac{1}{h}(\lambda^p_{k,k+1} - \lambda^p_{k-1,k}) &= -(m\,l^2)^{-1} \cdot \frac{1}{2}(\lambda^q_{k,k+1} + \lambda^q_{k-1,k}) \end{aligned} \tag{8.20}$$

To achieve conservation of the discrete Hamiltonian $\mathcal{H}^d_{k,k+1}$ for a mechanical system described with one generalized coordinate, the discrete second derivative of the potential energy has to be of the form

$$\bar{\nabla}_{qq} V(q_{k-1}, q_k, q_{k+1}) = \frac{\bar{\nabla}_q V(q_k, q_{k+1}) - \bar{\nabla}_q V(q_{k-1}, q_k)}{q_{k+\frac{1}{2}} - q_{k-\frac{1}{2}}} \tag{8.21}$$

that means for the energy consistent discretization of the Hamilton equations of motion, introduced in Eqs. (8.6) and (8.7),

$$\bar{\nabla}_{qq}V(q_{k-1},q_k,q_{k+1}) = -m\,g\,l\cdot\frac{\frac{\sin q_{k+1}-\sin q_k}{q_{k+1}-q_k} - \frac{\sin q_k-\sin q_{k-1}}{q_k-q_{k-1}}}{q_{k+\frac{1}{2}}-q_{k-\frac{1}{2}}} \tag{8.22}$$

Two properties have to be fulfilled to obtain a discrete gradient of the Hamiltonian which yields conservation of the discrete Hamiltonian, that is validity of Eq. (2.19). On the one hand, the discrete second derivative of the potential function has to satisfy the directionality property given by

$$\begin{aligned}&\frac{1}{2}(\lambda^p_{k,k+1}+\lambda^p_{k-1,k})\cdot\bar{\nabla}_{qq}V(q_{k-1},q_k,q_{k+1})\cdot(q_{k+\frac{1}{2}}-q_{k-\frac{1}{2}})\\ &+\frac{1}{2}(\bar{\nabla}_qV(q_k,q_{k+1})+\bar{\nabla}_qV(q_{k-1},q_k))\cdot(\lambda^p_{k,k+1}-\lambda^p_{k-1,k})\\ &=\lambda^p_{k,k+1}\cdot\bar{\nabla}_qV(q_k,q_{k+1})-\lambda^p_{k-1,k}\cdot\bar{\nabla}_qV(q_{k-1},q_k)\end{aligned} \tag{8.23}$$

which can be recast in the form

$$\begin{aligned}&\frac{1}{2}(\lambda^p_{k,k+1}+\lambda^p_{k-1,k})\cdot\bar{\nabla}_{qq}V(q_{k-1},q_k,q_{k+1})\cdot(q_{k+\frac{1}{2}}-q_{k-\frac{1}{2}})\\ &=\frac{1}{2}(\lambda^p_{k,k+1}+\lambda^p_{k-1,k})\cdot(\bar{\nabla}_qV(q_k,q_{k+1})-\bar{\nabla}_qV(q_{k-1},q_k))\end{aligned} \tag{8.24}$$

or alternatively

$$\bar{\nabla}_{qq}V(q_{k-1},q_k,q_{k+1})\cdot(q_{k+\frac{1}{2}}-q_{k-\frac{1}{2}}) = \bar{\nabla}_qV(q_k,q_{k+1})-\bar{\nabla}_qV(q_{k-1},q_k) \tag{8.25}$$

The condition in Eq. (8.25) is fulfilled for the formula in Eq. (8.21) by construction. By application of a similar proceeding for the first part of the discrete equations of motion given in Eq. $(8.18)_1$ and taking into account the discrete control equation given in Eq. $(8.18)_5$ for the remaining parts of the discrete Hamiltonian, the conservation of the discrete Hamiltonian has been proven. On the other hand, the discrete second derivative has to satisfy the consistency property, which means that the discrete gradient has to converge locally against the second derivative of the potential function evaluated at the midpoint of the two involved time steps. It is worth mentioning that the application of a constant time step size is mandatory for the validity of the above given proceeding. Notice that Eq. (8.21) yields a formula, which has similarities to the Greenspan formula in Eq. (8.7), necessary for achieving energy consistency. Remember that total energy consistency is not valid, if a simple midpoint evaluation of the gradient of the potential energy will be applied. However, conservation of the discrete Hamiltonian given in Eq. (8.17) can be achieved in the present case by use of equation

$$\bar{\nabla}_{qq}V(q_{k-1},q_k,q_{k+1}) = -m\,g\,l\cdot\frac{\cos q_{k+\frac{1}{2}}-\cos q_{k-\frac{1}{2}}}{q_{k+\frac{1}{2}}-q_{k-\frac{1}{2}}} \tag{8.26}$$

thus only the special approximation of the second derivative generally given in Eq. (8.21) is of decisive importance.

Numerical experiments In the following, a mathematical pendulum with values taken from Gerdts [49] will be investigated within optimal control. The mass is given by $m = 1$, the length is $l = 1$ and a gravitational force is acting on the pendulum with gravitational constant $g = 9.81$. Boundary conditions for the configuration are given by $q_0 = 0$ and $q_f = \frac{\pi}{2}$. The system starts and ends at rest, thus $p_0 = p_f = 0$. Additionally, the total time of the movement is $t_f = 3$. The time step size in this example is $h = \frac{t_f}{N}$, where $N = 20$ is the number of time steps.

As results, the curves of the control torque and the angle for the optimal movement of the mathematical pendulum are given in Fig. 8.2. Furthermore, the kinetic energies and the sum of the total energy $T + V$ and the work of the control forces W are plotted in Fig. 8.3. Notice that application of the Greenspan Scheme leads to energy consistency, while the same is not valid for the Midpoint Scheme.

Additionally, the convergence behaviour of the Hamiltonian has been plotted in Fig. 8.4. If the optimal solution is calculated by a direct method, in this case, with the SQP solver fmincon in MATLAB without provided gradients, then the discrete Hamiltonian is not conserved. If the optimal solution is calculated by use of the DNCO with the discrete costate equations given in Eq. (8.20) together with the special approximation given in Eq. (8.21), then the discrete Hamiltonian is conserved. As a crucial difference to the consistency properties in the forward dynamics case, it has to be noted that the value of the Hamiltonian differs for different time step sizes.

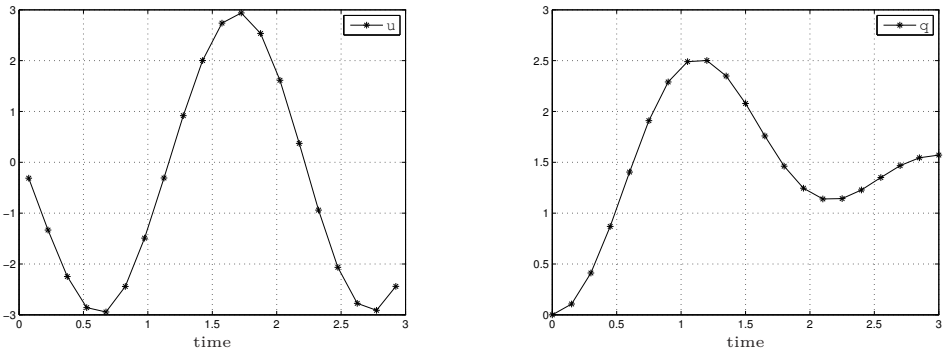

Figure 8.2.: Optimal control of a Mathematical Pendulum for Greenspan Scheme ($N = 20$): 1. Resulting torque (Left). 2. Resulting angle (Right).

8.2. Systems with several degrees of freedom

In this section, a particle of unit mass in a three-dimensional gravitational field and the 3-link manipulator depicted in Fig. 6.1 will be investigated within the framework of optimal control. Both mechanical systems serve as prototypical

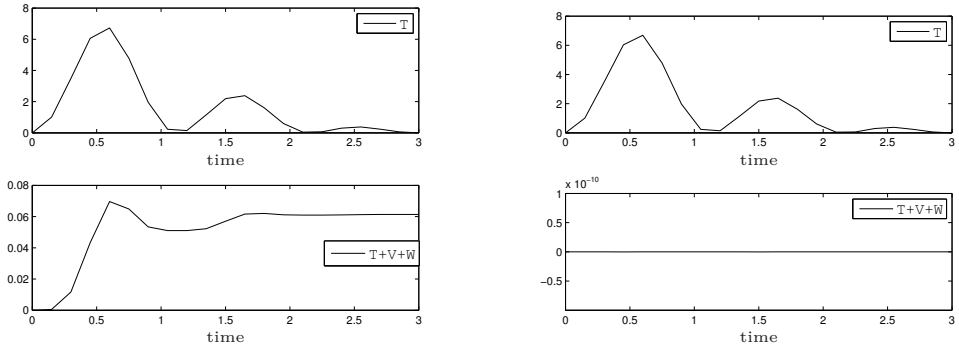

Figure 8.3.: Optimal control of a Mathematical Pendulum (N=20): 1. Resulting energies for Midpoint Scheme (Left). 2. Resulting energies for Greenspan Scheme (Right).

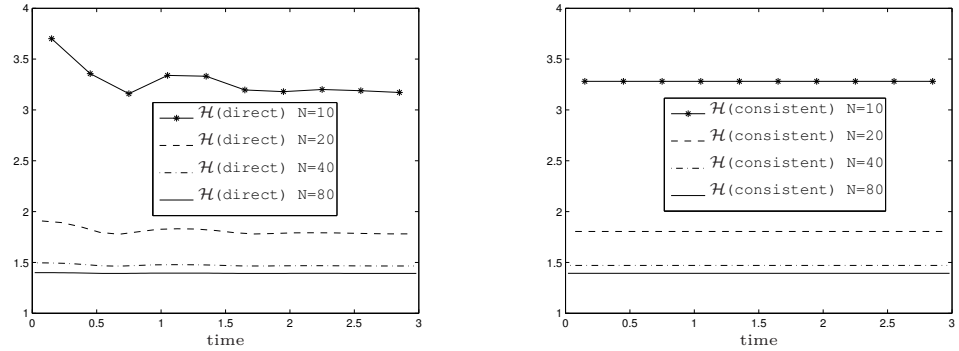

Figure 8.4.: Optimal control of a Mathematical Pendulum for Greenspan Scheme: 1. Convergence of the Hamiltonian for a direct method (Left). 2. Convergence of the Hamiltonian for a consistent discretization of the necessary conditions of optimality (Right).

examples of systems with several degrees of freedom. While Cartesian coordinates will be employed for the central force problem, angles will be applied for the description of the 3-link manipulator. The equations of motion will be discretized by application of an energy consistent time-stepping scheme based on the discrete derivative of Gonzalez introduced in Gonzalez [53]. For that purpose, the transition to the Hamiltonian formulation of the equations of motion is necessary. Additionally, an indirect optimal control method which conserves the underlying discrete Hamiltonian of the optimal control problem will be introduced. As in the forward dynamics case, the latter necessitates the application of the Hamilton equations of motion. To achieve conservation of the discrete Hamiltonian, a discretization of the costate equations is necessary which is inspired by the discrete derivative of Gonzalez used for the discretization of the state equations.

Consistent discretization of the equations of motion In the following, a discretization of the equations of motion for a multi degree of freedom system, which yields energy consistency will be described. For this aim, the kinetic and the potential energy has to be formulated using the generalized coordinates arranged in the vector $\boldsymbol{q} \in \mathbb{R}^n$ together with the momenta arranged in the vector $\boldsymbol{p} \in \mathbb{R}^n$. The kinetic energy for the multi degree of freedom system can be written in the form

$$T(\boldsymbol{q}, \boldsymbol{p}) = \frac{1}{2} \boldsymbol{p} \cdot \boldsymbol{M}(\boldsymbol{q})^{-1} \boldsymbol{p} \tag{8.27}$$

The potential energy $V(\boldsymbol{q})$ is, at this point, a general nonlinear function. Both energies will be combined in the Hamilton function given by

$$H(\boldsymbol{q}, \boldsymbol{p}) = T(\boldsymbol{q}, \boldsymbol{p}) + V(\boldsymbol{q}) \tag{8.28}$$

Furthermore, the work of the control forces for the multi degree of freedom system is given by

$$W = \int_{t_0}^{t} \boldsymbol{u} \cdot \boldsymbol{M}(\boldsymbol{q})^{-1} \boldsymbol{p} \, dt \tag{8.29}$$

For the description of the dynamic behaviour, the Hamiltonian formulation of the equations of motion given by

$$\begin{aligned} \dot{\boldsymbol{q}} &= \nabla_{\boldsymbol{p}} H(\boldsymbol{q}, \boldsymbol{p}) \\ \dot{\boldsymbol{p}} &= -\nabla_{\boldsymbol{q}} H(\boldsymbol{q}, \boldsymbol{p}) - \boldsymbol{u} \end{aligned} \tag{8.30}$$

will be employed. By application of a more compact form, the Hamilton equations of motion take the form

$$\dot{\boldsymbol{x}} = \mathbb{J} \, \nabla_{\boldsymbol{x}} H(\boldsymbol{x}) - (\boldsymbol{0}, \boldsymbol{u}) \tag{8.31}$$

where $\boldsymbol{x} = (\boldsymbol{q}, \boldsymbol{p}) \in \mathbb{R}^{2n}$ is the state vector and

$$\mathbb{J} = \begin{bmatrix} \boldsymbol{0} & \boldsymbol{I} \\ -\boldsymbol{I} & \boldsymbol{0} \end{bmatrix} \tag{8.32}$$

the symplectic matrix. Accordingly, the motion is specified by a system of $2n$ first-order differential equations instead of n second-order differential equations, which would be the case for the Lagrange equations of motion. Using the compact form of Eq. (8.31), the discrete equations of motion take the form

$$\frac{1}{h}(\boldsymbol{x}_{k+1} - \boldsymbol{x}_k) = \mathbb{J} \, \bar{\nabla}_{\boldsymbol{x}} H(\boldsymbol{x}_k, \boldsymbol{x}_{k+1}) - (\boldsymbol{0}, \boldsymbol{u}_{k,k+1}) \tag{8.33}$$

where the time derivative has been approximated with the difference quotient. Furthermore, to achieve total energy consistency for a mechanical system described with several generalized coordinates, the discretization of the gradient of the Hamilton function has to be of the form

$$\bar{\nabla}_{\boldsymbol{x}} H(\boldsymbol{x}_k, \boldsymbol{x}_{k+1}) = \boldsymbol{H}_{\alpha} + \frac{H(\boldsymbol{x}_{k+1}) - H(\boldsymbol{x}_k) - \boldsymbol{H}_{\alpha} \cdot \Delta \boldsymbol{x}}{\Delta \boldsymbol{x} \cdot \Delta \boldsymbol{x}} \, \Delta \boldsymbol{x} \tag{8.34}$$

where

$$\Delta \boldsymbol{x} = \boldsymbol{x}_{k+1} - \boldsymbol{x}_k \tag{8.35}$$

The component $\boldsymbol{H}_\alpha$ can be chosen as

$$\boldsymbol{H}_1 = \nabla_{\boldsymbol{x}} H(\boldsymbol{x}_{k+\frac{1}{2}}) \tag{8.36}$$

or alternatively

$$\boldsymbol{H}_2 = \frac{1}{2}(\nabla_{\boldsymbol{x}} H(\boldsymbol{x}_{k+1}) + \nabla_{\boldsymbol{x}} H(\boldsymbol{x}_k)) \tag{8.37}$$

The option given in Eq. (8.36) will be chosen in the numerical examples at the end of this section. The formula in Eq. (8.34) yields the well-known method of Gonzalez introduced in Gonzalez [53]. Two properties have to be fulfilled to obtain a discrete gradient which yields total energy consistency for mechanical systems with several degrees of freedom. On the one hand, the discrete gradient of the Hamilton function has to satisfy the directionality property given by

$$\bar{\nabla}_{\boldsymbol{x}} H(\boldsymbol{x}_k, \boldsymbol{x}_{k+1}) \cdot (\boldsymbol{x}_{k+1} - \boldsymbol{x}_k) = H(\boldsymbol{x}_{k+1}) - H(\boldsymbol{x}_k) \tag{8.38}$$

which is fulfilled for the formula in Eq. (8.34) by construction. On the other hand, the discrete gradient has to satisfy the consistency property, which means that the discrete gradient has to converge locally against the gradient of the Hamilton function evaluated at the midpoint. Finally, the discrete work of the control forces for the multi degree of freedom system takes the form

$$W_k = h \cdot \sum_{i=0}^{k-1} \boldsymbol{u}_{i,i+1} \cdot \boldsymbol{M}(\boldsymbol{q}_{i+\frac{1}{2}})^{-1} \boldsymbol{p}_{i+\frac{1}{2}} \tag{8.39}$$

Necessary conditions of optimality Again, the task is minimizing the control effort which is necessary for moving the mechanical system from an initial configuration into a final one. This control effort can be described by the continuous quadratic function

$$\mathcal{L}(\boldsymbol{u}) = \frac{1}{2}\, \boldsymbol{u} \cdot \boldsymbol{u} \tag{8.40}$$

to be inserted into the cost function in Eq. (2.3) with the control torques arranged in the vector $\boldsymbol{u}$. The Hamilton equations of motion for the multi degree of freedom system will be applied, hence the continuous Hamiltonian is given by

$$\mathcal{H} = -\mathcal{L}(\boldsymbol{u}) + \begin{bmatrix} \boldsymbol{\lambda}^q \\ \boldsymbol{\lambda}^p \end{bmatrix} \cdot \begin{bmatrix} \nabla_p H(\boldsymbol{q}, \boldsymbol{p}) \\ -\nabla_q H(\boldsymbol{q}, \boldsymbol{p}) - \boldsymbol{u} \end{bmatrix} \tag{8.41}$$

The Hamiltonian can be used for the derivation of the NCO, which take the form

$$\begin{aligned} \dot{\boldsymbol{q}} &= \nabla_p H(\boldsymbol{q}, \boldsymbol{p}) \\ \dot{\boldsymbol{p}} &= -\nabla_q H(\boldsymbol{q}, \boldsymbol{p}) - \boldsymbol{u} \\ \dot{\boldsymbol{\lambda}}^q &= \nabla_{qq} H(\boldsymbol{q}, \boldsymbol{p}) \cdot \boldsymbol{\lambda}^p - \nabla_{pq} H(\boldsymbol{q}, \boldsymbol{p}) \cdot \boldsymbol{\lambda}^q \\ \dot{\boldsymbol{\lambda}}^p &= \nabla_{qp} H(\boldsymbol{q}, \boldsymbol{p}) \cdot \boldsymbol{\lambda}^p - \nabla_{pp} H(\boldsymbol{q}, \boldsymbol{p}) \cdot \boldsymbol{\lambda}^q \\ \boldsymbol{0} &= \boldsymbol{u} + \boldsymbol{\lambda}^p \end{aligned} \tag{8.42}$$

By application of a more compact form, the continuous Hamiltonian takes the form

$$\mathcal{H} = -\mathcal{L}(\boldsymbol{u}) + \boldsymbol{\lambda} \cdot \Big[\mathbb{J}\, \nabla_{\boldsymbol{x}} H(\boldsymbol{x}) - (\boldsymbol{0}, \boldsymbol{u})\Big] \tag{8.43}$$

A compact form of the continuous necessary conditions of optimality then is given by

$$\begin{aligned} \dot{\boldsymbol{x}} &= \mathbb{J}\, \nabla_{\boldsymbol{x}} H(\boldsymbol{x}) - (\boldsymbol{0}, \boldsymbol{u}) \\ \dot{\boldsymbol{\lambda}} &= -(\boldsymbol{\lambda}^T\, \mathbb{J}\, \nabla_{\boldsymbol{x}\boldsymbol{x}} H(\boldsymbol{x}))^T \\ \boldsymbol{0} &= \nabla_{\boldsymbol{u}} \mathcal{H}(\boldsymbol{x}, \boldsymbol{u}, \boldsymbol{\lambda}) \end{aligned} \tag{8.44}$$

As in the one-dimensional case, fulfilment of the NCO in Eq. (8.44) involves conservation of the Hamiltonian.

Direct transcription approach The discrete version of the continuous function introduced in Eq. (8.40), which has to be inserted into the discrete cost function in Eq. (2.14), reads

$$\mathcal{L}(\boldsymbol{u}_{k,k+1}) = \frac{1}{2}\, \boldsymbol{u}_{k,k+1} \cdot \boldsymbol{u}_{k,k+1} \tag{8.45}$$

where the discrete controls are arranged in the vector $\boldsymbol{u}_{k,k+1}$. Furthermore, the compact form of the discrete Hamiltonian for systems with several degrees of freedom is given by

$$\mathcal{H}^d_{k,k+1} = -\mathcal{L}(\boldsymbol{u}_{k,k+1}) + \boldsymbol{\lambda}_{k,k+1} \cdot \Big[\mathbb{J}\, \bar{\nabla}_{\boldsymbol{x}} H(\boldsymbol{x}_k, \boldsymbol{x}_{k+1}) - (\boldsymbol{0}, \boldsymbol{u}_{k,k+1})\Big] \tag{8.46}$$

and can be used for deriving the discrete necessary conditions of optimality (DNCO) within a direct transcription method. If the gradient of the Hamilton function in the state equations will be evaluated in the midpoint, the discrete necessary conditions of optimality take the form

$$\begin{aligned} \frac{1}{h}(\boldsymbol{x}_{k+1} - \boldsymbol{x}_k) &= \mathbb{J}\, \bar{\nabla}_{\boldsymbol{x}} H(\boldsymbol{x}_k, \boldsymbol{x}_{k+1}) - (\boldsymbol{0}, \boldsymbol{u}_{k,k+1}) \\ \frac{1}{h}(\boldsymbol{\lambda}_{k,k+1} - \boldsymbol{\lambda}_{k-1,k}) &= -\frac{1}{2}\{\boldsymbol{\lambda}^T_{k,k+1}\, \mathbb{J}\, \bar{\nabla}_{\boldsymbol{x}\boldsymbol{x}} H(\boldsymbol{x}_k, \boldsymbol{x}_{k+1}) \\ &\qquad + \boldsymbol{\lambda}^T_{k-1,k}\, \mathbb{J}\, \bar{\nabla}_{\boldsymbol{x}\boldsymbol{x}} H(\boldsymbol{x}_{k-1}, \boldsymbol{x}_k)\}^T \\ \boldsymbol{0} &= \boldsymbol{u}_{k,k+1} + \boldsymbol{\lambda}^p_{k,k+1} \end{aligned} \tag{8.47}$$

where the discrete second derivative of the Hamilton function is given by

$$\bar{\nabla}_{\boldsymbol{x}\boldsymbol{x}} H(\boldsymbol{x}_k, \boldsymbol{x}_{k+1}) = \nabla_{\boldsymbol{x}\boldsymbol{x}} H(\boldsymbol{x}_{k+\frac{1}{2}}) \tag{8.48}$$

Comments similar to those for the one-dimensional case given in Section 8.1 can be stated for systems with several degrees of freedom.

Consistent discretization of the necessary conditions of optimality Alternatively, an indirect transcription approach leading to a conserved discrete Hamiltonian can be employed. For that purpose, the costate equations will be discretized in the form

$$\frac{1}{h}(\boldsymbol{\lambda}_{k,k+1}-\boldsymbol{\lambda}_{k-1,k})=-\frac{1}{2}\left\{(\boldsymbol{\lambda}_{k,k+1}+\boldsymbol{\lambda}_{k-1,k})^T\,\mathbb{J}\,\bar{\nabla}_{\boldsymbol{xx}}H(\boldsymbol{x}_{k-1},\boldsymbol{x}_k,\boldsymbol{x}_{k+1})\right\}^T \tag{8.49}$$

To achieve conservation of the discrete Hamiltonian $\mathcal{H}^d_{k,k+1}$ for a mechanical system described with several generalized coordinates, the discrete second derivative of the Hamilton function has to be of the form

$$\bar{\nabla}_{\boldsymbol{xx}}H(\boldsymbol{x}_{k-1},\boldsymbol{x}_k,\boldsymbol{x}_{k+1})=\boldsymbol{H}_\beta+\frac{\bar{\nabla}_{\boldsymbol{x}}H(\boldsymbol{x}_k,\boldsymbol{x}_{k+1})-\bar{\nabla}_{\boldsymbol{x}}H(\boldsymbol{x}_{k-1},\boldsymbol{x}_k)-\boldsymbol{H}_\beta\Delta\boldsymbol{x}}{\Delta\boldsymbol{x}\cdot\Delta\boldsymbol{x}}\,\Delta\boldsymbol{x}^T \tag{8.50}$$

with

$$\Delta\boldsymbol{x}=\boldsymbol{x}_{k+\frac{1}{2}}-\boldsymbol{x}_{k-\frac{1}{2}}=\frac{1}{2}(\boldsymbol{x}_{k+1}-\boldsymbol{x}_{k-1}) \tag{8.51}$$

The component $\boldsymbol{H}_\beta$ can be chosen as

$$\boldsymbol{H}_1=\nabla_{\boldsymbol{xx}}H(\boldsymbol{x}_k) \tag{8.52}$$

or alternatively

$$\boldsymbol{H}_2=\frac{1}{2}(\nabla_{\boldsymbol{xx}}H(\boldsymbol{x}_{k+\frac{1}{2}})+\nabla_{\boldsymbol{xx}}H(\boldsymbol{x}_{k-\frac{1}{2}})) \tag{8.53}$$

As in the forward dynamics case, the option given in Eq. (8.52) will be chosen in the numerical examples at the end of this section. Two properties have to be fulfilled to obtain a discrete gradient of the Hamiltonian which yields conservation of the discrete Hamiltonian, that is validity of Eq. (2.19). On the one hand, the discrete second derivative of the Hamilton function has to satisfy the directionality property given by

$$\begin{aligned}&\frac{1}{2}(\boldsymbol{\lambda}_{k,k+1}+\boldsymbol{\lambda}_{k-1,k})^T\,\mathbb{J}\,\bar{\nabla}_{\boldsymbol{xx}}H(\boldsymbol{x}_{k-1},\boldsymbol{x}_k,\boldsymbol{x}_{k+1})\cdot(\boldsymbol{x}_{k+\frac{1}{2}}-\boldsymbol{x}_{k-\frac{1}{2}})\\+&\frac{1}{2}(\mathbb{J}\,\bar{\nabla}_{\boldsymbol{x}}H(\boldsymbol{x}_k,\boldsymbol{x}_{k+1})+\mathbb{J}\,\bar{\nabla}_{\boldsymbol{x}}H(\boldsymbol{x}_{k-1},\boldsymbol{x}_k))\cdot(\boldsymbol{\lambda}_{k,k+1}-\boldsymbol{\lambda}_{k-1,k})\\=&\boldsymbol{\lambda}^T_{k,k+1}\,\mathbb{J}\,\bar{\nabla}_{\boldsymbol{x}}H(\boldsymbol{x}_k,\boldsymbol{x}_{k+1})-\boldsymbol{\lambda}^T_{k-1,k}\,\mathbb{J}\,\bar{\nabla}_{\boldsymbol{x}}H(\boldsymbol{x}_{k-1},\boldsymbol{x}_k)\end{aligned} \tag{8.54}$$

which can be recast in the form

$$\begin{aligned}&\frac{1}{2}(\boldsymbol{\lambda}_{k,k+1}+\boldsymbol{\lambda}_{k-1,k})^T\,\mathbb{J}\,\bar{\nabla}_{\boldsymbol{xx}}H(\boldsymbol{x}_{k-1},\boldsymbol{x}_k,\boldsymbol{x}_{k+1})\cdot(\boldsymbol{x}_{k+\frac{1}{2}}-\boldsymbol{x}_{k-\frac{1}{2}})\\=&\frac{1}{2}(\boldsymbol{\lambda}_{k,k+1}+\boldsymbol{\lambda}_{k-1,k})^T\,\mathbb{J}\,(\bar{\nabla}_{\boldsymbol{x}}H(\boldsymbol{x}_k,\boldsymbol{x}_{k+1})-\bar{\nabla}_{\boldsymbol{x}}H(\boldsymbol{x}_{k-1},\boldsymbol{x}_k))\end{aligned} \tag{8.55}$$

or alternatively

$$\bar{\nabla}_{\boldsymbol{xx}}H(\boldsymbol{x}_{k-1},\boldsymbol{x}_k,\boldsymbol{x}_{k+1})\cdot(\boldsymbol{x}_{k+\frac{1}{2}}-\boldsymbol{x}_{k-\frac{1}{2}})=\bar{\nabla}_{\boldsymbol{x}}H(\boldsymbol{x}_k,\boldsymbol{x}_{k+1})-\bar{\nabla}_{\boldsymbol{x}}H(\boldsymbol{x}_{k-1},\boldsymbol{x}_k) \tag{8.56}$$

The condition in Eq. (8.56) is fulfilled for the formula in Eq. (8.50) by construction. By taking into account the discrete control equation given in Eq. $(8.47)_3$

for the remaining parts of the discrete Hamiltonian, the conservation of the discrete Hamiltonian has been proven. On the other hand, the discrete second derivative has to satisfy the consistency property, which means that the discrete gradient has to converge locally against the second derivative of the Hamilton function evaluated at the midpoint of the two involved time steps. As in the one-dimensional case, the application of a constant time step size is mandatory for the validity of the above given proceeding. Notice that Eq. (8.50) yields a discrete derivative similar to Eq. (8.34), necessary for achieving energy consistency.

Numerical experiments: Central force problem In the following, a particle of unit mass in a three-dimensional gravitational field will be investigated within optimal control. A two-dimensional version of this example has been treated in Grizzle & Marcus [56]. Let $\boldsymbol{q} = (q_1, q_2, q_3)$ be the position vector and $\boldsymbol{p} = (p_1, p_2, p_3)$ the corresponding momentum. The particle will be controlled by thrusters acting in the q_1, q_2 and q_3 directions, hence $\boldsymbol{u} = (u_1, u_2, u_3)$. The potential energy for this example is given by

$$V(\boldsymbol{q}) = -(q_1^2 + q_2^2 + q_3^2)^{-\frac{1}{2}} \tag{8.57}$$

The constant mass matrix in this example is equal to the 3×3 identity matrix. Consequently, the transition to the Hamilton formalism can be done in a straightforward way. Furthermore, the boundary conditions on configuration level are chosen as $\boldsymbol{q}_0 = (1, 0, 0)$ and $\boldsymbol{q}_f = (0, 0, 1.5)$, the boundary conditions on momentum level as $\boldsymbol{p}_0 = (0, 1, 0)$ and $\boldsymbol{p}_f = (0, -1, 0)$. Additionally, the total time of the movement is given by $t_f = \pi$. The time step size in this example is $h = \frac{t_f}{N}$, where $N = 20$ is the number of time steps.

The numerical results for the given example are depicted in Fig. 8.5. The energy consistency plotted in the first diagram has been achieved by application of the discrete derivative of Gonzalez for the discretization of the state equations. Similarly, the consistency of the Hamiltonian has been obtained by the additional application of the newly proposed discretization of the costate equations given in Eq. (8.49) together with Eq. (8.50). Furthermore, the resulting controls are depicted in the second diagram of Fig. 8.5. The trajectory of the particle is represented in the third diagram. Therein, a reference trajectory has been added, which has been achieved by a forward dynamics simulation with the given initial conditions and vanishing controls. Notice that the particle moves on a semi circle with radius one, if the total time is chosen as $t_f = \pi$. Finally, the last diagram shows the convergence behaviour of the third components of the Lagrange-multipliers as well as the Hamiltonian. Averaged values of the discrete quantities have been calculated by application of the formula

$$(\cdot)^{av} = \frac{1}{N} \sum_{k=0}^{N-1} (\cdot)_{k,k+1} \tag{8.58}$$

Obviously, the averaged value for the Hamiltonian is equal to its value on every time step within the present Hamiltonian conserving method. Furthermore, the

Lagrange-multipliers and the Hamiltonian have been calculated for $N = 10 \cdot 2^i$, $i = 0, ..., 6$ and compared with reference solutions calculated for $N = 1280$. Notice that all of the three quantities converge quadratically. In particular, the newly proposed discretization of the costate equations is second-order accurate.

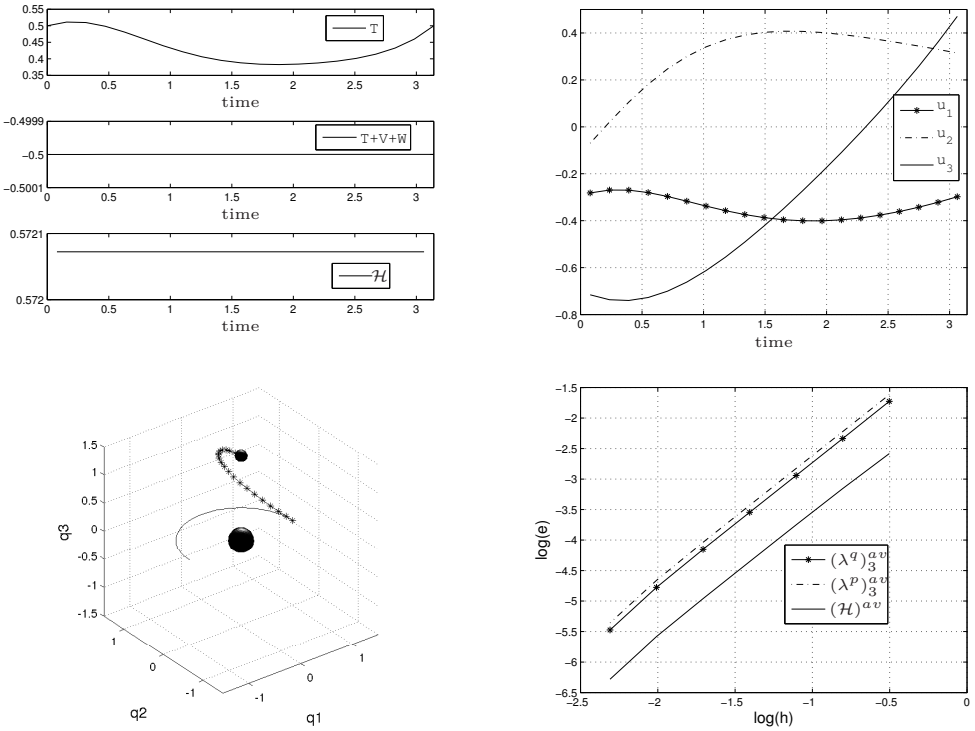

Figure 8.5.: Optimal control of a particle in a gravitational field with consistent discretization of the state and the costate equations ($N = 20$): 1. Resulting energies and Hamiltonian. 2. Resulting forces. 3. Resulting trajectory and reference trajectory. 4. Quadratic convergence of the averaged third components of the Lagrange-multipliers and the Hamiltonian.

Numerical experiments: 3-link manipulator Below, the 3-link manipulator introduced in Section 6.2 will be investigated within optimal control. Mass and geometric properties, boundary conditions for the configuration and the total time are given in Section 6.2. The boundary conditions on velocity level lead to similar ones on momentum level, that is $\boldsymbol{p}_0 = \boldsymbol{p}_f = 0$. The time step size in this example is $h = \frac{t_f}{N}$, where $N = 40$ is the number of time steps.

As results, the control torques and the angles for the optimal movement of the manipulator are given in Fig. 8.6. As expected, the curves are similar to those of the 3-link manipulator treated with the BEM in Section 7.3. Furthermore, the kinetic energy and the sum of the total energy $T + V$ and the work of the control forces W are plotted in Fig. 8.7. Notice that application of the discrete derivative of Gonzalez leads to energy consistency, while the same is not valid for the midpoint evaluation.

Additionally, the convergence behaviour of the Hamiltonian has been plotted in Fig. 8.8. If the optimal solution is calculated by a direct method, in this case, with the SQP solver fmincon in MATLAB without provided gradients, then the discrete Hamiltonian is not conserved. If the optimal solution is calculated by use of the DNCO with the newly proposed discretization of the costate equations given in Eq. (8.49) and Eq. (8.50) together with the Gonzalez-type discretization of the state equations, then the discrete Hamiltonian is conserved.

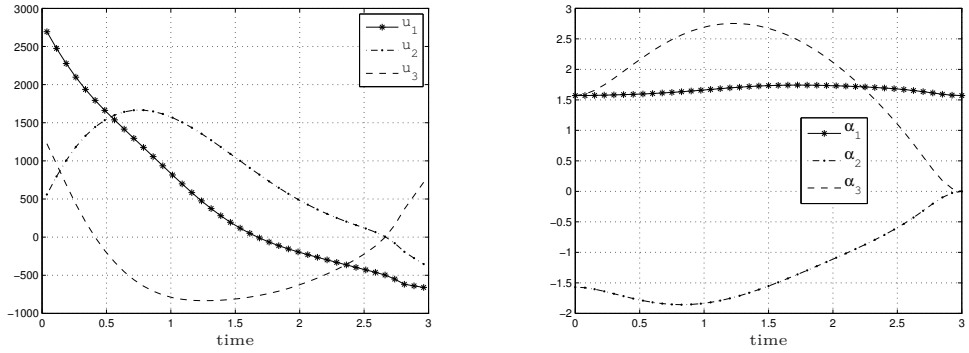

Figure 8.6.: Optimal control of a 3-link manipulator with energy consistent discretization ($N = 40$): 1. Resulting torques (Left). 2. Resulting angles (Right).

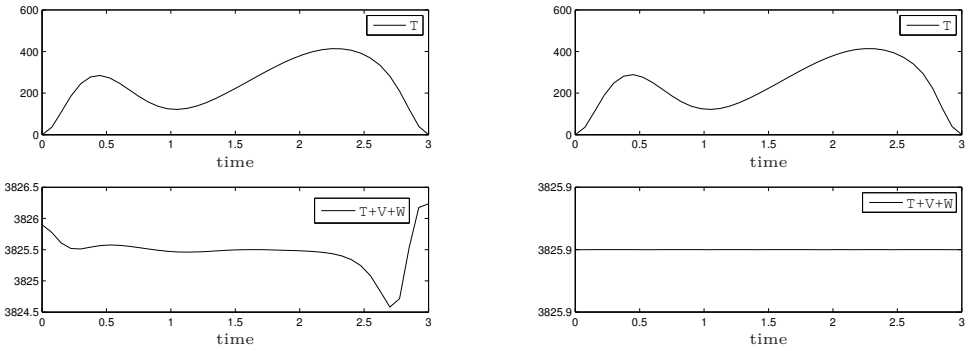

Figure 8.7.: Optimal control of a 3-link manipulator (N=40): 1. Resulting energies with midpoint evaluation (Left). 2. Resulting energies with energy consistent discretization (Right).

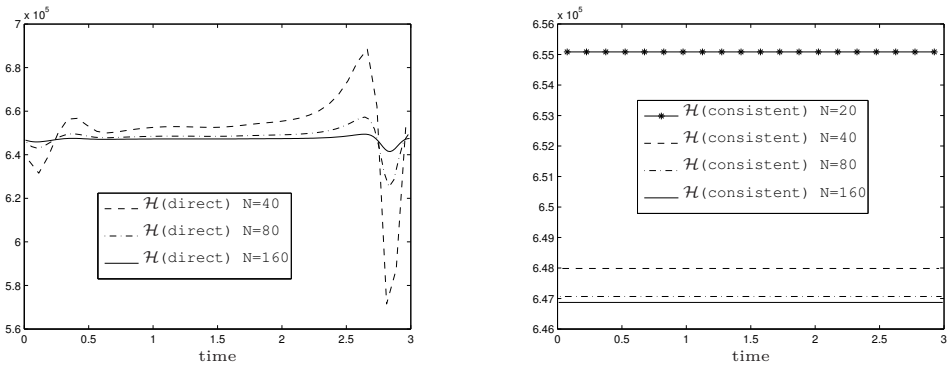

Figure 8.8.: Optimal control of a 3-link manipulator with energy consistent discretization: 1. Convergence of the Hamiltonian for a direct method (Left). 2. Convergence of the Hamiltonian for a consistent discretization of the necessary conditions of optimality (Right).

9. Summary and outlook

The main goal of the present work was the numerical treatment of optimal control problems in multibody dynamics. In a first step, a survey of different existing formulations of the underlying equations of motion for the mechanical system has been presented. Special attention has been given to the rotationless formulation, which is characterized by a constant mass matrix. The rotationless formulation is especially suitable for the development of mechanical integrators, which are algorithmically consistent regarding basic mechanical properties, namely the energy, the linear and the angular momentum. Energy-momentum schemes are well-known to possess superior numerical stability and robustness properties.

The applicability of the mentioned scheme for optimal control problems requires a consistent incorporation of control torques. A direct incorporation of the generalized torques using transformation matrices has been preferred to alternative methods like the coordinate augmentation technique. To achieve the consistency properties, a special evaluation of these transformation matrices turned out to be mandatory. In addition to the consistent incorporation of the control torques, a way for the consistent incorporation of the generalized velocities needed for the formulation of linear viscous friction has been demonstrated.

Beside the direction cosines leading to the rotationless formulation, also quaternions have been investigated in Chapter 5 of this work. The corresponding equations of motion exhibit a lower redundancy, but contain a configuration dependent mass matrix. For the transition to the Hamilton formalism, an invertible mass matrix has been derived by a reduction process from the mass matrix in the director formulation. A formulation of the kinetic energy with quadratic invariants together with a special discretization has been applied for deriving a new quaternion-based energy-momentum scheme. While the consistency properties have been demonstrated within a numerical example, benefits concerning the calculation time due to the lower redundancy could not be observed. Additionally, the extension to multibody systems turned out to be cumbersome within the quaternion-based energy-momentum scheme. Consequently, quaternions have not been employed in the optimal control problems later on.

Optimal control problems in multibody dynamics have been treated in Chapters 6 and 7. In a first step, direct transcription methods provided with equations of motion in ODE-form have been derived. By application of the REM, a numerical optimal control method has been introduced which is algorithmically consistent concerning the discrete energy, the discrete linear momentum, and the discrete angular momentum as basic properties of the mechanical system.

The widely used generalized coordinates formulation has been employed for the verification of the numerical results. For that purpose, representative numerical examples have been investigated. It is worth mentioning that the resulting ODE-formulation yields a minimal set of equations, but a high degree of nonlinearity. In a second step, a direct transcription method based on equations of motion in DAE-form has been derived. The corresponding equations of motion therein have been discretized by the BEM. In contrast to the ODE-based optimal control approaches, the DAE-based approach exhibits a large set of equations due to the redundancy of the rotationless formulation. However, the arising computational costs can be reduced significantly by exploiting sparsity of the simply structured equations, which has been investigated only rudimentary in this thesis. The numerical results have been compared to those achieved by the ODE-based optimal control methods. Finally, it should be remarked that a good initial guess seems to be more important for the DAE-based direct transcription method than for the ODE-based one.

In Chapter 8 of this thesis, it has been shown that conservation properties similar to the energy consistency in forward dynamics exist also in optimal control problems. Though the conservation of the Hamiltonian has to be valid along an optimal movement in the continuous setting, the corresponding discrete property is not fulfilled for the direct transcription methods applied previously. Accordingly, a special discretization of the costate equations has been performed to achieve an indirect optimal control method which conserves the Hamiltonian of the optimal control problem algorithmically. As a first step, this indirect transcription scheme has been employed for a formulation of the equations of motion with generalized coordinates. The extension to other formulations seems to be promising.

A lot of interesting research work is still open concerning the computational treatment of optimal control problems in multibody dynamics. A short survey of potential future directions will be given below.

- More research work has to be done regarding conservation properties in the optimal control of multibody dynamics. While in this work a Hamiltonian conserving method has been derived for the generalized coordinates formulation of the equations of motion, a similar approach may be developed for other choices of coordinates. Especially, the simple form of the basic energy-momentum scheme seems to be appropriate for deriving methods with similar properties. Furthermore, Hamiltonian conserving methods should be derived for other kind of optimal control problems than the mechanical ones treated in this thesis. The applicability does not seem to be limited to mechanical optimal control problems. In addition to the Hamiltonian of the optimal control problem, other kind of conservation properties may be derived for a mechanical system. While the conservation of the Hamiltonian has similarities to the energy consistency, further conservation properties similar to momentum and angular momentum conservation might be found. Furthermore, schemes satisfying these properties algorith-

mically should be applied for other optimal control methods like shooting or multiple shooting. An improved stability might be especially benefitting to methods with consecutively treated time steps.

- A challenging task is the optimal control of multibody systems specified with equations of motion in DAE-form. The determination of a good initial guess turns out to be especially important for mechanical systems described that way. Additionally, the redundancy of the DAE-formulation may lead to increasing computational costs within the transcription methods applied in this work. However, the computational costs can be reduced by exploiting the sparsity of the simply structured DAE-formulation. In this connection, the application of the widely used open source code IPOPT (see, for example, Wächter & Biegler [105]) should be considered. Furthermore, it should be tested if the mixed redundant formulation described in Becker [8] is a suitable compromise between the redundant formulation and the reduced one within optimal control problems.
- Assuming further developments of optimal control with equations of motion in DAE-form will be made, the incorporation of flexible components into the multibody systems can be approached. It is worth mentioning that schemes satisfying basic mechanical conservation properties are especially superior for forward dynamics problems of flexible multibody systems. Similar benefits can be expected for the optimal control of such systems. Additionally, an efficient DAE-formulation enables the treatment of closed kinematic chains within optimal control.
- Although the coordinate augmentation technique for the incorporation of rotational variables into the rotationless formulation has been avoided in this work, this method seems to be still necessary for multibody systems with torsional springs and winches. While this technique has been successfully applied for forward dynamics problems of such multibody systems (see Uhlar [99]), this procedure should also be employable for the more complex optimal control problems.

A. Details of the implementation of the REM

Below, some informations concerning the implementation of the direct transcription method used for the optimal control of the 3-link manipulator treated in Chapter 6 will be given. At this point, the dynamics of the mechanical system will be described by use of the reduced energy-momentum scheme (REM) with eliminated velocities. For simplicity both the incorporation of inequality constraints and the incorporation of dissipation will be neglected. The basic task for the solution of an optimal control problem with a direct transcription method is the formulation of the discrete augmented cost function given in Eq. (2.15). For this aim, the discrete quadratic function to be inserted into the discrete cost function in Eq. (2.14), takes the form

$$\mathcal{L}(\boldsymbol{u}_{k,k+1}) = \frac{1}{2}\boldsymbol{u}_{k,k+1} \cdot \boldsymbol{u}_{k,k+1} \tag{A.1}$$

In addition to that, the constraints consisting of both the discrete equations of motion $\boldsymbol{f}(\boldsymbol{x}_k, \boldsymbol{x}_{k+1}, \boldsymbol{u}_{k,k+1})$ and the final conditions on configuration and velocity level summarized in $\boldsymbol{\Psi}(\boldsymbol{x}_N)$ have to be incorporated by use of the discrete Lagrange-multipliers $\boldsymbol{\lambda}_{k,k+1}$ respectively $\boldsymbol{\mu}$. Correspondingly, the discrete equations of motion for the present REM take the form

$$\boldsymbol{f}(\boldsymbol{x}_k, \boldsymbol{x}_{k+1}, \boldsymbol{u}_{k,k+1}) = \boldsymbol{P}(\boldsymbol{q}_{k+\frac{1}{2}})^T \boldsymbol{a}^1_{k+1} + h\, \boldsymbol{u}_{k,k+1} \tag{A.2}$$

for $k = 0, ..., N-1$, where abbreviations necessary for the subsequent formulation of the gradients of the form

$$\boldsymbol{a}^1_{k+1} = \boldsymbol{M}(\boldsymbol{v}_{k+1} - \boldsymbol{v}_k) + h\, \nabla_q \boldsymbol{V} \tag{A.3}$$

have been applied. Notice that the form of the discrete equations of motion has been already adapted to the 3-link manipulator as example. Consequently, the defining relation for the transformation matrix $\boldsymbol{B}$ of the 3-link manipulator given in Eq. (6.10) has been inserted. Furthermore, in the present REM, the discrete state vector $\boldsymbol{x}_{k+1}$ is equal to the vector of local coordinates of minimal size $\boldsymbol{\theta}_{k+1}$, that is

$$\boldsymbol{x}_{k+1} = \boldsymbol{\theta}_{k+1} \tag{A.4}$$

for $k = 0, ..., N-1$. Hence, $\boldsymbol{\theta}_{k+1}$ will be used in the following for describing the gradients. Additionally, the mentioned constraints will be summarized in the vector of constraint functions denoted by $\boldsymbol{C}$.

In the next step, the necessary gradients for the direct transcription method used for the optimal control of the 3-link manipulator will be provided. Firstly, the gradient of the discrete cost function takes the form

$$\nabla_{(\boldsymbol{\theta},\boldsymbol{u})}\boldsymbol{\mathcal{L}} = \begin{bmatrix}\boldsymbol{0}_{1\times N(n-m)} & \boldsymbol{u}\end{bmatrix} \tag{A.5}$$

with the global vector of discrete controls and the global vector of local coordinates of minimal size defined by

$$\begin{aligned}\boldsymbol{u} &= \begin{bmatrix}\boldsymbol{u}_{0,1} & \cdots & \boldsymbol{u}_{N-1,N}\end{bmatrix}\\ \boldsymbol{\theta} &= \begin{bmatrix}\boldsymbol{\theta}_1 & \cdots & \boldsymbol{\theta}_N\end{bmatrix}\end{aligned} \tag{A.6}$$

Secondly, the gradient of the vector of constraint functions is given by

$$\nabla_{(\boldsymbol{\theta},\boldsymbol{u})}\boldsymbol{C} = \begin{bmatrix}\left\{\boldsymbol{A}^1\,\nabla_{\boldsymbol{q}}\left(\boldsymbol{q}_\circ\right) + \boldsymbol{A}^2\,\nabla_{\boldsymbol{q}}(\boldsymbol{v}_{\boldsymbol{\Delta}})\right\}\boldsymbol{A}^3 & \boldsymbol{A}^4\\ \nabla_{\boldsymbol{\theta}}\boldsymbol{\Psi} & \boldsymbol{0}_{2(n-m)\times N(n-m)}\end{bmatrix} \tag{A.7}$$

by use of the global matrices

$$\boldsymbol{A}^i = \begin{bmatrix}\boldsymbol{A}^i_1 & & \\ & \ddots & \\ & & \boldsymbol{A}^i_N\end{bmatrix} \tag{A.8}$$

with the locally defined abbreviations

$$\begin{aligned}\boldsymbol{A}^1_{k+1} &= \nabla_{\boldsymbol{q}_{k+1}}(\boldsymbol{P}(\boldsymbol{q}_{k+\frac{1}{2}})^T\boldsymbol{a}^1_{k+1})\\ \boldsymbol{A}^2_{k+1} &= \boldsymbol{P}(\boldsymbol{q}_{k+\frac{1}{2}})^T\boldsymbol{M}\\ \boldsymbol{A}^3_{k+1} &= \nabla_{\boldsymbol{\theta}_{k+1}}\boldsymbol{q}_{k+1}\\ \boldsymbol{A}^4_{k+1} &= h\,\boldsymbol{I}_{n-m}\end{aligned} \tag{A.9}$$

for $k = 0, ..., N-1$ and $i = 1, 2, 3, 4$. The remaining parts of the block-diagonal matrices in Eq. (A.8) are zero matrices of adequate size. Similar as the global vector of discrete controls and the global vector of local coordinates of minimal size introduced in Eq. (A.6), the global discrete configuration vector arising in Eq. (A.7) is defined by

$$\boldsymbol{q} = \begin{bmatrix}\boldsymbol{q}_1 & \cdots & \boldsymbol{q}_N\end{bmatrix} \tag{A.10}$$

Furthermore, the midpoint evaluation of the configuration vector in the null space matrix in Eq. (A.2) for the N time steps yields a gradient in the vector of constraint functions in Eq. (A.7) of the form

$$\nabla_{\boldsymbol{q}}\left(\boldsymbol{q}_\circ\right) = \begin{bmatrix}\boldsymbol{I}_n & \boldsymbol{0}_n & \cdots & \cdots & \boldsymbol{0}_n\\ \boldsymbol{I}_n & \ddots & \ddots & & \vdots\\ \boldsymbol{0}_n & \ddots & \ddots & \ddots & \vdots\\ \vdots & \ddots & \ddots & \ddots & \boldsymbol{0}_n\\ \boldsymbol{0}_n & \cdots & \boldsymbol{0}_n & \boldsymbol{I}_n & \boldsymbol{I}_n\end{bmatrix} \tag{A.11}$$

where $\boldsymbol{I}_n$ are $n \times n$ identity matrices and $\boldsymbol{0}_n$ zero matrices of the same size. Additionally, differentiating $\boldsymbol{v}_{\boldsymbol{\Delta}} = \boldsymbol{v}_{k+1} - \boldsymbol{v}_k$ with respect to the configuration vector $\boldsymbol{q}_{k+1}$ for $k = 0, ..., N-1$ and taking into account Eq. (3.33) yields a gradient in the vector of constraint functions in Eq. (A.7) given by

$$\nabla_{\boldsymbol{q}}(\boldsymbol{v}_{\boldsymbol{\Delta}}) = \frac{2}{h} \begin{bmatrix} \boldsymbol{I}_n & \boldsymbol{0}_n & \cdots & \cdots & \cdots & \cdots & \boldsymbol{0}_n \\ -3\boldsymbol{I}_n & \ddots & \ddots & & & & \vdots \\ +4\boldsymbol{I}_n & \ddots & \ddots & \ddots & & & \vdots \\ -4\boldsymbol{I}_n & \ddots & \ddots & \ddots & \ddots & & \vdots \\ +4\boldsymbol{I}_n & \ddots & \ddots & \ddots & \ddots & \ddots & \vdots \\ \vdots & \ddots & \ddots & \ddots & \ddots & \ddots & \boldsymbol{0}_n \\ \pm 4\boldsymbol{I}_n & \cdots & +4\boldsymbol{I}_n & -4\boldsymbol{I}_n & +4\boldsymbol{I}_n & -3\boldsymbol{I}_n & \boldsymbol{I}_n \end{bmatrix} \tag{A.12}$$

In the present 3-link manipulator example, the resulting matrix $\boldsymbol{A}_{k+1}^1 \in \mathbb{R}^{(n-m)\times n}$ in Eq. $(\text{A.9})_1$ solely consists of the components of $\boldsymbol{a}_{k+1}^1$. Furthermore, the matrix $\boldsymbol{A}_{k+1}^3$ in Eq. $(\text{A.9})_3$ is equal to the already available null space matrix $\boldsymbol{P}$, that is, the relation

$$\boldsymbol{A}_{k+1}^3 = \nabla_{\boldsymbol{\theta}_{k+1}} \boldsymbol{q}_{k+1} = \boldsymbol{P}(\boldsymbol{q}_{k+1}) \tag{A.13}$$

is valid. Finally, the gradient of the final conditions for both the configuration and the velocity level given in Eq. (6.3) has to be calculated. The gradient takes the form

$$\nabla_{\boldsymbol{\theta}} \boldsymbol{\Psi} = \begin{bmatrix} \nabla_{\boldsymbol{\theta}}(\boldsymbol{\theta}_N) \\ \left\{ \nabla_{\boldsymbol{q}_N}(\boldsymbol{B}(\boldsymbol{q}_N)\boldsymbol{v}_N)\, \nabla_{\boldsymbol{q}}(\boldsymbol{q}_N) + \boldsymbol{B}(\boldsymbol{q}_N)\, \nabla_{\boldsymbol{q}}(\boldsymbol{v}_N) \right\} \boldsymbol{A}_N^3 \end{bmatrix} \tag{A.14}$$

by use of the components

$$\begin{aligned} \nabla_{\boldsymbol{\theta}}(\boldsymbol{\theta}_N) &= \begin{bmatrix} \boldsymbol{0}_{(n-m)\times(N-1)\cdot(n-m)} & \boldsymbol{I}_{n-m} \end{bmatrix} \\ \nabla_{\boldsymbol{q}}(\boldsymbol{q}_N) &= \begin{bmatrix} \boldsymbol{0}_{n\times(N-1)\cdot n} & \boldsymbol{I}_n \end{bmatrix} \\ \nabla_{\boldsymbol{q}}(\boldsymbol{v}_N) &= \frac{2}{h} \begin{bmatrix} \pm 2\boldsymbol{I}_n & \cdots & -2\boldsymbol{I}_n & +2\boldsymbol{I}_n & -2\boldsymbol{I}_n & \boldsymbol{I}_n \end{bmatrix} \end{aligned} \tag{A.15}$$

At this point, all gradients needed for the direct transcription method have been provided.

The above gradients can be used for the solution of the optimal control problem with the SQP solver fmincon. Alternatively, they can be employed for the derivation of discrete necessary conditions for optimality (DNCO). For that purpose, the discrete costate equations and the discrete control equations have to be calculated by application of the formula

$$\nabla_{(\boldsymbol{\theta},\boldsymbol{u})} \boldsymbol{\mathcal{L}} + \boldsymbol{\lambda} \cdot \nabla_{(\boldsymbol{\theta},\boldsymbol{u})} \boldsymbol{C} = \boldsymbol{A}^T \tag{A.16}$$

In addition to the discrete equations of motion and the final conditions summed up in the vector of constraints $\boldsymbol{C}$, the discrete costate and control equations in $\boldsymbol{A}$ serve as DNCO. Finally, the DNCO can be solved using Newton's method.

B. Details of the implementation of the BEM

In the present chapter, details of the implementation for the direct transcription method used for the optimal control of the 3-link manipulator treated in Chapter 7 will be provided. The basic energy-momentum scheme (BEM) without eliminated velocities serves as basis for the formulation of the mechanical multibody system. As in Appendix A, both the incorporation of inequality constraints and the incorporation of dissipation will be neglected. To formulate the essential discrete augmented cost function given in Eq. (2.15), the discrete quadratic function introduced in Eq. (A.1) has to be inserted into the discrete cost function in Eq. (2.14). Additionally, the constraints consisting of both the discrete equations of motion $\boldsymbol{f}(\boldsymbol{x}_k, \boldsymbol{x}_{k+1}, \boldsymbol{x}_{k,k+1}, \boldsymbol{u}_{k,k+1})$ and the final conditions summarized in $\boldsymbol{\Psi}(\boldsymbol{x}_N)$ have to be incorporated by use of the discrete Lagrange-multipliers $\boldsymbol{\lambda}_{k,k+1}$ respectively $\boldsymbol{\mu}$. In the present BEM, the discrete equations of motion reads

$$\boldsymbol{f}(\boldsymbol{x}_k, \boldsymbol{x}_{k+1}, \boldsymbol{x}_{k,k+1}, \boldsymbol{u}_{k,k+1}) = \begin{bmatrix} \boldsymbol{q}_{k+1} - \boldsymbol{q}_k - h\, \boldsymbol{v}_{k+\frac{1}{2}} \\ \boldsymbol{M}(\boldsymbol{v}_{k+1} - \boldsymbol{v}_k) + h(\nabla_{\boldsymbol{q}} \boldsymbol{V} + \boldsymbol{a}^2_{k+1}) \\ \boldsymbol{\Phi}(\boldsymbol{q}_{k+1}) \end{bmatrix} \tag{B.1}$$

for $k = 0, ..., N-1$ for the first two parts of the equations of motion and $k = 0, ..., N-2$ for the constraints. Notice that the constraints at the final time t_N are enforced through the boundary conditions on configuration level. Furthermore, the abbreviations

$$\boldsymbol{a}^2_{k+1} = \boldsymbol{G}(\boldsymbol{q}_{k+\frac{1}{2}})^T \boldsymbol{\gamma}_{k,k+1} + \boldsymbol{B}(\boldsymbol{q}^{k+\frac{1}{2}})^T \boldsymbol{u}_{k,k+1} \tag{B.2}$$

have been employed in Eq. (B.1). Again, the mentioned constraints will be summarized in the vector of constraint functions denoted by $\boldsymbol{C}$.

In the next step, the required gradients for the direct transcription optimal control method based on the BEM will be provided. Firstly, the gradient of the discrete cost function takes the form

$$\nabla_{(\boldsymbol{q},\boldsymbol{v},\boldsymbol{\gamma},\boldsymbol{u})} \boldsymbol{\mathcal{L}} = \begin{bmatrix} \boldsymbol{0}_{1 \times N(2n+m)} & \boldsymbol{u} \end{bmatrix} \tag{B.3}$$

with the global vectors of discrete configurations, velocities, Lagrange-multipliers,

and controls defined by

$$\begin{aligned}\boldsymbol{q} &= \begin{bmatrix}\boldsymbol{q}_1 & \cdots & \boldsymbol{x}_N\end{bmatrix}\\ \boldsymbol{v} &= \begin{bmatrix}\boldsymbol{v}_1 & \cdots & \boldsymbol{v}_N\end{bmatrix}\\ \boldsymbol{\gamma} &= \begin{bmatrix}\boldsymbol{\gamma}_{0,1} & \cdots & \boldsymbol{\gamma}_{N-1,N}\end{bmatrix}\\ \boldsymbol{u} &= \begin{bmatrix}\boldsymbol{u}_{0,1} & \cdots & \boldsymbol{u}_{N-1,N}\end{bmatrix}\end{aligned} \tag{B.4}$$

Secondly, the gradient of the vector of constraint functions is given by

$$\nabla_{(\boldsymbol{q},\boldsymbol{v},\boldsymbol{\gamma},\boldsymbol{u})}\boldsymbol{C} = \begin{bmatrix} \nabla_{\boldsymbol{q}}(\boldsymbol{q}_{\boldsymbol{\Delta}}) & -\frac{h}{2}\nabla_{\boldsymbol{q}}(\boldsymbol{q}_{\circ}) & \boldsymbol{0} & \boldsymbol{0} \\ h(\boldsymbol{A}^5+\boldsymbol{A}^6)\,\nabla_{\boldsymbol{q}}(\boldsymbol{q}_{\circ}) & \nabla_{\boldsymbol{v}}(\boldsymbol{v}_{\boldsymbol{\Delta}}) & h\boldsymbol{A}^7 & h\boldsymbol{A}^8 \\ \begin{bmatrix}\boldsymbol{A}^9 & \boldsymbol{0}\end{bmatrix} & \boldsymbol{0} & \boldsymbol{0} & \boldsymbol{0} \\ \nabla_{\boldsymbol{q}}\boldsymbol{\Psi} & \nabla_{\boldsymbol{v}}\boldsymbol{\Psi} & \boldsymbol{0} & \boldsymbol{0} \end{bmatrix} \tag{B.5}$$

by use of the global matrices given in Eq. (A.8) with the local defined abbreviations

$$\begin{aligned}\boldsymbol{A}^5_{k+1} &= \nabla_{\boldsymbol{q}_{k+1}}(\boldsymbol{G}(\boldsymbol{q}_{k+\frac{1}{2}})^T\boldsymbol{\gamma}_{k,k+1})\\ \boldsymbol{A}^6_{k+1} &= \nabla_{\boldsymbol{q}_{k+1}}(\boldsymbol{B}(\boldsymbol{q}^{k+\frac{1}{2}})^T\boldsymbol{u}_{k,k+1})\\ \boldsymbol{A}^7_{k+1} &= h\,\boldsymbol{G}(\boldsymbol{q}_{k+\frac{1}{2}})^T\\ \boldsymbol{A}^8_{k+1} &= h\,\boldsymbol{B}(\boldsymbol{q}^{k+\frac{1}{2}})^T\\ \boldsymbol{A}^9_{k+1} &= \boldsymbol{G}(\boldsymbol{q}_{k+1})\end{aligned} \tag{B.6}$$

and zero matrices of adequate size. Notice that N matrices are located on the diagonal for $i = 5, 6, 7, 8$ due to $k = 0, ..., N-1$ and $N-1$ matrices are located on the diagonal for $i = 9$ due to $k = 0, ..., N-2$. The midpoint evaluation of the configuration vectors in Eq. (B.1) for the N time steps yields a gradient in the vector of constraint functions in Eq. (B.5) given by Eq. (A.11). Furthermore, differentiating $\boldsymbol{q}_{\boldsymbol{\Delta}} = \boldsymbol{q}_{k+1} - \boldsymbol{q}_k$ with respect to the configuration vector $\boldsymbol{q}_{k+1}$ for $k = 0, ..., N-1$ yields a gradient in the vector of constraint functions in Eq. (B.5) given by

$$\nabla_{\boldsymbol{q}}(\boldsymbol{q}_{\boldsymbol{\Delta}}) = \begin{bmatrix} \boldsymbol{I}_n & \boldsymbol{0}_n & \cdots & \cdots & \boldsymbol{0}_n \\ -\boldsymbol{I}_n & \ddots & \ddots & & \vdots \\ \boldsymbol{0}_n & \ddots & \ddots & \ddots & \vdots \\ \vdots & \ddots & \ddots & \ddots & \boldsymbol{0}_n \\ \boldsymbol{0}_n & \cdots & \boldsymbol{0}_n & -\boldsymbol{I}_n & \boldsymbol{I}_n \end{bmatrix} \tag{B.7}$$

Apparently, replacing the configuration by the velocity yields similar gradients. Concerning the matrices $\boldsymbol{A}^6_{k+1}$ in Eq. $(\text{B.6})_2$, the contravariant evaluation of the transformation matrix has to be taken into account for the calculation of the derivatives. In particular, the contravariant evaluated directors have to be derivated with respect to the corresponding covariant ones. Consequently, for each of the three rigid bodies and $i, j = 1, 2$ the formula

$$\frac{\partial(\boldsymbol{d}^j)^{k+\frac{1}{2}}}{\partial(\boldsymbol{d}_i)_{k+\frac{1}{2}}} = -\boldsymbol{R}^{k+\frac{1}{2}}\,\frac{\partial(\boldsymbol{d}_j)_{k+\frac{1}{2}}}{\partial(\boldsymbol{d}_i)_{k+\frac{1}{2}}}\,\boldsymbol{R}^{k+\frac{1}{2}} \tag{B.8}$$

has to be employed. The arising vectors and matrices therein have been introduced in Eqs. (6.12), (6.13), and (6.14). Finally, the gradients of the final conditions for both the configuration and the velocity level given in Eq. (7.11) have to be calculated. The derivative of the final conditions with respect to the configuration vector reads

$$\nabla_{\boldsymbol{q}} \boldsymbol{\Psi} = \begin{bmatrix} \nabla_{\boldsymbol{q}}(\boldsymbol{q}_N) \\ \nabla_{\boldsymbol{q}_N}(\boldsymbol{B}(\boldsymbol{q}_N)\boldsymbol{v}_N)\, \nabla_{\boldsymbol{q}}(\boldsymbol{q}_N) \end{bmatrix} \tag{B.9}$$

by use of the components given in Eq. $(A.15)_2$. Furthermore, the derivative of the final conditions with respect to the velocity takes the form

$$\nabla_{\boldsymbol{v}} \boldsymbol{\Psi} = \begin{bmatrix} \boldsymbol{0} \\ \boldsymbol{B}(\boldsymbol{q}_N)\, \nabla_{\boldsymbol{v}}(\boldsymbol{v}_N) \end{bmatrix} \tag{B.10}$$

where the component $\nabla_{\boldsymbol{v}}(\boldsymbol{v}_N)$ is equal to the one given in Eq. $(A.15)_2$. At this point, all gradients needed for the direct transcription method have been provided.

Similar as in the case of the REM elaborated in Appendix A, the provided gradients can be used for the solution of the optimal control problem with the SQP solver fmincon. As an alternative, they can be used for the formulation of discrete necessary conditions for optimality (DNCO). For this aim, the discrete costate equations and the discrete control equations have to be calculated by application of the formula

$$\nabla_{(\boldsymbol{q},\boldsymbol{v},\boldsymbol{\gamma},\boldsymbol{u})} \boldsymbol{\mathcal{L}} + \boldsymbol{\lambda} \cdot \nabla_{(\boldsymbol{q},\boldsymbol{v},\boldsymbol{\gamma},\boldsymbol{u})} \boldsymbol{C} = \boldsymbol{A}^T \tag{B.11}$$

In addition to the discrete equations of motion and the final conditions summed up in the vector of constraints $\boldsymbol{C}$, the discrete costate and control equations in $\boldsymbol{A}$ serve as DNCO. Finally, the DNCO can be solved using Newton's method.

Bibliography

[1] S.K. Agrawal, S. Li, and B.C. Fabien. Optimal trajectories of open-chain mechanical systems: An explicit optimality equation with a multiple shooting solution. *Mech. Struct. & Mach.*, 25(2):163–177, 1997.

[2] S.L. Altmann. *Rotations, Quaternions, and Double Groups*. Clarendon Press, Oxford, 1986.

[3] M. Arribas, A. Elipe, and M. Palacios. Quaternions and the rotation of a rigid body. *Celestial Mechanics and Dynamical Astronomy*, 96(3-4):239–251, 2006.

[4] U.M. Ascher, R.M.M. Mattheij, and R.D. Russell. *Numerical solution of boundary value problems for ordinary differential equations*. Classics in applied mathematics. Society for Industrial and Applied Mathematics, 1995.

[5] M. Athans and P.L. Falb. *Optimal control: an introduction to the theory and its applications*. Lincoln Laboratory publications. McGraw-Hill, 1966.

[6] A. Barclay, P. E. Gill, and J. B. Rosen. SQP methods and their application to numerical optimal control, 1997.

[7] O.A. Bauchau and C.L. Bottasso. On the design of energy preserving and decaying schemes for flexible, nonlinear multi-body systems. *Comput. Methods Appl. Mech. Engrg.*, 169:61–79, 1999.

[8] C. Becker. Verwendung einer gemischt redundanten Formulierung zur Modellierung und Simulation von Mehrkörpersystemen. Diploma thesis, University of Siegen, 2011.

[9] P. Betsch. The discrete null space method for the energy consistent integration of constrained mechanical systems. Part I: Holonomic constraints. *Comput. Methods Appl. Mech. Engrg.*, 194(50-52):5159–5190, 2005.

[10] P. Betsch, C. Hesch, N. Sänger, and S. Uhlar. Variational integrators and energy-momentum schemes for flexible multibody dynamics. *J. Comput. Nonlinear Dynam.*, 5(3):031001/1–11, 2010.

[11] P. Betsch and S. Leyendecker. The discrete null space method for the energy consistent integration of constrained mechanical systems. Part II: Multibody dynamics. *Int. J. Numer. Meth. Engng*, 67(4):499–552, 2006.

[12] P. Betsch and R. Siebert. Rigid body dynamics in terms of quaternions: Hamiltonian formulation and conserving numerical integration. *Int. J. Numer. Meth. Engng*, 79(4):444–473, 2009.

[13] P. Betsch, R. Siebert, and N. Sänger. Natural coordinates in the optimal control of multibody systems. *J. Comput. Nonlinear Dynam.*, 7(1):011009/1–8, 2012.

[14] P. Betsch and P. Steinmann. Inherently energy conserving time finite elements for classical mechanics. *Journal of Computational Physics*, 160:88–116, 2000.

[15] P. Betsch and P. Steinmann. Conservation properties of a time FE method. Part II: Time-stepping schemes for nonlinear elastodynamics. *Int. J. Numer. Meth. Engng*, 50:1931–1955, 2001.

[16] P. Betsch and P. Steinmann. Constrained integration of rigid body dynamics. *Comput. Methods Appl. Mech. Engrg.*, 191:467–488, 2001.

[17] P. Betsch and P. Steinmann. Conservation properties of a time FE method. Part III: Mechanical systems with holonomic constraints. *Int. J. Numer. Meth. Engng*, 53:2271–2304, 2002.

[18] P. Betsch and P. Steinmann. A DAE approach to flexible multibody dynamics. *Multibody System Dynamics*, 8:367–391, 2002.

[19] P. Betsch and S. Uhlar. Energy-momentum conserving integration of multibody dynamics. *Multibody System Dynamics*, 17(4):243–289, 2007.

[20] P. Betsch, S. Uhlar, and M. Quasem. Numerical integration of mechanical systems with mixed holonomic and control constraints. In K. Arczewski, J. Frączek, and M. Wojtyra, editors, *Proceedings of the ECCOMAS Thematic Conference on Multibody Dynamics*, Warsaw, Poland, 29th June - 2nd July 2009.

[21] J.T. Betts. Survey of numerical methods for trajectory optimization. *J. Guidance, Control and Dynamics*, 21(2):193–207, 1998.

[22] J.T. Betts. *Practical Methods for Optimal Control Using Nonlinear Programming*. SIAM, Philadelphia, PA, 2001.

[23] J.T. Betts, S.L. Campbell, and A. Engelsone. Direct transcription solution of optimal control problems with higher order state constraints: theory vs practice. *Optim Eng*, 8:1–19, 2007.

[24] J.T. Betts and W.P. Huffman. Mesh refinement in direct transcription methods for optimal control. *Optim. Control Appl. Meth.*, 19:1–21, 1998.

[25] T. Binder, L. Blank, H.G. Bock, R. Bulirsch, W. Dahmen, M. Diehl, T. Kronseder, W. Marquardt, J.P. Schlöder, and O. von Stryk. Introduction to model based optimization of chemical processes on moving horizons. In M. Grötschel, S.O. Krumke, and J. Rambau, editors, *Online Optimization of Large Scale Systems*, pages 295–340. Springer-Verlag, 2001.

[26] W. Blajer and K. Kołodziejczyk. A geometric approach to solving problems of control constraints: Theory and a DAE framework. *Multibody System Dynamics*, 11(4):343–364, 2004.

[27] H.G. Bock and K.J. Plitt. A multiple shooting algorithm for direct solution of optimal control problems. In *IFAC 9th Triennal World Congress*, pages 1603–1608, Budapest, Hungary, 1984.

[28] P. T. Boggs and J. W. Tolle. Sequential quadratic programming, 1995.

[29] J.F. Bonnans and J. Laurent-Varin. Computation of order conditions for symplectic partitioned Runge-Kutta schemes with application to optimal control. *Numer. Math.*, 103(1):1–10, 2006.

[30] M. Borri, L. Trainelli, and A. Croce. The embedded projection method: A general index reduction procedure for constrained system dynamics. *Comput. Methods Appl. Mech. Engrg.*, 195(50-51):6974–6992, 2006.

[31] C.L. Bottasso and A. Croce. Optimal control of multibody systems using an energy preserving direct transcription method. *Multibody System Dynamics*, 12(1):17–45, 2004.

[32] C.L. Bottasso, A. Croce, L. Ghezzi, and P. Faure. On the solution of inverse dynamics and trajectory optimization problems for multibody systems. *Multibody System Dynamics*, 11(1):1–22, 2004.

[33] A.E. Bryson and Y.-C. Ho. *Applied Optimal Control*. John Wiley & Sons, 1975.

[34] C. Büskens and M. Knauer. Higher order real-time approximations in optimal control of multibody-systems for industrial robots. *Multibody System Dynamics*, 15(1):85–106, 2006.

[35] C. Büskens and H. Maurer. Nonlinear programming methods for real-time control of an industrial robot. *Journal of Optimization Theory and Applications*, 107(3):505–527, 2000.

[36] C. Büskens and H. Maurer. SQP-methods for solving optimal control problems with control and state constraints: adjoint variables, sensitivity analysis and real-time control. *Journal of Computational and Applied Mathematics*, 120(1-2):85–108, 2000.

[37] R. Callies and P. Rentrop. Optimal control of rigid-link manipulators by indirect methods. *GAMM-Mitt.*, 31(1):27–58, 2008.

[38] E. Celledoni and N. Säfström. A Hamiltonian and multi-Hamiltonian formulation of a rod model using quaternions. *Computer Methods in Applied Mechanics and Engineering*, 199(45-48):2813–2819, 2010.

[39] J.C.K. Chou. Quaternion kinematic and dynamic differential equations. *IEEE Trans. Robotics and Automat.*, 8(1):53–64, 1992.

[40] V. Cossalter and R. Lot. A motorcycle multi-body model for real time simulations based on the natural coordinates approach. *Vehicle System Dynamics*, 37(6):423–447.

[41] M. Diehl. Script for Numerical Optimal Control Course. ETH Zurich, 2011.

[42] M. Diehl, H.G. Bock, H. Diedam, and P.-B. Wieber. Fast direct multiple shooting algorithms for optimal robot control. In M. Diehl and K. Mombaur, editors, *Fast Motions in Biomechanics and Robotics*, volume 340 of *Lecture Notes in Control and Information Sciences (LNCIS)*, pages 65–93. Springer Berlin Heidelberg, 2006.

[43] M. Diehl, H.G. Bock, J.P. Schlöder, R. Findeisen, Z. Nagy, and F. Allgöwer. Real-time optimization and nonlinear model predictive control of processes governed by differential-algebraic equations. *J. Proc. Contr.*, 12(4):577–585, 2002.

[44] A. Engelsone, S.L. Campbell, and J.T. Betts. Direct transcription solution of higher-index optimal control problems and the virtual index. *Applied Numerical Mathematics*, 57:281–296, 2007.

[45] P. J. Enright and B. A. Conway. Discrete approximations to optimal trajectories using direct transcription and nonlinear programming. *Journal of Guidance, Control, and Dynamics*, 15(4):994–1001, 1992.

[46] J. García de Jalón. Twenty-five years of natural coordinates. *Multibody System Dynamics*, 18(1):15–33, 2007.

[47] J. García de Jalón, M.A. Serna, F. Viadero, and J. Flaquer. A simple numerical method for the kinematic analysis of spatial mechanisms. *ASME J. Mech. Design*, 104:78–82, 1982.

[48] M. Gerdts. Direct shooting method for the numerical solution of higher-index DAE optimal control problems. *Journal of Optimization Theory and Applications*, 117(2):267–294, 2003.

[49] M. Gerdts. *Optimal Control of Ordinary Differential Equations and Differential-Algebraic Equations*. Habilitation thesis, Department of Mathematics, University of Bayreuth, 2006.

[50] M. Gerdts and M. Kunkel. A globally convergent semi-smooth Newton method for control-state constrained DAE optimal control problems. *Computational Optimization and Applications*, pages 1–33, 2009.

[51] J.M. Goicolea and J.C. Garcia Orden. Dynamic analysis of rigid and deformable multibody systems with penalty methods and energy-momentum schemes. *Comput. Methods Appl. Mech. Engrg.*, 188:789–804, 2000.

[52] O. Gonzalez. Time integration and discrete Hamiltonian systems. *J. Nonlinear Sci.*, 6:449–467, 1996.

[53] O. Gonzalez. Mechanical systems subject to holonomic constraints: Differential-algebraic formulations and conservative integration. *Physica D*, 132:165–174, 1999.

[54] O. Gonzalez and J.C. Simo. On the stability of symplectic and energy-momentum algorithms for non-linear Hamiltonian systems with symmetry. *Comput. Methods Appl. Mech. Engrg.*, 134:197–222, 1996.

[55] D. Greenspan. Conservative numerical methods for $\ddot{x} = f(x)$. *Journal of Computational Physics*, 56:28–41, 1984.

[56] J. Grizzle and S. Marcus. The structure of nonlinear control systems possessing symmetries. *Automatic Control, IEEE Transactions on*, 30(3):248–258, 1985.

[57] M. Groß, P. Betsch, and P. Steinmann. Conservation properties of a time FE method. Part IV: Higher order energy and momentum conserving schemes. *Int. J. Numer. Meth. Engng*, 63:1849–1897, 2005.

[58] W.W. Hager. Runge-Kutta methods in optimal control and the transformed adjoint system. *Numer. Math.*, 87(2):247–282, 2000.

[59] R. Hannemann and W. Marquardt. Continuous and discrete composite adjoints for the Hessian of the Lagrangian in shooting algorithms for dynamic optimization. *SIAM Journal on Scientific Computing*, 31(6):4675–4695, 2010.

[60] C.R. Hargraves and S.W. Paris. Direct trajectory optimization using nonlinear programming and collocation. *J. Guidance*, 10(4):338–342, 1987.

[61] A. Hartwich, K. Stockmann, C. Terboven, S. Feuerriegel, and W. Marquardt. Parallel sensitivity analysis for efficient large-scale dynamic optimization. *Optimization and Engineering*, 12:489–508, 2011.

[62] E.J. Haug. *Computer-Aided Kinematics and Dynamics of Mechanical Systems. Volume I: Basic Methods.* Allyn & Bacon, 1989.

[63] G.A. Hicks and W.H. Ray. Approximation methods for optimal control systems. *Can. J. Chem. Engng.*, 49:522–528, 1971.

[64] D.G. Hull. Conversion of optimal control problems into parameter optimization problems. *J. Guidance, Control, and Dynamics*, 20(1):57–60, 1997.

[65] C. Kraus, H. G. Bock, and H. Mutschler. Parameter estimation for biomechanical models based on a special form of natural coordinates. *Multibody System Dynamics*, 13(1):101–111, 2005.

[66] C. Kraus, M. Winckler, and H.G. Bock. Modeling mechanical DAE using natural coordinates. *Mathematical and Computer Modelling of Dynamical Systems*, 7(2):145–158, 2001.

[67] P. Krysl. Explicit momentum-conserving integrator for dynamics of rigid bodies approximating the midpoint Lie algorithm. *Int. J. Numer. Meth. Engng*, 63:2171–2193, 2005.

[68] J.B. Kuipers. *Quaternions and rotation sequences*. Princeton University Press, 1999.

[69] P. Kunkel and V. Mehrmann. Optimal control for unstructured nonlinear differential-algebraic equations of arbitrary index. *Math. Control Signals Systems*, 20(3):227–269, 2008.

[70] H. Lang, J. Linn, and M. Arnold. Multi-body dynamics simulation of geometrically exact Cosserat rods. *Multibody System Dynamics*, 25(3):285–312, 2011.

[71] B. Leimkuhler and S. Reich. *Simulating Hamiltonian Dynamics*. Cambridge University Press, 2004.

[72] D. B. Leineweber, I. Bauer, H. G. Bock, and J. P. Schlöder. An efficient multiple shooting based reduced SQP strategy for large-scale dynamic process optimization - Part I: Theoretical aspects. *Comput. Chem. Engng*, 27(2):157–166, 2003.

[73] D. B. Leineweber, A. Schäfer, H. G. Bock, and J. P. Schlöder. An efficient multiple shooting based reduced SQP strategy for large-scale dynamic process optimization - Part II: Software aspects and applications. *Comput. Chem. Engng*, 27(2):167–174, 2003.

[74] E.V. Lens, A. Cardona, and M. Géradin. Energy preserving time integration for constrained multibody systems. *Multibody System Dynamics*, 11(1):41–61, 2004.

[75] A. Lew, Marsden J.E., M. Ortiz, and M. West. Variational time integrators. *Int. J. Numer. Meth. Engng*, 60:153–212, 2004.

[76] S. Leyendecker, P. Betsch, and P. Steinmann. The discrete null space method for the energy consistent integration of constrained mechanical systems. Part III: Flexible multibody dynamics. *Multibody System Dynamics*, 19(1-2):45–72, 2008.

[77] S. Leyendecker, S. Ober-Blöbaum, J.E. Marsden, and M. Ortiz. Discrete mechanics and optimal control for constrained systems. *Optimal Control Applications and Methods*, 31(6):505–528, 2010.

[78] A.J. Maciejewski. Hamiltonian formalism for Euler parameters. *Celestial Mechanics*, 37:47–57, 1985.

[79] J.E. Marsden and T.S. Ratiu. *Introduction to Mechanics and Symmetry*. Springer-Verlag, 2nd edition, 1999.

[80] J.E. Marsden and M. West. Discrete mechanics and variational integrators. *Acta Numerica*, 10:357–514, 2001.

[81] F.C. Moon. *Applied Dynamics with Applications to Multibody and Mechatronic Systems*. John Wiley & Sons, 1998.

[82] H.S. Morton, Jr. Hamiltonian and Lagrangian formulations of rigid-body rotational dynamics based on the Euler parameters. *The Journal of the Astronautical Sciences*, 41:569–591, 1993.

[83] P.C. Müller. Some aspects of the optimal control of non-linear descriptor systems. *J. Appl. Maths Mechs*, 65(5):769–776, 2001.

[84] P.C. Müller. Optimal control of proper and nonproper descriptor systems. *Archive of Applied Mechanics*, 72(11-12):875–884, 2003.

[85] P.E. Nikravesh. *Computer-aided analysis of mechanical systems*. Prentice-Hall, 1988.

[86] S. Ober-Blöbaum, O. Junge, and J.E. Marsden. Discrete mechanics and optimal control: an analysis. *ESAIM: Control, Optimisation and Calculus of Variations, 17*, pages 322–352, 2011.

[87] O.M. O'Reilly and P.C. Varadi. Hoberman's sphere, Euler parameters and Lagrange's equations. *Journal of Elasticity*, 56:171–180, 1999.

[88] E.R. Pinch. *Optimal Control and the Calculus of Variations*. Oxford University Press, 1993.

[89] M.A. Puso. An energy and momentum conserving method for rigid-flexible body dynamics. *Int. J. Numer. Meth. Engng*, 53:1393–1414, 2002.

[90] P.J. Rabier and W.C. Rheinboldt. *Nonholonomic motion of rigid mechanical systems from a DAE viewpoint*. SIAM, Philadelphia, PA, 2000.

[91] I. Romero. Formulation and performance of variational integrators for rotating bodies. *Computational Mechanics*, 42:825–836, 2008.

[92] N. Sänger. *Elemente für die Dynamik flexibler Mehrkörpersysteme*. Phd thesis, University of Siegen, 2011.

[93] N. Sänger, P. Betsch, and C. Hesch. A computational framework for large deformation problems in flexible multibody dynamics. In J.C. Samin and P. Fisette, editors, *Proceedings of the ECCOMAS Thematic Conference on Multibody Dynamics*, Brussels, Belgium, 4th July - 7nd July 2011.

[94] R. Siebert and P. Betsch. Energy-momentum consistent optimal control of multibody systems. In J.C. Samin and P. Fisette, editors, *Proceedings of the ECCOMAS Thematic Conference on Multibody Dynamics*, Brussels, Belgium, 4th July - 7nd July 2011.

[95] J.C. Simo and N. Tarnow. The discrete energy-momentum method. Conserving algorithms for nonlinear elastodynamics. *Z. angew. Math. Phys. (ZAMP)*, 43:757–792, 1992.

[96] J.C. Simo, N. Tarnow, and K.K. Wong. Exact energy-momentum conserving algorithms and symplectic schemes for nonlinear dynamics. *Comput. Methods Appl. Mech. Engrg.*, 100:63–116, 1992.

[97] J.C. Simo and K.K. Wong. Unconditionally stable algorithms for rigid body dynamics that exactly preserve energy and momentum. *Int. J. Numer. Meth. Engng*, 31:19–52, 1991.

[98] E.D. Sontag. *Mathematical Control Theory*. Springer, 1990.

[99] S. Uhlar. *Energy consistent time-integration of hybrid multibody systems*. Phd thesis, University of Siegen, 2009.

[100] S. Uhlar and P. Betsch. On the derivation of energy consistent time stepping schemes for friction afflicted multibody systems. *Computers and Structures*, 88(11-12):737–754, 2010.

[101] C. Vallee, A. Hamdouni, F. Isnard, and D. Fortune. The equations of motion of a rigid body without parametrization of rotations. *J. Appl. Maths Mechs*, 63(1):25–30, 1999.

[102] R. von Schwerin. *MultiBody System SIMulation*. Springer-Verlag, 1999.

[103] O. von Stryk. Numerical solution of optimal control problems by direct collocation. In *In Optimal Control - Calculus of Variation, Optimal Control Theory and Numerical Methods, 111, 129-143, International Series of Numerical Mathematics, Birkhäuser*, 1993.

[104] O. von Stryk and R. Bulirsch. Direct and indirect methods for trajectory optimization. *Annals of Operations Research*, 37:357–373, 1992.

[105] A. Wächter and L. T. Biegler. On the implementation of an interior-point filter line-search algorithm for large-scale nonlinear programming. *Mathematical Programming*, 106:25–57, 2006.

[106] J.M. Wendlandt and J.E. Marsden. Mechanical integrators derived from a discrete variational principle. *Physica D*, 106:223–246, 1997.

[107] W.L. Wood. *Practical Time-stepping Schemes*. Oxford University Press, 1990.

Schriftenreihe des Lehrstuhls für Numerische Mechanik

Bisher in dieser Reihe erschienen:

Band I

Mechanische Integratoren für Kontaktvorgänge deformierbarer Körper unter großen Verzerrungen,
C. Hesch, Dissertation, 2007, urn:nbn:de:hbz:467-3156

Band II

Higher-order accurate and energy-momentum consistent discretisation of dynamic finite deformation thermo-viscoelasticity,
M. Groß, Habilitationsschrift, 2009, urn:nbn:de:hbz:467-3890

Band III

Energy Consistent Time-Integration of Hybrid Multibody Systems,
S. Uhlar, Dissertation, 2009, urn:nbn:de:hbz:467-4086

Band IV

Elemente für die Dynamik flexibler Mehrkörpersysteme,
N. Sänger, Dissertation, 2011, urn:nbn:de:hbz:467-5611

Band V

Mechanical integrators for the optimal control in multibody dynamics,
R. Siebert, Dissertation, 2012, urn:nbn:de:hbz:467-6520